Minnesota Department of Transportation

RESEARCH SERVICES & LIBRARY

Office of Transportation System Management

Evaluation of Concrete and Mortars for Partial Depth Repairs

Eshan V. Dave, Principal Investigator
Department of Civil Engineering
University of Minnesota Duluth

November 2014

Research Project
Final Report 2014-41

To request this document in an alternative format call 651-366-4718 or 1-800-657-3774 (Greater Minnesota) or email your request to ADArequest.dot@state.mn.us. Please request at least one week in advance.

Technical Report Documentation Page

1. Report No.	2.	3. Recipients Accession No.	
MN/RC 2014-41			
4. Title and Subtitle Evaluation of Concrete and Mortars for Partial Depth Repairs		5. Report Date November 2014 6.	
7. Author(s) Eshan V. Dave, Jay Dailey and Eric Musselman		8. Performing Organization Report No.	
9. Performing Organization Name and Address Department of Civil Engineering, University of Minnesota Duluth Department of Civil and Environmental Engineering, Villanova University		10. Project/Task/Work Unit No. CTS Project #2013028 11. Contract (C) or Grant (G) No. (C) 99008, (wo) 48	
12. Sponsoring Organization Name and Address Minnesota Department of Transportation Research Services & Library 395 John Ireland Boulevard, MS 330 St. Paul, Minnesota 55155-1899		13. Type of Report and Period Covered Final Report 14. Sponsoring Agency Code	
15. Supplementary Notes http://www.lrrb.org/pdf/201441.pdf			

16. Abstract (Limit: 250 words)

Partial-depth patching mixes must rapidly gain strength to allow the roadway to be reopened to traffic quickly. A patch should also bond well to the substrate to prevent the patch from separating from the existing material and be durable enough to withstand harsh winters. The objective of the research described in this report is to develop improved guidelines for evaluation of pre-bagged commercial patching mixtures and to recommend effective construction practices. To achieve these objectives, 13 different cementitious materials were selected and tested to determine key properties including strength gain, shrinkage, bond strength, and durability. The impact of the proposed research will be a better performing patch material as well as performance criteria that can be used to compare the materials tested in this program to new materials that will certainly be developed in the future.

This research was conducted in four main phases, literature review and development of a testing plan and three phases of laboratory testing campaigns. The most commonly available acceptance specification for partial-depth patching materials is the ASTM C928. This specification was followed and the outcomes of each of the recommended tests were evaluated in context of the performance of the patching materials. Several additional tests were developed and conducted to evaluate the bonding properties of patching materials; correlations between lab measured properties were also evaluated. Through aforementioned testing and analysis, a laboratory testing based acceptance procedure was developed for partial-depth patching materials to be used by MnDOT.

17. Document Analysis/Descriptors	18. Availability Statement		
Partial depth repair, Concrete pavements, Repairing, Patching, Freeze thaw durability	No restrictions. Document available from: National Technical Information Services, Alexandria, Virginia 22312		
19. Security Class (this report)	20. Security Class (this page)	21. No. of Pages	22. Price
Unclassified	Unclassified	233	

Evaluation of Concrete and Mortars for Partial Depth Repairs

Final Report

Prepared by:

Eshan V. Dave and Jay Dailey
Department of Civil Engineering,
University of Minnesota Duluth

Eric Musselman
Department of Civil and Environmental Engineering,
Villanova University

November 2014

Published by:

Minnesota Department of Transportation
Research Services Section
395 John Ireland Boulevard, MS 330
St. Paul, Minnesota 55155-1899

Table of Contents

List of Tables

List of Figures

Executive Summary

Over the course of their service life, concrete pavements undergo significant traffic and climatic loading leading to gradual accumulation of damage. This accumulation of damage and distress comes from the effects of changing weather conditions (temperature and moisture) and continuous vehicular traffic. All of this environmental and traffic loading often leads to cracking and spalling of the concrete at the joint edges. This pavement distress can also be created from stresses in the concrete due to incompressible material collecting in the joint, which leads to the slab not being able to expand and contract properly. Deficient aggregates also will cause spalling. All of these areas of distress need to be patched prior to the point when their severity impedes safe and smooth traffic operations on the roadway.

The partial-depth patching mixes must rapidly gain strength to allow the roadway to be reopened to traffic quickly. In addition, the patch should bond well to the substrate to prevent the patch from separating from the existing material and be durable enough to withstand the harsh Minnesota winters. The objective of the research described in this report is to develop improved guidelines for evaluation of pre-bagged commercial patching mixtures to evaluate the effects of chemical admixtures on a standard MnDOT patching mix and to recommend effective construction practices. To achieve these objectives, 13 different cementitious materials were selected and tested to determine key properties including strength gain, shrinkage, bond strength, and durability. The impact of the proposed research will be a better performing patch material as well as performance criteria that can be used to compare the materials tested in this program to new materials that will certainly be developed in the future.

This research project was conducted in four main phases, namely literature review and development of testing plan and three phases of laboratory testing campaigns. The most commonly available acceptance specification for partial-depth patching materials is the ASTM C928. This specification followed the present study and the outcomes of each of the recommended tests were evaluated in context of the performance of the patching materials. Several additional tests were developed and conducted to evaluate the bonding properties of patching materials; correlations between lab measured properties were also evaluated. Through aforementioned testing and analysis, a laboratory testing based acceptance procedure was developed for partial-depth patching materials to be used by MnDOT.

The main benefits of this research are realized through improvement of the performance of the "Bagged Portland Cement Concrete Patching Mix (Grade 3Ul8)" through the use of chemical admixtures, the development of improved guidelines for the acceptance of pre-bagged commercial patching mixes, and the determination of effective construction practices for partial-depth patches.

Chapter 1:
Introduction

This is a report on testing for the acceptance of partial-depth patching materials for research contract number 99008 work order number 48. This comprehensive report provides literature review, research methodology, testing plan, test methods, test results and recommendations on basis of test results in context of patching material selection process.

The findings also are the basis for a draft of best practices manual for two areas of interest; material acceptance and construction techniques.

Partial-Depth Repair

Damage to rigid pavements can be anywhere from slight surface damage to cracks extending to the bottom of the slab. When this damage is contained in the upper 1/3 to ½ of the slab thickness, partial-depth repair (PDR) is used (Symons, 1999). If the spall penetrates to a depth below ½ of the slab thickness a full depth repair is usually recommended (Johnson, 2012). Many state's Departments of Transportation (DOTs) utilize PDR as routine practice to maintain the concrete pavements. For example, Minnesota, Iowa, California, Colorado, Kansas, Missouri and Wisconsin DOTs use this method. The process of partial-depth repair actually started in Minnesota in the early 1980's (International Grooving and Grinding Association, 2011). One of the first projects was the repair of portions of Trunk Highway 61 near Hastings and Duluth using the PDR. The first removal method used was a sawing and chipping process of the distressed area. The early projects were not met with success; this led to MnDOT proposing a grinder for material removal which led to much higher rates of success (International Grooving and Grinding Association, 2011).

The study being performed deals directly with the materials involved in PDR. MnDOT has three different classifications of partial-depth repairs. These are Type BA, Type BE and Type B3 (Masten, 2011). A comparison of the three types is presented in Table 1. Diagrams of the repair types are located in Appendix A.

Table 1: Partial-depth repair types

Type	Definitions
BA	• Repair is contained above the level of the dowel bars • Patch width is minimum of 10" wide • Patch is a maximum of 6' long
BE	• Repair depth is below dowel bars (full depth) • Tie bar steel reinforcement must be provided in patch • Reinforcement must extend a minimum of 4" into sound concrete and be exposed a minimum of 4" into the patch material
B3	• Same as type BA except the patch length is longer than 6'

Even though the Type BE repair extends to the full depth of the pavement it is not considered a full depth repair by MnDOT. Full depth repair as defined by MnDOT includes the replacement of load transferring devices, dowel bars.

Motivation

Partial-depth patching is of growing concern in the colder climate regions of North America. Aging infrastructures of rigid pavements are showing signs of increased distresses. The research conducted for this particular project was proposed to improve the reliability of the products being used to patch these distresses.

Research Objectives

There are many important material properties that must be considered when selecting a patching material. The focus of this study was to determine which of these properties should be tested and what the threshold of the results should be for the acceptance rapid setting patch materials to be used for partial-depth repair.

The outcomes of the research conducted include:

- Comprehensive recommendation of laboratory tests to be conducted on patching materials for use in cold climate patching applications
- The acceptable limits for the results of those tests
- Best practices manual on proper construction techniques for PDR

Scope of Testing and Products/Materials

Testing and Products used in Task 2 of the Study

The first portion of the project consisted of six different tests: compressive strength gain, flexural strength at 4 hours, setting time, freeze-thaw durability, shrinkage and bond strength. The tests were performed by following the ASTM C928 specification for rapid setting, pre-bagged cementitious materials. The only deviation from that standard is the bond strength test, which is described herein.

The thirteen materials that were chosen to undergo the testing during task two of the project included:

1. MnDOT 3U18 (produced by TCC)
2. MnDOT 3U18M (produced by TCC)
3. Akona Rapid Patch
4. MnDOT District 3 Mix1, 3U18 based
5. MnDOT District 3 Mix2, 3U18 based
6. Five Star Highway Patch
7. Futura-15
8. Futura-45 Extended
9. Mono Patch
10. Pavemend SL

11. Pavemend SLQ
12. Rapid Set Concrete Mix
13. TCC Taconite-based Mix (Rapid Patch)

These products were chosen in conjunction with the technical advisory panel of the project. Most of the patching materials were delivered to the University of Minnesota Duluth by mid-December 2012. The TCC Taconite Mix arrived at the facility on April 4th 2013.

Testing and Products used in Task 3 of the Study

The second phase of the project consisted of six different tests: coefficient of thermal expansion, abrasion resistance, modulus of elasticity, length change in sulfate, scaling resistance to deicing chemicals and the slant shear bond test. The tests were performed by following the ASTM C928 specification for rapid setting, pre-bagged cementitious materials.

The four materials that were chosen to undergo testing during task three of the project included:

1. MnDOT 3U18M (produced by TCC)
2. MnDOT District 3 Mix 2, 3U18 based
3. Futura-45 (Non-Extended version)
4. Rapid Set Concrete Mix

These products were chosen in conjunction with the technical advisory panel of this project.

Testing, Products and Construction Methods used in Task 4 of the Study

The final testing portion of the project consisted of the pop-out bond tests. The test was proposed by Eric Musselman with the intention of evaluating construction techniques on representative pavement slabs. The test was conducted with four main parameters in place:

1. Using water as a bonding agent.
2. Using a cement/water grout mixture as a bonding agent.
3. Four test subjects were cast and stored at a temperature of 50 degrees Fahrenheit.
4. Cement paste bonding agent (Villanova)

The three materials that were chosen to undergo testing during task four of the project includes:

1. MnDOT 3U18M (produced by TCC)
2. MnDOT District 3 Mix 2, 3U18 based
3. Futura 45 (Villanova)

These products were chosen in conjunction with the technical advisory panel of this project.

Organization of the Report

This report is organized into six chapters and four appendices. Chapter 2 provides the literature review that was conducted through task-1 of the study. The literature review also helped develop the testing

plan for the tasks 2 thru 4 of the study and helped develop list of products that were evaluated. Chapter 3 describes all the testing procedures and methods that were employed throughout the project. This chapter also briefly describes the analysis of the test results and the implications associated with the findings. Chapters 4 and 5 present the results from the testing conducted through task 2, and tasks 3 and 4 respectively. Along with presentation of results, discussions are provided on the findings from the laboratory testing campaign. On the basis of research conducted through this project a laboratory testing based acceptance procedure for cementitious materials used in partial-depth repair of rigid pavements was developed, this procedure is outlined in Chapter 6 of this report. Finally, Chapter 7 summarizes the study and lists the key conclusions and recommendations. The MnDOT approved partial-depth repair techniques are attached for reader's reference as Appendix A. On basis of the site visits and through experience gained in testing patching materials a best practices recommendation is put together by the researchers, this is attached as Appendix B. The raw data from laboratory testing is attached as Appendix C and the detailed presentation of testing campaign undertaken at the Villanova university is attached as Appendix D.

Chapter 2:
Literature Review and Research Approach

Literature Review

Minnesota Department of Transportation currently has 34 approved bag mixes of rapid set cementitious materials used for concrete pavement repair (CPR). (MnDOT, 2012) These products have passed the minimum requirements set forth by MnDOT. The approval process is directly based on the ASTM C 928 specifications. The ASTM C 928 has requirements on minimum compressive strength, bond strength, aversion to length change, consistency and scaling resistance. Table 3 shows the tests and the required values of the properties. The requirements are for three different classes of concrete or mortar: R1, R2 and R3.

Table 2 (A & B): Tests and property requirements of ASTM C 928 specification for acceptance of patching mixes.

Property (A: Time dependent)	Test Specification	3 hour	1 day	7 days	28 days
Compressive strength min. (psi)	ASTM C39/C109				
R1 concrete/mortar		500	2000	4000	
R2 concrete/mortar		1000	3000	4000	
R3 concrete/mortar		3000	5000	5000	
Bond strength min. (psi)	ASTM C882				
R1, R2, R3 concrete/mortar			1000	1500	
Length change based on	ASTM C157				
3 hour length (% change)					
Max increase in water @ 28 days					0.15
Max decrease in air @ 28 days					-0.15

Property (B: Time independent)	Test Specification	Consistency	
Consistency of concrete/mortar	ASTM C143	R1 consistency 15 minutes after mixing liquid is added	R2 and R3 consistency 5 minutes after mixing liquid is added
Slump of concrete (in)		3	3
Flow of mortar (%)		100	100
Scaling resistance to deicing chemicals after 25 cycles of freezing and thawing	ASTM C672	Concrete: Max visual rating of 2.5 Mortar: Max scaled material of 1 lb/ft^2	

Other very important material properties are only recommended by ASTM C 928 and MnDOT, not required. These include, set time, coefficient of thermal expansion and freeze-thaw resistance. MnDOT

standard construction specifications reference the pre-bagged patch mix grade 3U18. This mix is only specified for mix proportions and aggregate gradation. Other DOT's also rely on the ASTM C 928 specification for purposes of material acceptance. In South Dakota another requirement for patching materials is that the concrete mix design must reach 4,000 psi within 6 hours. Ziegler and Levi recommended that all spall repairs must be conducted when the air temperature is above 40 °F (2008). The NDDOT specifies a maximum water content and minimum placing temperature. The specification also lists AASHTOM-85 high early strength cement (Type III) for spall repairs (Ziegler and Levi, 2008). Iowa DOT requires a maximum slump of 4 inch as well as 6.5% air entrainment. The specification does not require a minimum working temperature but instead requires the patching material to be at least 65 °F prior to placement. Table 3 lists the additional requirements of Minnesota's bordering states for partial-depth repairs.

Table 3: Additional requirements by state

State	Additional requirements to the ASTM C928 specification
Iowa	• Maximum slump of 4” • 6.5% air entrainment • No minimum air temperature but does requires the mix to be at least 65° F prior to placement
Michigan	• Has no specification for partial-depth repair
North Dakota	• Maximum water content values given in a table • Minimum air temperature 40° F • Specifies ASTM M-85 high early cement for spall repair
South Dakota	• Materials must reach 4000 psi @ 6 hours • Spall repair to be done above 40° F
Wisconsin	• Follows ASTM C928 with no additional requirements

Several research studies have also focused on comparative evaluation of various CPR materials. Factors such as cost, workability and durability are often used as evaluation parameters for making recommendations regarding the material selection. Several products were tested in each of the previous research project. Different types of rapid set cementitious materials were considered. These include dry mix PCC concrete, magnesium phosphate cement, polymer concrete and polymer modified concrete (Cervo and Schokker, 2008, Markey et al., 2006, Good et al., 1993, Platte et al., 2009). The most common concrete mix in previous studies is based on the Type III Portland cement. Magnesium Phosphate has been used to accelerate set times and lower the permeability of the concrete (Cervo and Schokker, 2008). Polymer concrete is a composite mixture in which a polymerization of a monomer produces the bond between the cement and the aggregate added to the patch mixture. Polymer modified concrete is different in the fact that the synthetic polymer only replaces a portion, 10-15%, of the binding agent in Portland cement (Cervo and Schokker, 2008). The previous research studies that undertook laboratory tests on the CPR products typically included: compressive strength, flexural strength, set time, freeze-thaw resistance, abrasion resistance, and length change resistance measurements.

The literature review also found three major field studies. The field study research was conducted in regions where the climate is warmer than that found in Minnesota. A study by the National Transportation Product Evaluation Program (NTPEP) was performed on a bridge deck in Ohio testing six different products (Platte et al., 2009). The Strategic Highway Research Program (SHRP) set up a field study covering four states: Utah, Arizona, Pennsylvania and South Carolina (Mojab et al., 1993). The Texas Transportation Institute’s (TTI) field tests were all conducted in Texas (Markey et al., 2006).

The NTPEP study tested the materials in 9 foot long by 3 foot wide by 4 inch deep patches. The edges were all saw cut with vertical interfaces. Materials included in the study are in Table 4.

Table 4: NTPEP Ohio bridge deck test materials

Manufacturer	Product name	Product type
Henkel Loctite	Fixmaster Magnacrete	Cementitious concrete
Quikrete Companies	Fastset DOT Deck repair Polymer with fibers	Polymer modified concrete
SpecChem	RepCon 928	Polymer modified concrete
W.R.Meadows	Sealtight Futura-15	Cementitious concrete
Willamette Valley Co.	FastPatch	Polymer concrete
CeraTech Inc.	Pavemend EX	Cementitious concrete

None of the products exhibited any spalling after 2 years. All of the materials showed mid-panel cracking of 1/32" except for the Willamette Valley FastPatch which had no mid-panel cracking. However the Willamette Valley FastPatch had the most edge cracking at 1/16" and showed 4% delamination. The most severe delamination occurred with the W.R. Meadows Futura-15, it was recorded at 66%.

The multistate SHRP study is one of the most extensive research projects on partial-depth patching (Mojab et al., 1993). Ten different products were used and are listed in Table 5.

Table 5: SHRP field test materials

Manufacturer	Product name	Product type
Generic	Type III PCC	Cementitious
United States Gypsum Co.	Duracal	Gypsum cement
Set Products Inc.	Set-45	Magnesium Phosphate cement
Five Star Products Inc.	Five Star HP	3 part epoxy grout
Sika Corporation	SikaPronto 11	2 part modified methacrylate
Accelerated Systems Technology Corporation	Penatron R/M-3003	2 part flexible polyurethane
Lone Star Industries Inc.	Pyrament 505	Cementitious
None provided	MC-64	2 part epoxy
GeoCHEM Inc.	Percol FL	2 part flexible polyurethane resin
Unique Paving Materials Corporation	UPM High Performance Cold Mix	Premixed bituminous

Once the patches were in place they were evaluated at 1, 3, 6, 12 and 18 months. Distresses and severity were recorded. Failure was based on the serviceability of the roadway, and is subjective (Mojab et al., 1993). The results of patch failures are in Table 6.

Table 6: Results of SHRP study

Material	% Failed
Pyrament 505	11.4
Percol FL	5.0
Set-45	4.3
Five Star HP	2.6
Type III PCC	1.2
Duracal	0
MC-64	0
SikaPronto 11	0
Penatron R/M 3003	0
UPM High Performance Cold Mix	0

The research conducted by TTI was performed in two locations across Texas; Houston and Fort Worth. Several products were used in the study (Table 7).

Table 7: Products used in the TTI field study.

Product	**Type of Material**	**Usage/ Time to Traffic**	**Storage Life (yrs)**	**Material Cost ($/cft)**
Delpatch	Polyurethane Polymer Concrete	1 hour	2	$145.00
RSP	Polyurethane Polymer Concrete	8-10 minute set time	0.5	$52.00
Wabo ElastoPatch	Polyurethane Polymer Concrete	1 hour	1	$152.00
FlexPatch (SSI)	Epoxy Polymer Concrete	1-2 hours	1	$115.00
FlexKrete	Thermosetting Vinyl Polymer Concrete	45-90 minutes	0.5	$110.00
EucoSpeed MP	Magnesium Polyphosphate	1 hour	1	$43.00
MgKrete	Magnesium Polyphosphate	30 minutes	0.5	$62.00
Pavemend 15	Magnesium Polyphosphate	1.5 hours	1-3	$90.00
Rapid Set	Hydraulic Cement	1 hour	1	$26.00
Fibrescreed	Polymer Modified Bitumen	15-60 minutes	2	$101.00

Each of the ten products involved in the TTI study were evaluated and ranked for four different variables; bond strength, cost, place ability and overall utility. The two study areas were reported separately (Table 8 and Table 9).

Table 8: Ranking of repair materials from Houston district

	Product	Bond Strength		Scores			
Rank	Matrix	Value (psi)	Adequacy	Cost	Placeability	Overall Utility	Total
1	MgKrete	250	No	9.8	4.5	7.8	7.94
2	RSP	85	No	9.8	6.5	6.8	7.93
3	Rapid Set	95	No	9.8	6.2	6.8	7.89
4	Pavemend	78	No	9.7	4.1	7.8	7.83
5	EucoSpeed	121	No	9.8	5.7	6.8	7.79
6	FlexPatch	168	No	9.7	3.9	7.8	7.77
7	Delpatch	50	No	9.6	4.1	7.8	7.76
8	FlexKrete	141	No	9.7	5.7	6.8	7.74
9	Fibrescreed	250	No	9.7	3.5	7.8	7.7
10	WaboCrete	61	No	9.5	5.7	6.8	7.68

Table 9: Ranking of repair materials from Fort Worth district

	Product	Bond Strength		Scores			
Rank	Matrix	Value (psi)	Adequacy	Cost	Placeability	Overall Utility	Total
1	EucoSpeed	121	No	9.8	6.5	6.8	7.94
2	RSP	85	No	9.8	6.5	6.8	7.93
3	Rapid Set	95	No	9.8	6.2	6.8	7.89
4	MgKrete	200	No	9.8	4.2	7.8	7.88
5	FlexKrete	141	No	9.7	5.7	6.8	7.74
6	Fibrescreed	250	No	9.7	3.5	7.8	7.7
7	WaboCrete	172	No	9.5	5.7	6.8	7.76
8	Pavemend	78	No	9.7	3.2	7.8	7.67
9	Delpatch	91	No	9.6	3.5	7.8	7.65
10	FlexPatch	108	No	9.5	3.2	7.8	7.63

Tests and Standards for Concrete Patching Materials

Current ASTM C 928 specifications require rapid set cementitious materials to pass certain criteria. The five criteria that are required include minimum compressive strength, bond strength, aversion to length change, consistency and scaling resistance. All of the products in this study were tested to measure these quantities. In addition, other criteria were also considered during this study. These include sulfate resistance, modulus of elasticity measurement, coefficient of thermal expansion and abrasion resistance.

Research Approach

The goal for the project was to develop a list of tests for the acceptance of rapid set cementitious materials used for partial-depth repair. The basic approach was to conduct all currently required laboratory tests as well as all recommended laboratory tests prescribed in the ASTM C928 on a

predetermined study group of patching materials. In addition to these tests there were others that were developed by the research staff in conjunction with the technical advisory panel.

The data from all of the tests was analyzed to determine which tests produced the most useful results for cold climate consideration.

Chapter 3:
Testing Procedures and Methodology

Procedures and Methods used in Task 2 of the Study

The phase one tests conformed to the ASTM C928 standard specification for testing rapid set materials. The tests and their corresponding ASTM designations are located in Table 10.

Table 10: Properties evaluated and preliminary test methods for Task 2

Property	Preliminary Test Method
Set time	ASTM C191 – Standard Test Method for Time of Setting of Hydraulic Cement by Vicat Needle
Strength gain	Time interval testing (3 hours, 24 hours, 7 days and 28 days) using ASTM C 39 – Standard Test Method for Compressive Strength of Cylindrical Concrete Specimens
Flexural strength	ASTM C78 – Standard Test Method for Flexural Strength of Concrete (at 4 hours)
Shrinkage	ASTM C490 - Standard Practice for Use of Apparatus for the Determination of Length Change of Hardened Cement Paste, Mortar, and Concrete
Bond strength	Modified version of ASTM C900 – Standard Test Method for Pullout Strength of Hardened Concrete
Freeze-thaw durability	ASTM C666 - Standard Test Method for Resistance of Concrete to Rapid Freezing and Thawing

Setting Time

The ASTM C191 is the standard test of setting time for hydraulic cement using the Vicat Needle apparatus. The testing of set times is crucial for determining the working time of concrete (Koehler and Fowler, 2003). The Vicat needle setup pictured meets ASTM specifications. (Figure 1)

Figure 1: Vicat needle apparatus

Strength Gain

Compressive strength gain measurements were obtained using the ASTM C39 standard test. The tests were conducted at time intervals of 3 hours, 1 day, 7 days and 28 days. (Figure 2)

Figure 2: Compression Test Setup

Flexural Strength

The flexural strength was determined using the ASTM C78 test. The test was performed at 4 hours after casting of specimen. The result is the modulus of rupture which is an indicator of the flexural strength.

Figure 3: Third-point Bending Test Fixture in Compression Frame

Length Change

Shrinkage testing was done using the ASTM C490 standard. Samples are cast in 2 inch by 2 inch by 11 inch prisms and then measured at 2 hours and 28 days to determine the amount of length change that they undergo in that time frame. Length change is important because it can directly affect the bond between the patch and the pavement slab. The more a material shrinks or expands the more potential for the patch to fail due to breaking of the bond interface.

Figure 4: Length change measuring device with the standardized bar and test specimen

Freeze Thaw / Durability Factor

The ASTM C666 test for rapid freeze-thaw is a cyclic test to measure durability of the material in cold climates. Data from this test indicates how resistant the concrete material will be to rapid temperature swings in the field. Considering the climate in Minnesota the need for this test is apparent.

Figure 5: Freeze-thaw chamber and digital control box

Modified Bond Strength Test

The bond strength is the only test performed for task two that deviates from the ASTM C928 specification. The test to be used in our lab is an adaptation of the ASTM C900 pull out test. An adaptation was made because the ASTM C900 is a test of the pullout strength of a homogenous section of concrete and is generally intended for testing anchorages.

Figure 6: Bond pullout testing fixture in the MTS machine

A rendering of the specimen to be used for the adapted test is shown in Figure 7. Results from this test are qualitative and used for comparison purposes only. The values obtained are not an indicator of the longevity of the patching material.

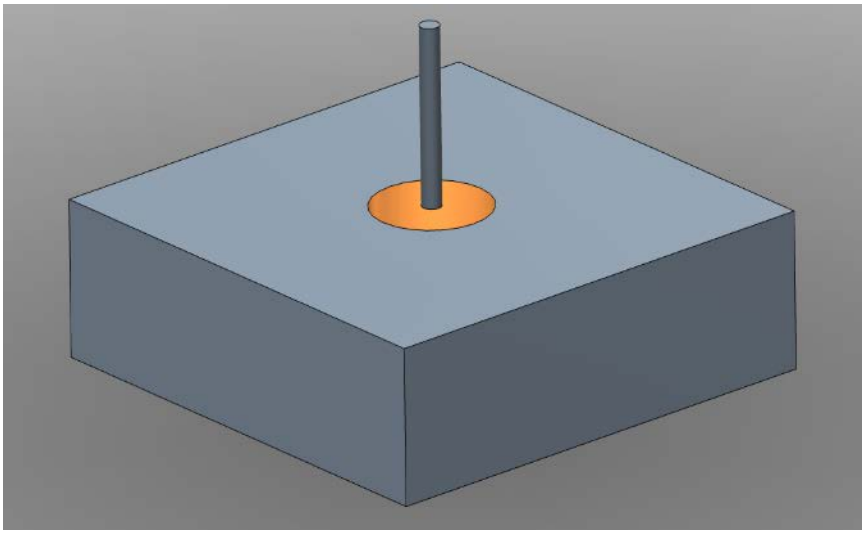

Figure 7: Pull out specimen schematic

Procedures and Methods used in the Task 3 of Study

The second phase tests primarily conformed to the ASTM C928 standard specification for testing rapid set materials. The tests and their corresponding ASTM designations are located in Table 11.

Table 11: Properties evaluated and preliminary test methods for Task 3.

Property	Preliminary Test Method
CoTE	ASTM C531—Standard test method for Linear Shrinkage and Coefficient of Thermal Expansion of Chemical-Resistant Mortars, Grouts, Monolithic Surfacings, and Polymer Concretes
Modulus of Elasticity	ASTM C 469 – Standard Test Method for Static Modulus of Elasticity and Poisson's Ratio of Concrete in Compression
Abrasion Resistance	ASTM C418 – Standard Test Method for Abrasion Resistance of Concrete by Sandblasting
Length Change in Sulfate	ASTM C1012 - Standard Test Method for Length Change of Hydraulic-Cement Mortars Exposed to a Sulfate Solution
Scaling Resistance	ASTM C672 – Standard Test Method for Scaling Resistance of Concrete Surfaces Exposed to Deicing Chemicals
Slant Shear Bond Test	ASTM C882 – Standard Test Method for Bond Strength of Epoxy-Resin Systems Used With Concrete By Slant Shear (Performed at Villanova University)

Coefficient of Thermal Expansion

The ASTM C531 is the standard test used to determine the coefficient of thermal expansion (CoTE). The CoTE is a property that quantifies how much a material expands and contracts during temperature fluctuation. This information is imperative when considering materials that will be used in colder climates. The test involves casting samples in 1 X 1 X 11 inch prism molds (Figure 8), and then measuring the samples at 73°F. Once that is done the samples are heated to 210°F and another length measurement is recorded. The difference in the two measured lengths at a given temperature variation leads to the calculation of the CoTE. The CoTE (k) can then be used in the formula for thermal deformation, $\Delta D = L_0 * k * \Delta T(°F/°C)$.

- ΔD is the calculated change in length
- L_0 is the initial length of the specimen
- k is the CoTE
- ΔT is the change in temperature

Figure 8: CoTE molded specimens.

Modulus of Elasticity

The ASTM C469 covers the modulus of elasticity (*E*) and Poisson's ratio. For the purposes of this study only the modulus of elasticity was determined. Modulus of elasticity measures a material's stiffness by comparing the stress over a body versus the strain on that body.

The quantity is a measure of the stiffness only while a material is within the elastic region, before any permanent deformation occurs. The units for strain are length/length and therefor cancel out of the modulus ratio.

The apparatus for determining the modulus of elasticity is used in a compression frame and measures deflection of a cylinder (Figure 2).

Figure 9: Modulus of elasticity apparatus with dial gage.

Abrasion Resistance

The abrasion resistance testing follows the ASTM C418 specification. The specification calls for a sandblaster to be used on a concrete specimen at a distance of 3 inches for the duration of one minute.

This creates a concave hole in the surface of the specimen. The abrasion coefficient, A_c, is calculated by dividing the volume of the void by the area that was abraded. This study used fine silica sand of a known density to determine the volume of the voids.

Abrasion resistance is an important property to consider when choosing patching materials for use in colder climates. The pavements in colder regions have to cope with not only everyday traffic abrasion but also with the direct contact of steel from snow plows.

Cylindrical specimens were used for this test with 4 inch diameter and 4 inch length (Figure 10).

Figure 10: Abrasion resistance sample cylinder.

Length Change in Sulfate

The ASTM C1012 specification measures the length change of a 2 X 2 X 11inch prism shaped specimen (Figure 11). This assesses the products resistance to a sulfate solution; the solution contains 50 grams of sodium sulfate (Na_2SO_4) per liter of water. Specimens are stored in an airtight container filled with the solution and measured at prescribed time intervals; 1, 2, 3, 4, 8, 13, and 15 weeks.

Figure 11: Length change in sulfate specimen mold.

Scaling Resistance to Deicing Chemicals

Due to the colder climate, highways in Minnesota are exposed to large quantities of deicing chemicals each year. The ASTM C672 test procedure was chosen for this reason to evaluate the effects of deicing chemicals on the patching mixes. This test submerges the surface of the specimen in a solution of calcium chloride and water. At prescribed times the surface is visually rated on a scale from 0 to 5.

- Zero – No scaling
- 1 – Very slight scaling, no coarse aggregate visible
- 2 – Slight to moderate scaling
- 3 – Moderate scaling, some coarse aggregate visible
- 4 – Moderate to severe scaling
- 5 – Severe scaling, coarse aggregate visible over the entire surface

The specimen is subjected to a freezing cycle for 16-18 hours followed by a 6-8 hour thawing period, once every 5 cycles each specimen is washed and rinsed to be visually rated before undergoing more cycles. The entire test lasts for a total of 50 cycles. Specimens are cast at a depth of 3 inches and must have the ability to contain the deicing solution on their surface (Figure 12).

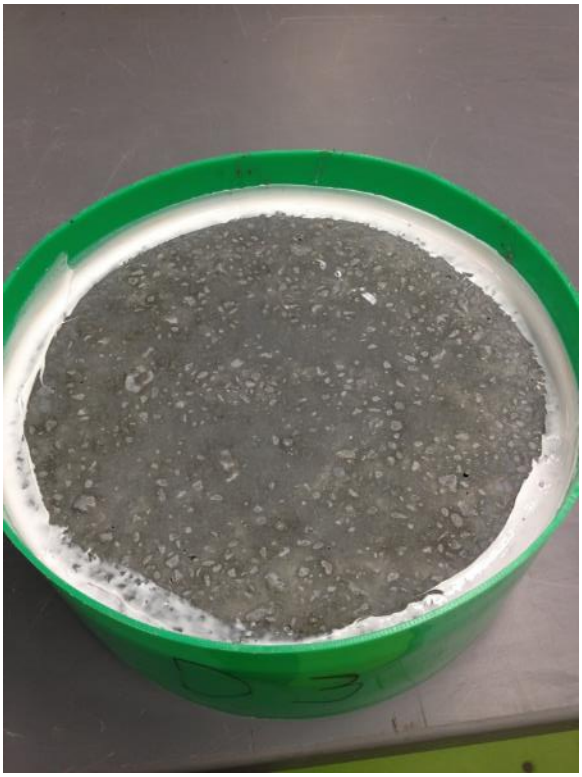

Figure 12: Scaling resistance to deicing chemicals specimen.

Slant Shear Bond Test

The ASTM C882 slant shear test is used extensively for bond strength (Pattnaik, 2006). The test was found to not be repeatable on a regular basis. Several of the composite cylinders tested in previous research programs did not break along the slanted interface which led to different bond strengths for the same material (Pattnaik, 2006). The geometry of the slant shear test involves a normal force that results in higher bond strengths because some of the force exerted by the testing apparatus does not directly load the bond (Ferraro, 2008). This normal force produces a friction force that is not representative of the actual failure mechanism (Trevino et al., 2003). The schematic of the slant-shear bond test is shown in. This test was intended for testing various epoxies that can be used to bond two concrete faces to one another.

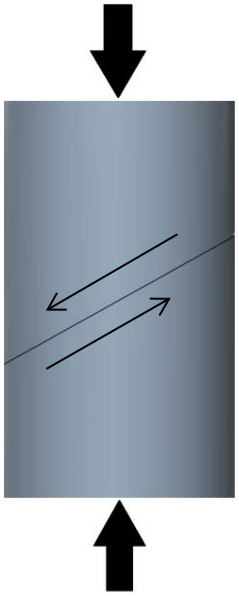

Figure 13: Schematic of the Slant Shear Bond Test.

Slant shear bond tests were conducted for this study at Villanova University under the direction of Eric Musselman. The results displayed a large variation from sample to sample. These variations ranged from 23%-55% (Figure 14).

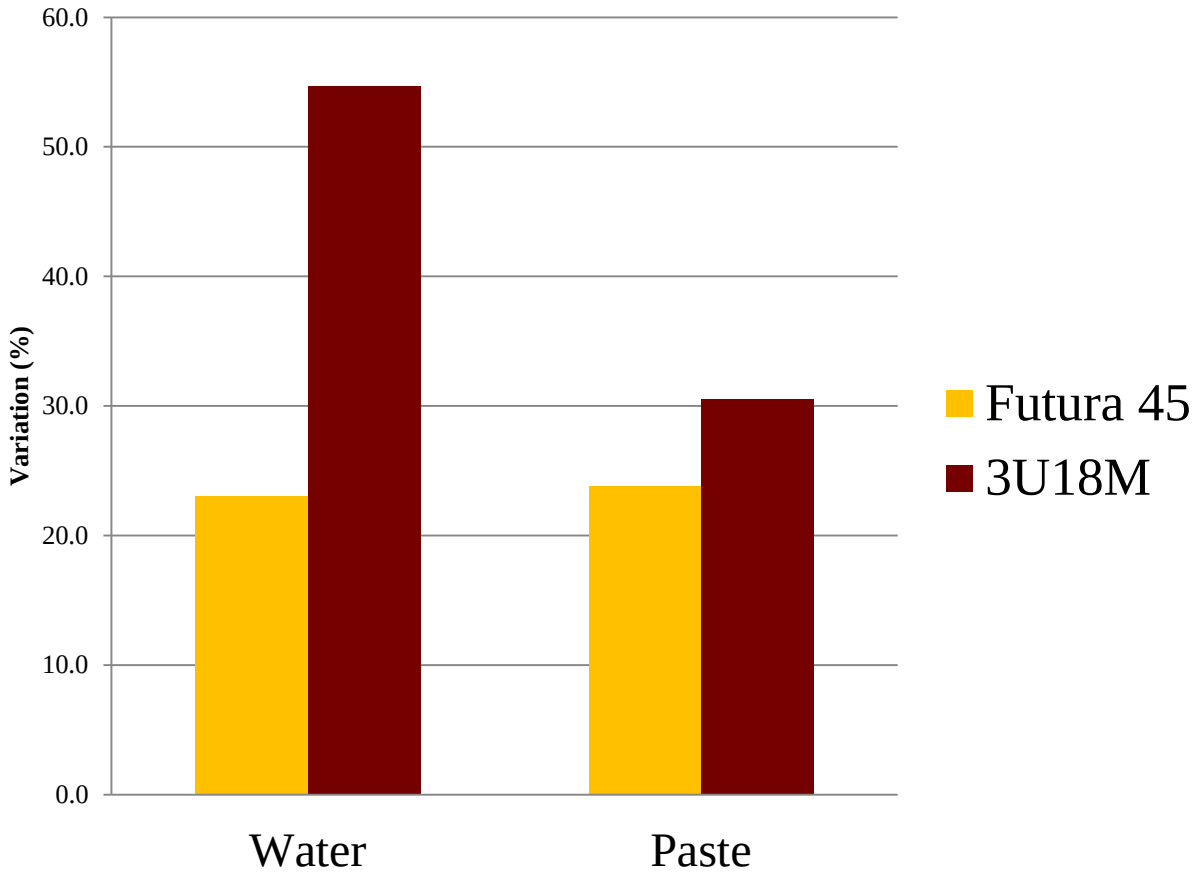

Figure 14: Slant shear variation (Panzitta & Musselman)

Previous research done at Penn State University by Cervo and Schokker also revealed a large variation of results obtained using the slant shear bond method. The data that was analyzed contained two separate testing times: 1 day and 3 days (Figure 15 and Figure 16).

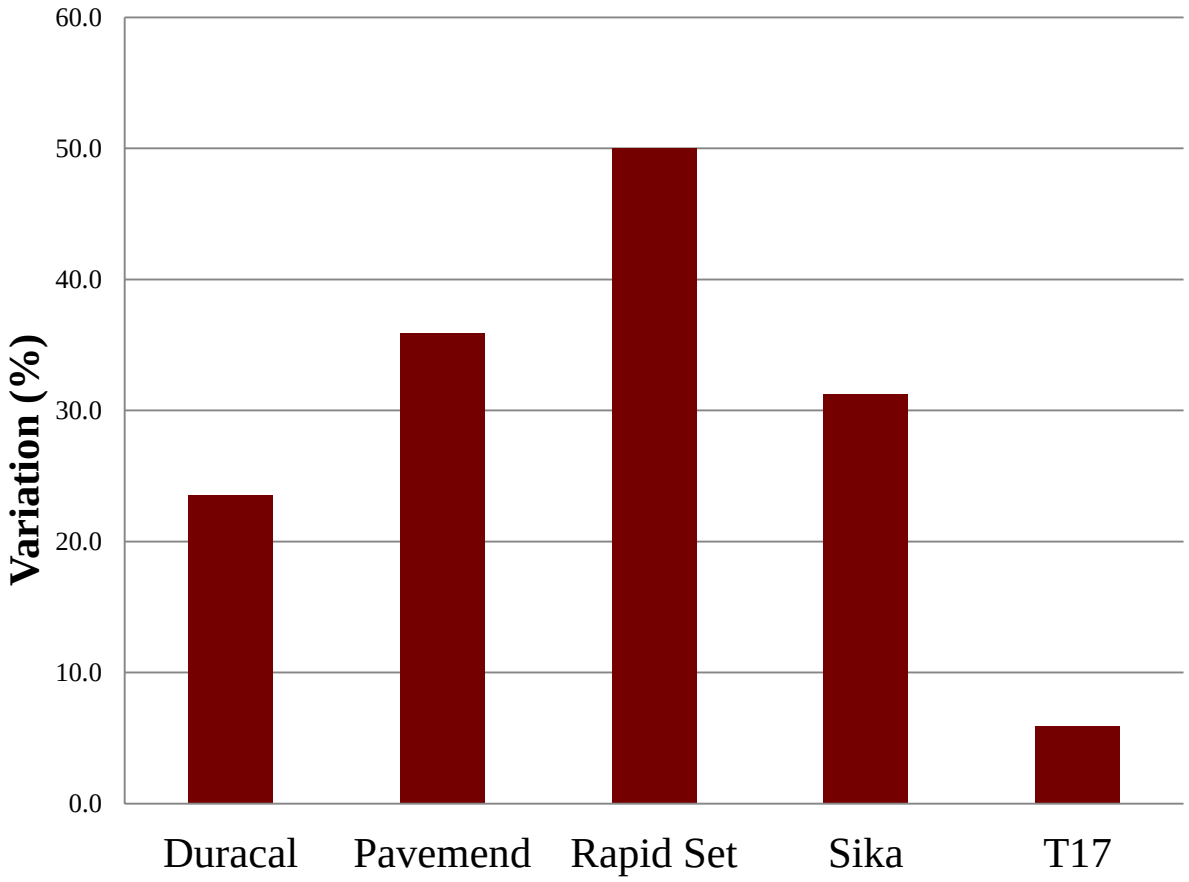

Figure 15: One day average variation of three replicate samples tested by Cervo and Schokker.

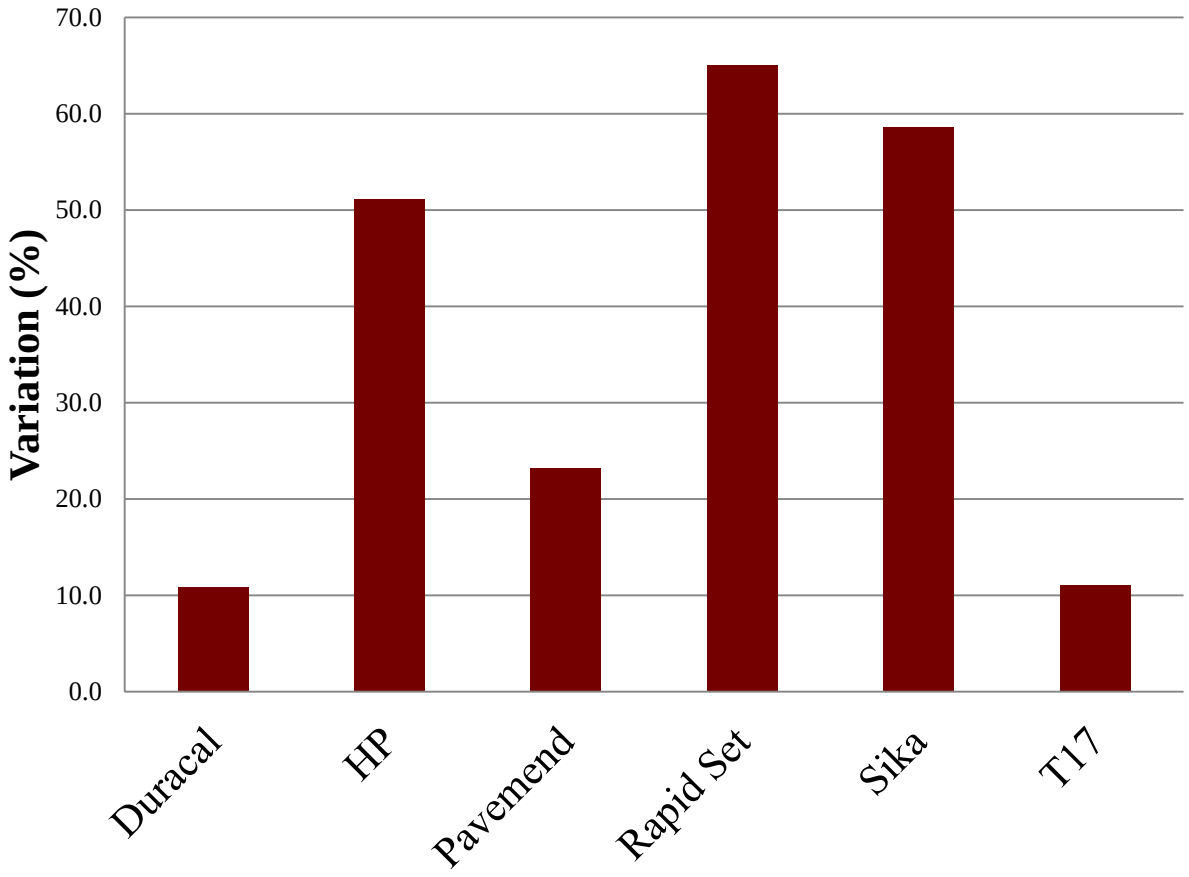

Figure 16: Three day average variation of three replicate samples tested by Cervo and Schokker.

Considering the data from previous research, the decision was made not to include the slant shear bond test in the testing regimen at the University of Minnesota Duluth.

Procedures and Methods used in the Task 4 of Study

University of Minnesota Duluth Testing

The pop-out bond test involved the casting of representative pavement slabs. The data collected during the test was empirical and was used for comparison purposes only. The slabs were 45 X 24 X 7 ½ inches in size. Once the slabs had cured completely a partial-depth repair milling machine was used to make a groove in the center of each slab (Figure 17).

Figure 17: Pavement milling machine used to groove test slabs.

The grooved areas were approximately 18 X 15 X 2 ¾ inches in size (Figure 18). The grooving head produced a hole with a sidewall that measured between 70 and 90 degrees, steeper than is allowed. A 15 pound jack hammer was used to slope the sidewalls to fall into MnDOT patching specifications, 30-60 degrees. The patch area preparation then followed current construction guidelines and were sandblasted to create a micro textured surface.

Figure 18: Test slabs containing partial-depth simulated repair areas.

After the grooving and sandblasting operation was complete a walk behind concrete saw was used to cut the slabs into two pieces longitudinally. This was done so that there would be an exposed edge of the patching material; this simulated the condition of actual patches in the field (Figure 19).

Figure 19: Slab after being cut longitudinally to expose the patch material edge.

Prior to casting the patch material the slabs were set up with a bond breaker similar to what is used in the field (Figure 20). This was done to simulate field conditions as closely as possible.

Figure 20: Half slab ready to have patching material added.

The flexural test was performed on the half slab specimens by supporting them at either end with the patch facing downward (Figure 21). A simple third point bending set up was used for the test. The specimen was placed into an MTS loading frame, this allowed a precise data acquisition of load and deformation (Figure 22).

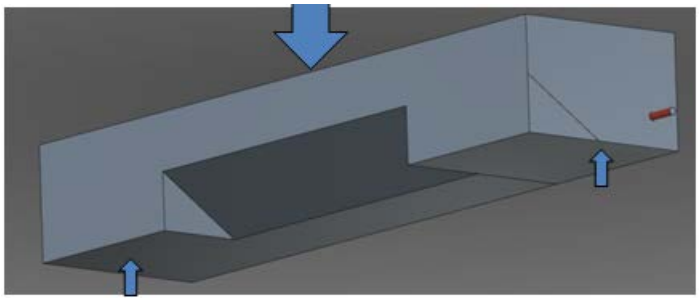

Figure 21: Half slab test schematic

Figure 22: Half slab in the MTS loading frame

Villanova University Testing

The testing completed at Villanova University focused on the bond behavior of partial-depth patching materials. The primary focus of the testing program was the evaluation of slab samples with both milled and saw cut and chipped patches. A detailed description of the testing program can be found in Appendix D, with a brief summary provided here.

The slabs being patched had dimensions equal to 24” X 47” X 7 1/8”, and were reinforced with 4 - #4 bars as shown in Figure 23. The concrete used to cast the slabs had 28 day strength of 6,500 psi. Patches were either saw cut and chipped or milled using a milling attachment for a skid steer, with the patch located at the center of the slab to a depth of approximately 3 inches. Other variables examined in the testing program in included the surface preparation (water or cement slurry) and the patching material (District 3 modified 3U18 or Futura 45).

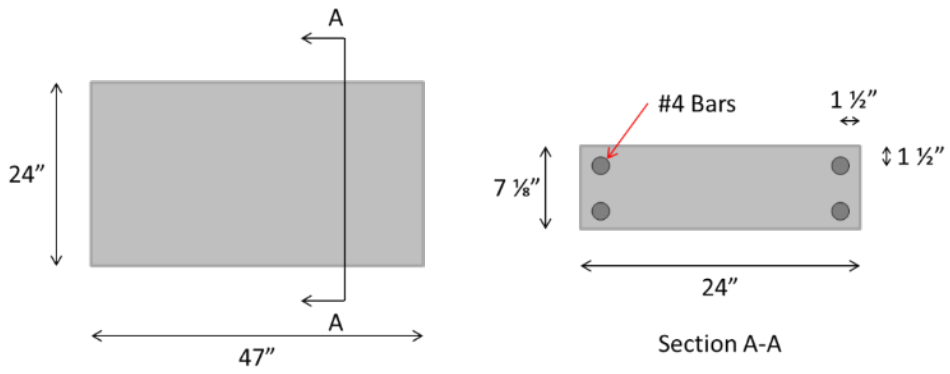

Figure 23: Villanova Slab bending specimen dimensions

The slabs were placed into the test setup shown in Figure 24, and loaded using a computer controlled, servo-hydraulic actuator. The slabs we loading using either a monotonic load, or a cyclical load consisting of 1,000 cycles at multiple displacement amplitudes that increased as the test progressed. Strain gages were placed at 3 locations on the patch for samples tested under cyclical loads to help indicate when bond loss between the patch and slab occurred. In addition to the strain data, the applied load and deflection of the actuator were also recorded.

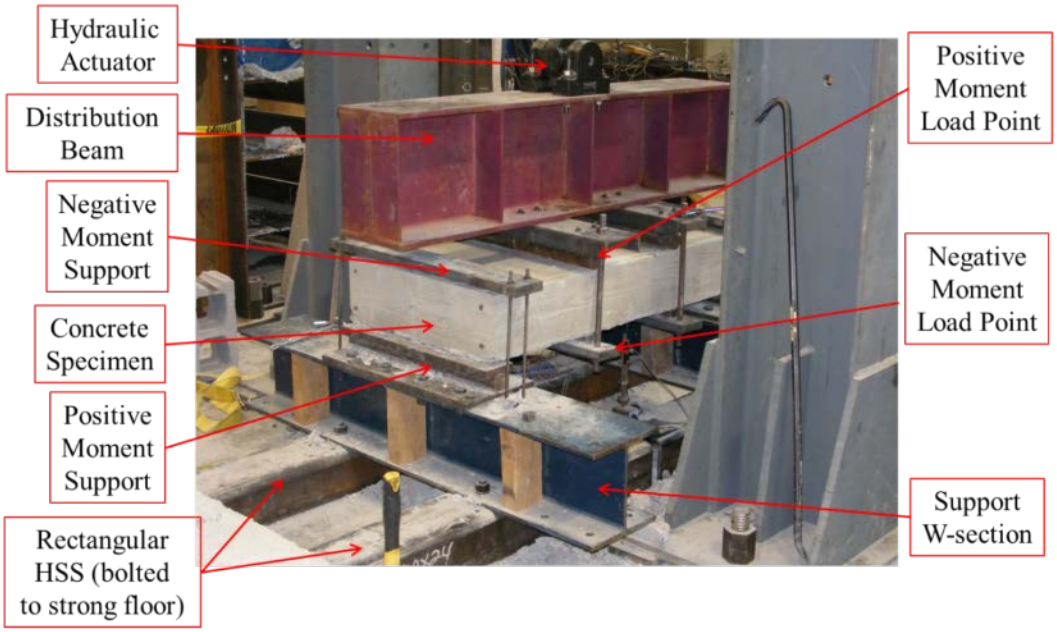

Figure 24: Components of slab bending load apparatus

Laboratory Mixing and Specimen Preparation

Mixing instructions for each product were provided from the manufacturers or developers. All specified gradations, proportions and water amounts were adhered to closely. The extremely rapid setting materials were mixed using a drill and paddle in five gallon buckets. These products included: Pavemend SL, Pavemend SLQ, Mono Patch and Futura-15. The remaining materials were mixed in a small concrete drum mixer.

Figure 25: Drill and paddle with a bucket and a standard concrete mixer

The materials were comprised of both proprietary mixes and mixes that required additional proportioning. Items listed as 1 and 7-13 (Page 2) were all proprietary and only required the addition of water. Materials listed 2-6 (Page 2) are bagged as cementitious materials and required admixtures as well as additional aggregates. Water was the primary fluid used as the hydrator, however the TCC Taconite mix came with a manufacturer provided activator liquid. Admixtures included super plasticizer/accelerator and air entrainment liquids. The aggregate used for the MnDOT District 3 mixes was provided by MnDOT District 3. The 3U18M, Akona Rapid Patch and the Five Star were extended using locally sourced aggregates. The gradation of the local coarse aggregate is CA-5.

The concrete used for the task four representative roadway slabs met the required MnDOT specifications. This mix was ordered from an approved concrete contractor, “Arrowhead Concrete Works” for the testing at UMD, and JDM Materials for the testing at Villanova.

Chapter 4:
Phase 1 Testing Results and Discussion (Task 2)

Compressive Strength Gain

The data in Figure 26 represents the compressive strength of each mix at 3 hours, 1 day, 7 days and 28 days on a log scale axis. Take note that the majority of the mixes that started towards the low end of the scale made large gains over time. These mixes are the products that are Type III cement based. Also note that the products that achieved a high early strength did not increase greatly in magnitude over time.

When Portland cement concrete goes through the hydration process it forms crystals which ultimately give the concrete its strength. This can be thought of as a bond matrix. The patching materials that have very rapid strength gain hydrate more quickly and therefor develop a shorter bond matrix. Because of this the ultimate compressive strength gain will be lower than the products that require more time to hydrate.

Considering the ultimate compressive strength as a measure of the quality of a patching material can be misleading. A patch material that reaches a compressive strength sufficient enough to support traffic is the goal.

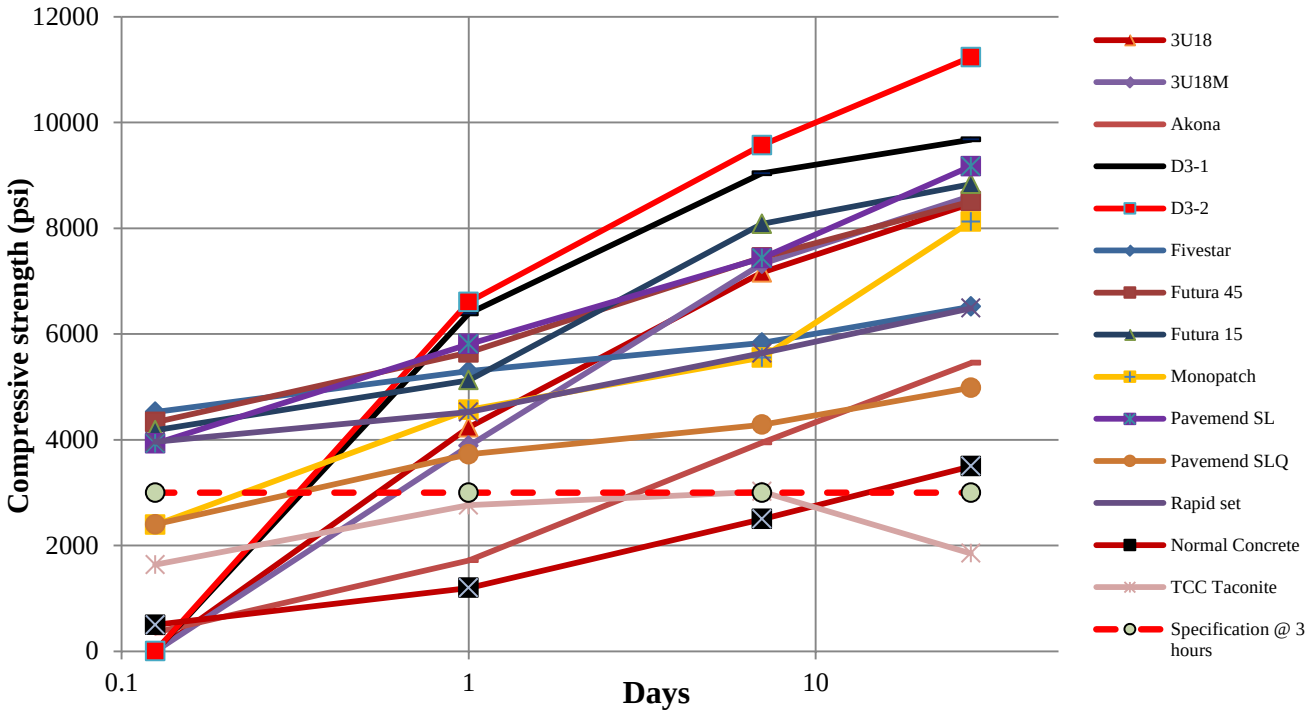

Figure 26: Compressive strength gain results

The values in Table 12 are ultimate compressive strengths and corresponding strengths expressed as a percentage of the ultimate strength.

Table 12: Compressive strength gains at 3 hour, 1 day and 7 day (expressed as percent of 28 day compressive strength)

Product	28 Day Comp (psi)	3 Hour (% of 28 Day)	1 Day (% of 28 Day)	7 Day (% of 28 Day)
3U18	8463	-	50.0	84.6
3U18M	8610	-	45.1	85.1
Akona	5454	6.5	31.5	72.4
District 3 Mix 2	11236	-	58.8	85.2
District 3 Mix 1	9677	-	66.0	93.4
Five star	6518	69.5	81.3	89.5
Futura 15	8838	47.3	58.0	91.5
Futura 45	8509	50.9	66.4	87.5
Mono Patch	8126	29.4	56.2	68.4
Pavemend SL	9172	42.8	63.4	81.1
Pavemend SLQ	4985	48.2	74.7	86.0
Rapid Set Concrete Mix	6488	61.1	69.8	86.9
TCC Taconite	1852	88.4	149.0	163.0

Flexural Strength/ Modulus of Rupture

The flexural strength measurement was recorded at 4 hours. The data in Figure 27 indicates that most of the products do not meet or exceed the modulus of rupture for normal concrete; however the concrete reading on this plot was measured at 28 days. Eight of the mixes reach at least 50% of the flexural strength of cured concrete in 4 hours.

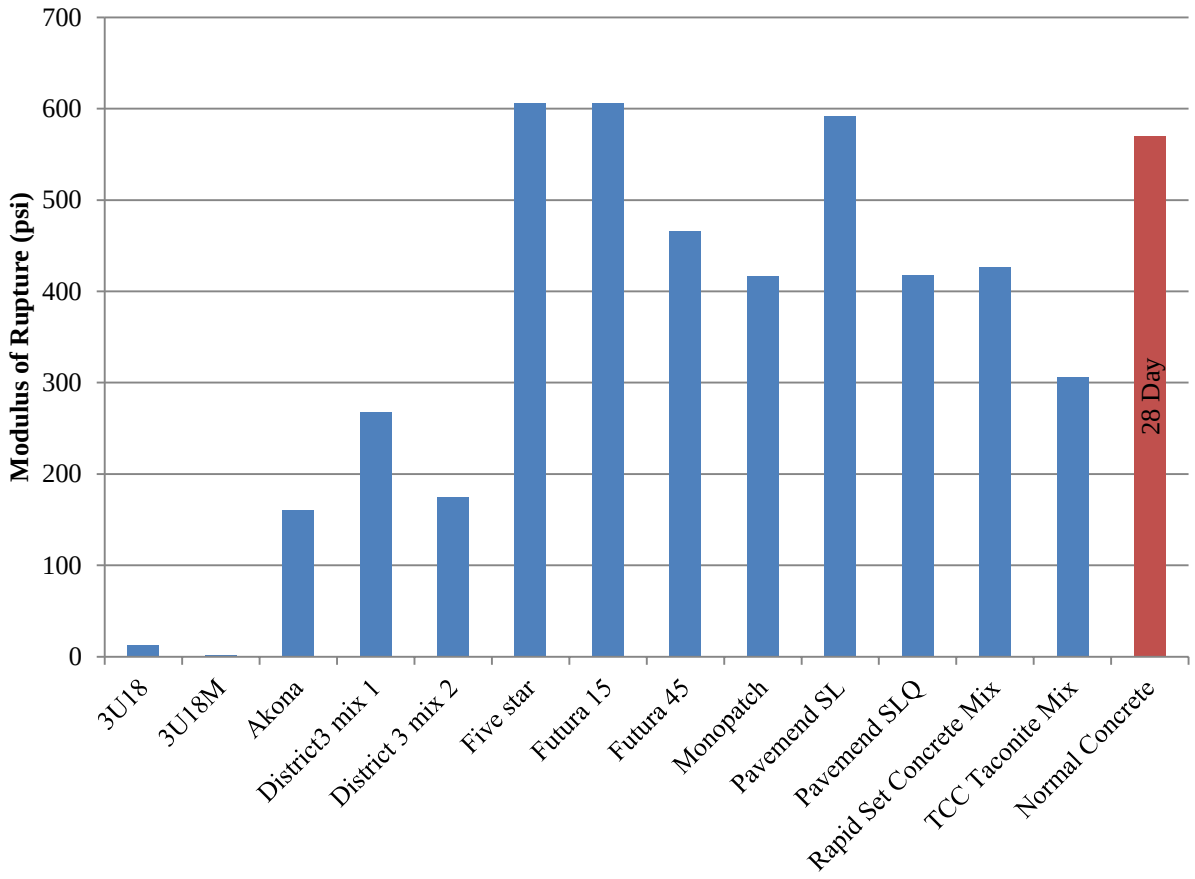

Figure 27: Measured modulus of rupture (Flexural strength)

An estimation of the modulus of rupture from the compressive strength is presented in Table 9. The estimation formula, $M_R = k\sqrt{f'c}$, was used for the calculations. The *k* is a multiplication factor that ranges from 7.5 to 10 (Mamlouk and Zaniewski, 2011, page 293). The *f'c* term is the compressive strength of the material. The minimum value in Table 9 was calculated using *k* = 7.5 and the maximum was calculated using *k* = 10.

The estimation formula method was unsuccessful for two of the products; Futura 45 and Rapid Set Concrete Mix. Four products could not be estimated as they had no measurable compressive strength at 3 hours.

Table 13: Estimation of the modulus of rupture

Material	Modulus of Rupture (psi)		
	Estimated value		Measured value
	Min	Max	
3U18	-	-	13
3U18M	-	-	0
Akona	141	188	160
District 3 Mix 1	-	-	268
District 3 Mix 2	-	-	175
Five star	505	673	606
Futura 15	485	646	606
Futura 45	494	658	***466***
Mono Patch	367	489	417
Pavemend SL	470	627	592
Pavemend SLQ	368	490	418
Rapid Set Concrete Mix	472	630	***426***
TCC Taconite	303	430	306

Setting Time

The setting time is an important variable to consider for choosing a rapid patch material when considering the amount of time required for opening a lane to traffic. The testing of set times is crucial in for determining working time of the concrete (Koehler and Fowler, 2003). This variable is not an indicator of overall patch performance or the longevity for a patch. Results from the actual tests can be found in Figure 28.

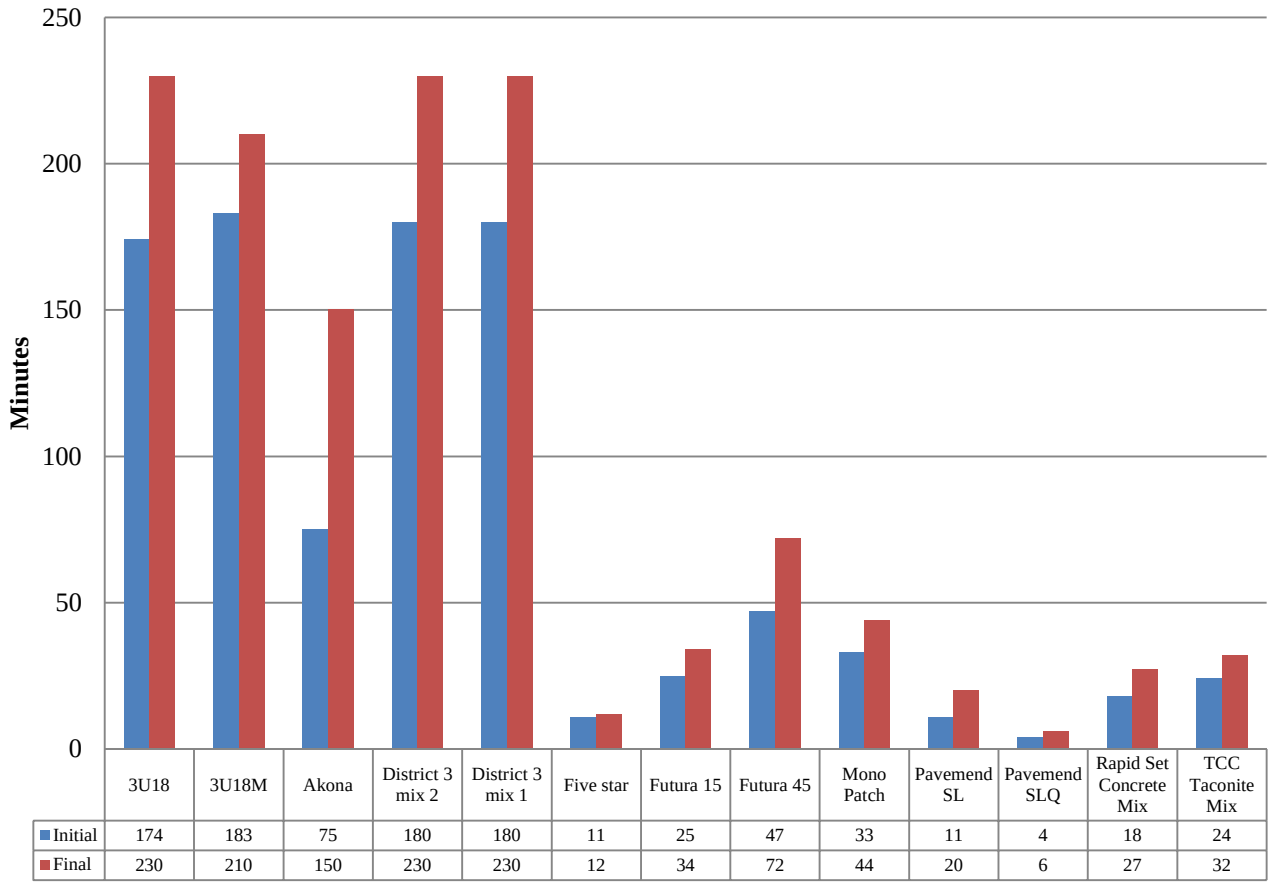

	3U18	3U18M	Akona	District 3 mix 2	District 3 mix 1	Five star	Futura 15	Futura 45	Mono Patch	Pavemend SL	Pavemend SLQ	Rapid Set Concrete Mix	TCC Taconite Mix
Initial	174	183	75	180	180	11	25	47	33	11	4	18	24
Final	230	210	150	230	230	12	34	72	44	20	6	27	32

Figure 28: Setting times

Freeze-thaw durability

The freeze-thaw durability of concrete and mortars are typically expressed by a durability factor. The freeze thaw durability contains two different extremes as can be seen in Figure 29. The overall trend is a durability factor between 15 and 25. Three of the products performed very well in comparison to the others. Theoretically the durability factor should not be over 100. The Pavemend SLQ finished over 100 which indicated that it cured significantly after being placed into the freeze thaw chamber. The materials were placed into the chamber after curing for 14 days as per the ASTM C666 specification.

*Note that the normal concrete durability factor was measured on a sample that had 5.5% air entrainment.

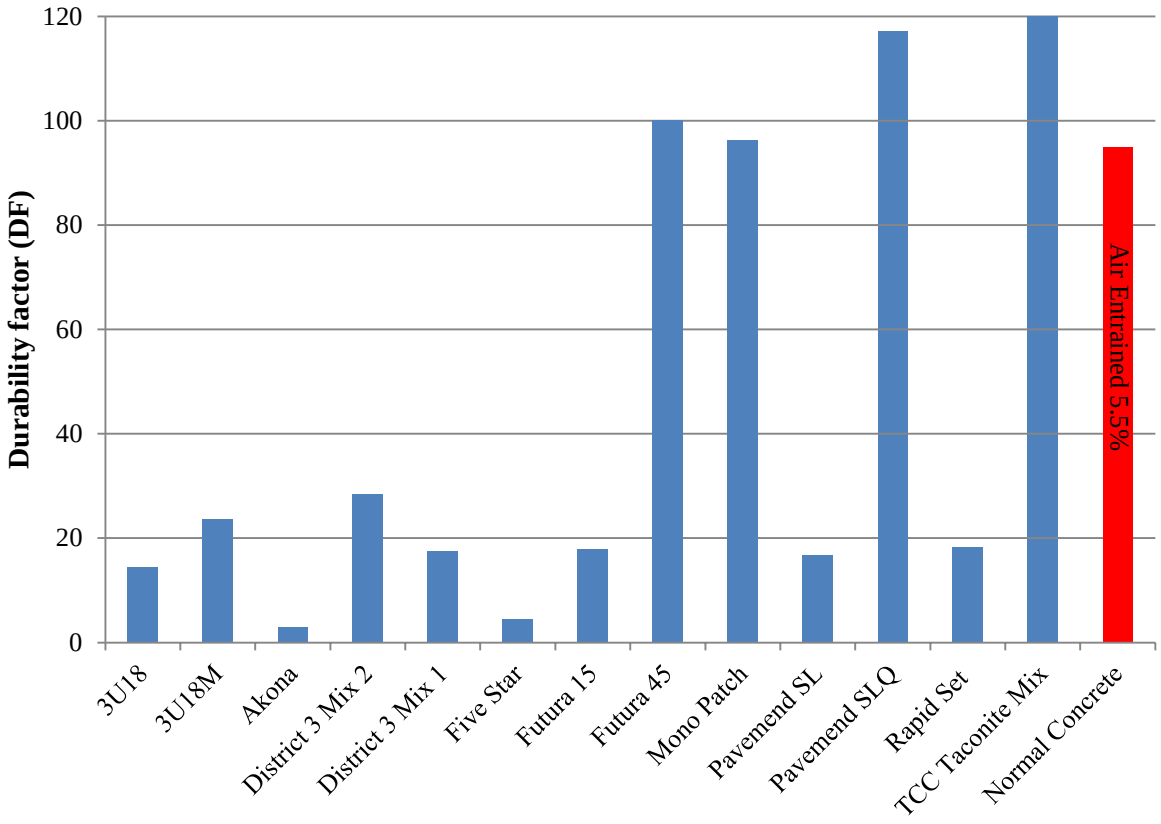

Figure 29: Freeze-thaw durability factors

A plot of the change in the relative dynamic modulus (RDM) compared to the number of cycles shows how the dynamic modulus changed over time (Figure 30). Each cycle in the freeze thaw chamber represents approximately 3 hours. During the 3 hour cycle the specimen is heated to 4°C and then cooled to -18°C.

The RDM is a measure of the current dynamic modulus compared to the material's initial dynamic modulus. The results of the freeze thaw test show the ability of a material to retain its dynamic modulus. This is NOT an indicator of which material has greater or lower modulus than the others.

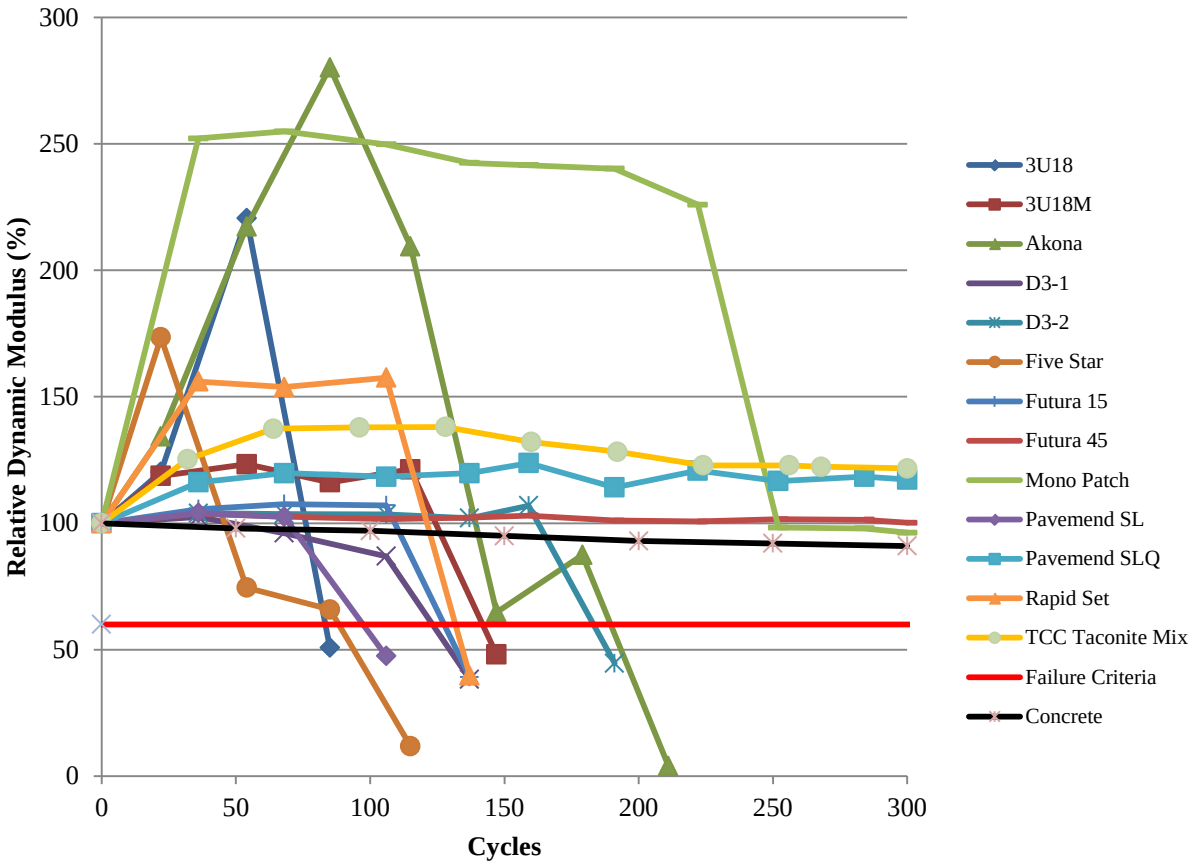

Figure 30: Fluctuation of the RDM vs. the number of cycles spent in the freeze-thaw chamber

In order to compare the actual stiffness of each material to one another the dynamic modulus must be calculated from the fundamental transverse frequency. To realize the effects of freeze thaw the dynamic modulus is plotted versus the number of cycles in Figure 31.

The data series that have black markers are the products that reached the maximum allowable number of cycles during the ASTM C666 freeze thaw test. Solid black lines indicate the four products chosen to move forward to task 3.

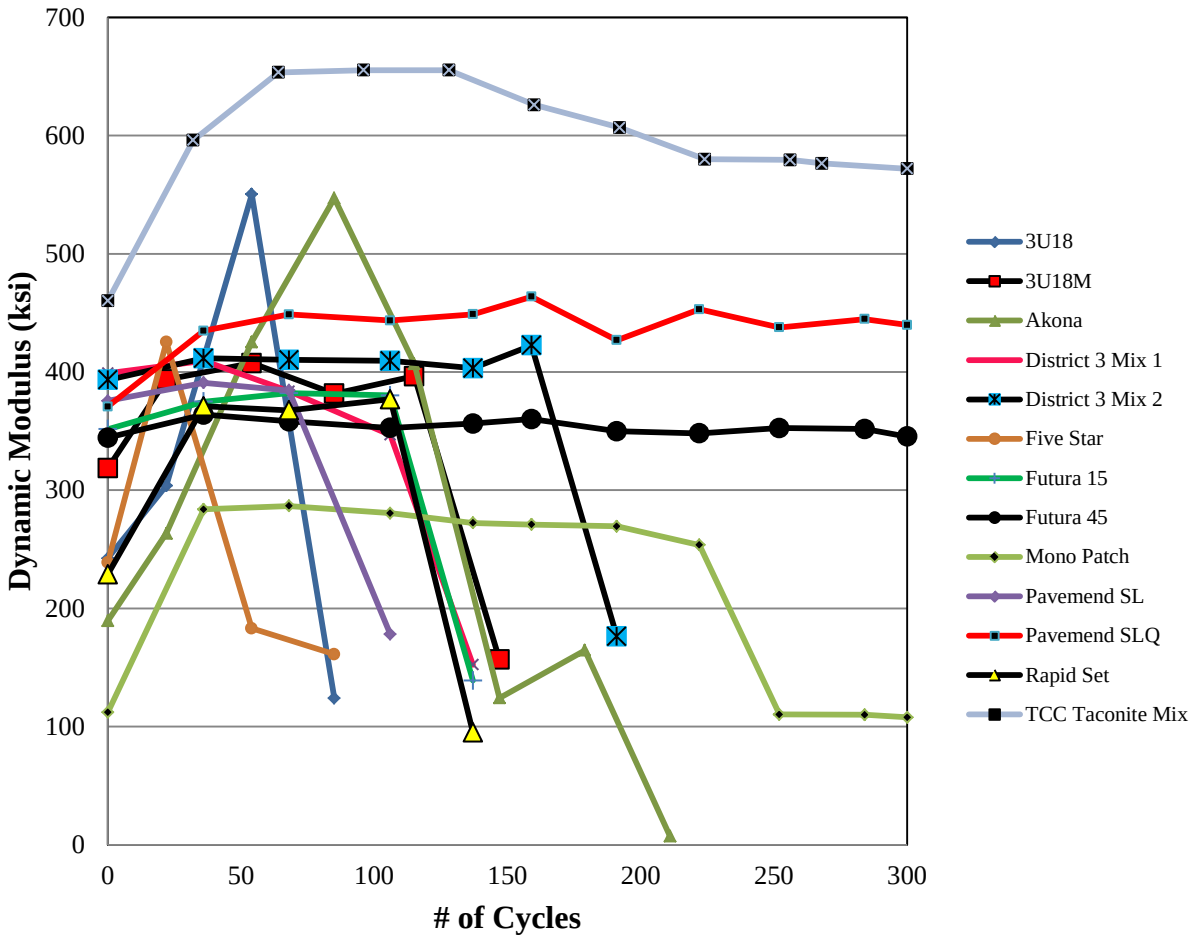

Figure 31: Dynamic modulus vs. the number of freeze thaw cycles

The change in mass of each product was also recorded (Figure 32). This measurement did not directly correlate with the RDM change for the same number of cycles. Some materials lost mass while maintaining their RDM as they went through freeze-thaw cycles. In some instances the mass loss was quite substantial. Thus, it can be summarized that the measure of material durability only in terms of RDM might be inadequate and the loss of mass should also be considered in the evaluation of patching mixes. There were materials that gained mass throughout the freeze thaw process; one theory is that those products were producing gypsum as part of the curing process.

The data for the normal concrete was obtained from a study done by the Federal Highway Administration (FHWA, 2006).

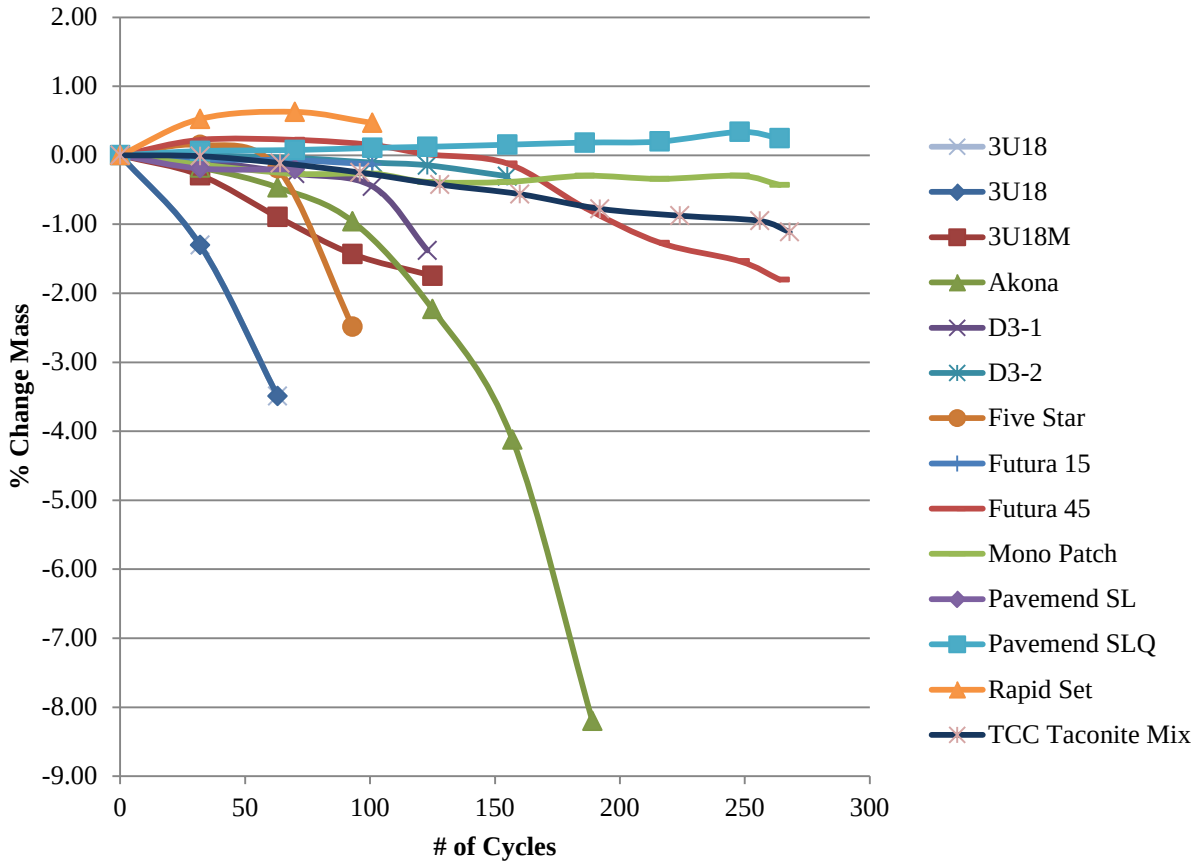

Figure 32: Percent change in mass vs. the number of cycles

Shrinkage (Length Change)

Length change yielded two unique results. There are two products that expanded while curing in air. Both of those products are magnesium phosphate based. Magnesium Phosphate has been used to accelerate set times and lower the permeability of the concrete (Cervo and Schokker, 2008). There were two products that failed to meet the ASTM C928 specification; Mono Patch and the TCC Taconite mix. Mono Patch expanded in water beyond the limit, which is shown as the black line on Figure 33. The TCC Taconite mix exhibited shrinkage in both air and water. The excessive shrinkage of TCC Taconite mix is partly due to thermal contraction of the specimen as the material hardened at relatively high temperature (approximately 130 °F). The length change in water was within the limit for this material; however the shrinkage in air could not be accurately measured due to the fact that it was no longer within the limits of the testing apparatus.

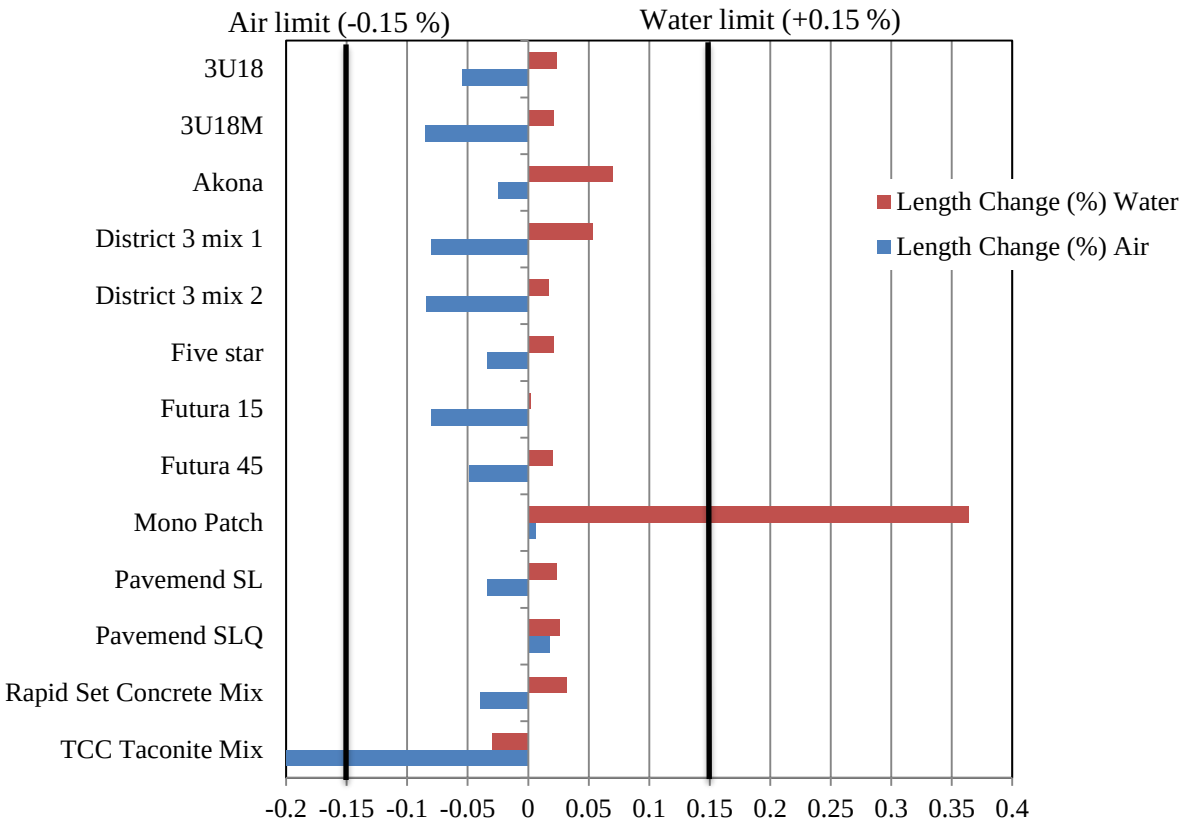

Figure 33: Length change in air and water at 28 days

Bond strength

The modified ASTM C900 bond strength test yielded results that suggest that the physical bond between the materials and the slabs is not an area of concern. Seven of the thirteen mixes developed enough load to break the slab before the bond interface failed.

The results of this test are inconclusive as to whether or not it should be added to the testing regimen for rapid set patching materials. There was a large variability in the results obtained for two separate replicate tests of the same product. The loads achieved at the initial break of either the slab or the bond interfaces are in Figure 34. Included for the purpose of comparison is a sample of normal concrete and asphalt. In general, the loads were relatively high and thus in an overall sense it can be observed that bond failure of the patching mixes in shear/sliding mode may not be of concern. A more representative bond evaluation of the patching mixes will be conducted through this project at a later stage where a combination of flexural and tensile stresses will be experienced by patches cast in miniaturized pavement slabs.

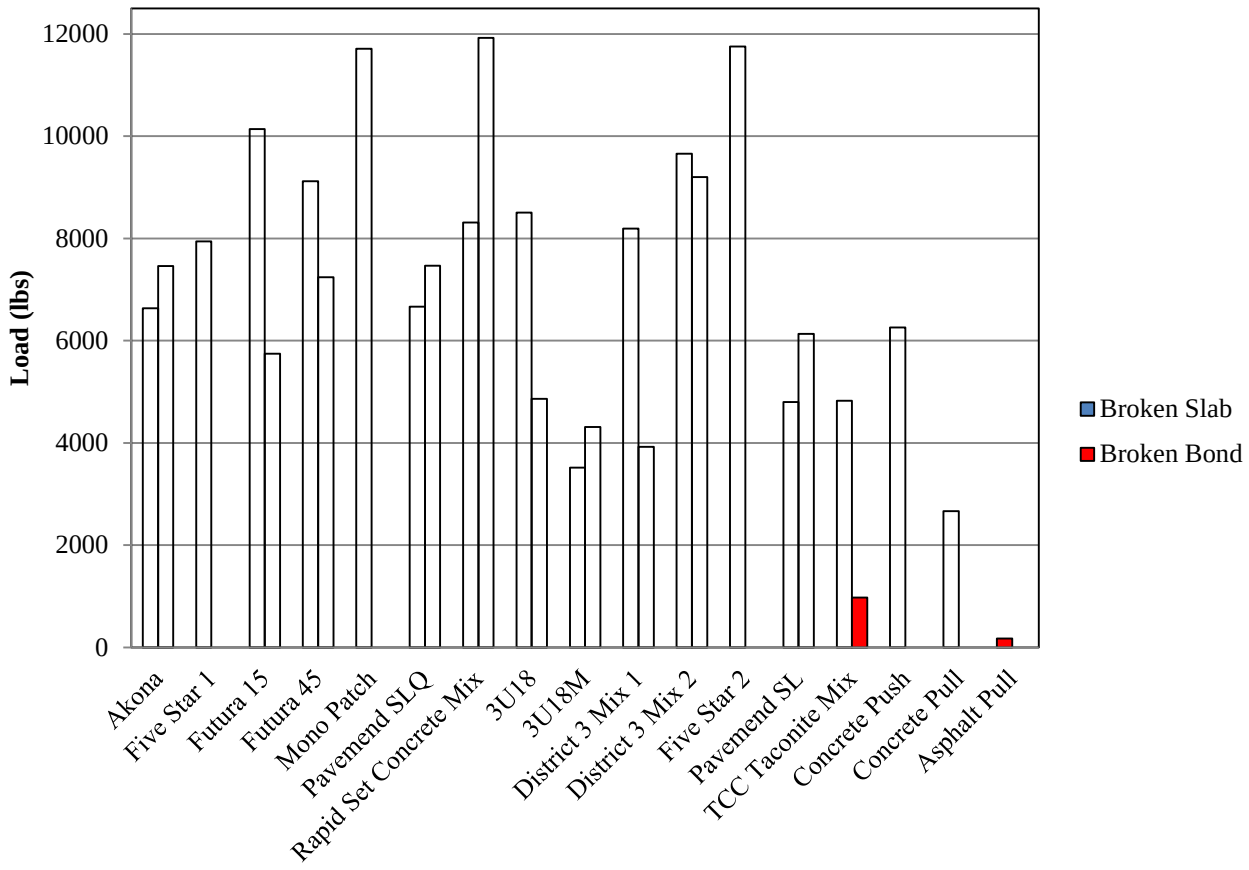

Figure 34: Load that caused the initial breakage in the sample for pull-out test

Performance Review of Products in Task 2

Each of the thirteen products possessed qualities which are conducive for use as patching materials. There are many important properties to be considered for the use of any material. This study was intended to determine which products possess these properties prior to their acceptance as patching materials. Thus far the standard acceptance testing has been conducted with additional testing to follow. This is a discussion about the results of the current acceptance criteria.

The list of materials mentioned here is alphabetically tabulated and is in no way a reflection of a ranking system. These notes serve to summarize the findings and were used by the technical advisory panel to select the materials that would be subjected to additional testing in task 3.

MnDOT 3U18

Mixing instructions were followed as per the manufacturer's specifications. The mix was held to a one inch slump which made workability low. Liquid admixture was used to achieve 5.5% air entrainment.

This mix fails to meet the compressive strength and slump requirement set forth by the ASTM C928. The flexural strength was the lowest of the products that could be measured. Freeze thaw durability ranked the third lowest among all products.

Figure 35: 3U18 compression, freeze thaw and pull out specimens

MnDOT 3U18M

This product contains an air entrainment admixture within the pre-bagged cementitious mix. It is much the same as the standard 3U18.

There are similar failures of the ASTM C928 spec, compressive strength and slump. The formed beam specimen for flexural strength was unable to support its own weight at four hours.

Figure 36: 3U18M compressive, freeze-thaw and pull out specimens

Akona Rapid Patch

This product is listed by the manufacturer as gypsum based cement. When cured the surface was smooth and shiny.

Compressive strength at three hours was negligible as the molded cylinders could not carry load. The flexural test did yield results; however, the interior of the beam specimen was still moist. The freeze thaw durability was the lowest among all products.

Figure 37: Akona compressive, freeze-thaw, flexural and pull out specimens

MnDOT District 3 Mix 1 (3U18 based)

A proportioned mix developed by Dan Labo at District 3. This contained calcium chloride as well a liquid plasticizer admixture.

The mix did not achieve ASTM C928 specified strength requirements. When broken during the flexural test there was sufficient internal bond developed to break individual aggregate pieces even though the interior was still moist.

Figure 38: District 3 Mix 1 compressive, freeze-thaw, flexural and pull out specimens

MnDOT District 3 Mix 2 (3U18 based)

This mix design is close to the District 3 Mix 1. The difference being that micro silica comprises 5% of the cementitious material.

Once again the compressive strength was insufficient at three hours. This mix did achieve the highest overall compressive strength at twenty eight days, over 11,000 psi. At four hours the flexural strength test proved that the internal bond was present and aggregate was broken. The interior as well as the exterior was moist at the time of the flexural test.

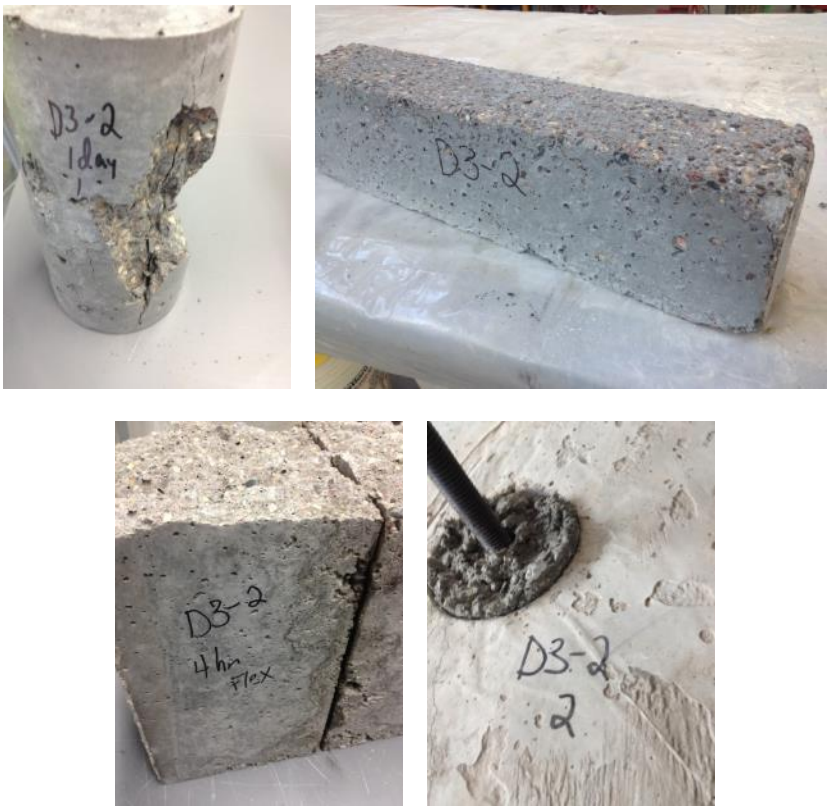

Figure 39: District 3 Mix 2 compressive, freeze-thaw, flexural and pull out specimens

Five Star Highway Patch

This mix starts off smooth and shiny, much like the Akona, but upon curing it takes on a low luster and becomes rougher. The cementitious material of this product is not listed by the manufacturer.

Strength gain at three hours was the highest among all products. Five Star also possessed the highest modulus of rupture at four hours. When broken for the flexural test the interior was completely dry and set. The resistance to freeze thaw was the second lowest of the group.

Figure 40: Five Star compressive, freeze-thaw, flexural and pull out specimens

Futura 15

The composition of this product was not disclosed by the manufacturer. The mixing, workability and finishing was similar to normal concrete.

Three hour compressive strength was among the top performers of the group. Even though it had achieved over 3,000 psi at three hours the interior of the cylinder molds was moist. It also displayed great compressive gains at 28 days. The modulus of rupture was the highest of the group and contained broken aggregate with a dry interior. Freeze thaw durability factor was below twenty.

Figure 41: Futura-15 compressive, freeze-thaw, flexural and pull out specimens

Futura 45 Extended

This product was similar to the Futura-15 except it has a longer set time. A slump of nine inches made workability easy.

Compressive strength gain was virtually identical to the Futura-15. The modulus of rupture was among the top performers. What set this apart was a large durability factor associated with freeze thaw resistance.

Figure 42: Futura-45 compressive, freeze-thaw, flexural and pull out specimens

Mono Patch

This is a magnesium phosphate based proprietary product. Workability was high with a 7 ¾ inch slump. This mix produced a moderate amount of heat during the curing phase; the concrete reached a temperature of 116°F at three hours.

Compressive strength at three hours was below the ASTM C928 specification. Modulus of rupture was on the higher end of the overall group. When the flexural test was complete the interior of the beam was dry and set but the product contained several spherical voids ranging from 1/16 to 1/8 inches in diameter. This may have contributed to the higher freeze thaw durability. However this product exhibited a failure during the length change specification. It showed high amounts of expansion in water as well as slight expansion in air.

Figure 43: Mono Patch compressive, freeze-thaw, flexural and pull out specimens

Pavemend SL

This is listed as high alumina cement by the manufacturer. Workability was high, this was a self-leveling mix.

The compressive strength at 3 hours was above the 3,000 psi mark. There was a great increase in the compressive strength at 28 days, it attained over 9,000 psi. This mix had the third highest modulus of rupture and was dry and set on the interior of the flexural beam. Freeze thaw durability was on par with most others which were below twenty.

Figure 44: Pavemend SL compressive, freeze-thaw, flexural and pull out specimens

Pavemend SLQ

Specialty Products lists this proprietary mix as magnesium phosphate based. This mix also was a self-leveling product. Even though it had high workability, care had to be taken as the working time was three minutes.

Three hour compressive strength was below the ASTM C928 specification. It did exceed the 3,000 psi level at one day. This product has high freeze thaw durability with a durability factor above 100. The flexural strength was in the middle of the range for the group, when the beam was broken the interior was found to be dry and set. Like the Mono Patch, which was also magnesium phosphate based, this product expanded while curing in air as well as in water.

Figure 45: Pavemend SLQ compressive, freeze-thaw, flexural and pull out specimens

Rapid Set Concrete Mix

Portland cement based product that most likely contains some accelerator given the fast setting times. Workability was high and the there was an adequate 15 minute working time.

Compressive strength gain was above the ASTM C928 specification. Freeze thaw durability was in the low range being below twenty. Flexural strength was in the middle of the group; the interior of the beam was dry and set.

Figure 46: Rapid Set compressive, freeze-thaw, flexural and pull out specimens

TCC Taconite Based Mix

The aggregate is from taconite tailings and the cementitious material is a product labeled as Akona. The mix also included a liquid component labeled as an activator which eliminated the need for mixing water.

The first attempt at mixing these components in the lab was not met with success. The product began to set up in the bucket while the mixing was still taking place. The following attempt was conducted outside on a day when the temperature was 31°F. The three components were placed outside for two hours prior to mixing. The resulting mixture yielded a more reasonable five minute working time. This product generates considerable heat while curing. It reached a temperature of 129°F thirty minutes after the liquid was added (Figure 47).

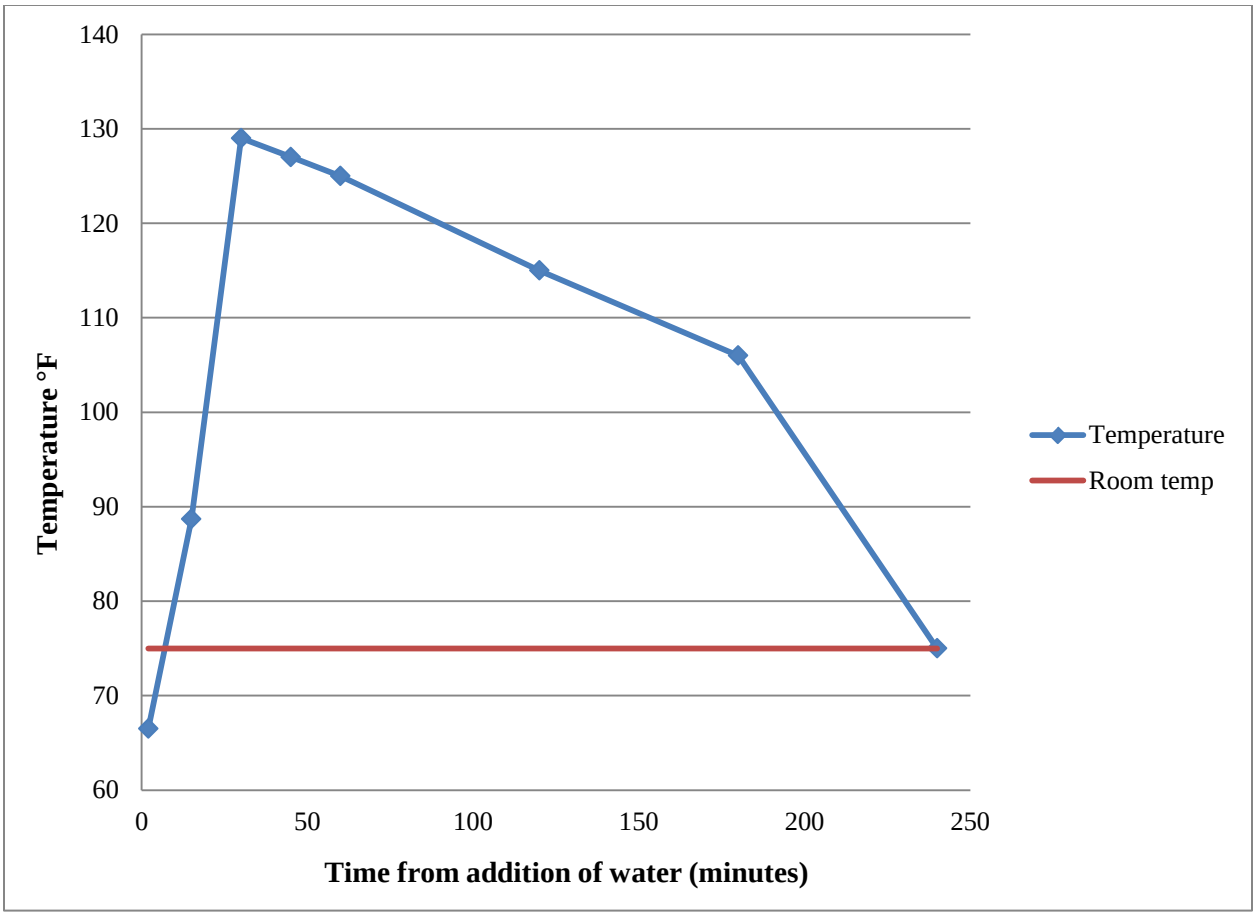

Figure 47: Heat of hydration for TCC taconite mix

Compressive strength at three hours was below the ASTM C928 specification. The 7 day strength was just above the MnDOT required minimum of 3,000 psi. Modulus of rupture was comparable to most of the other products. The interior of the flexural test beam contained several clay balls which were comprised of the taconite tailings aggregate. These clay balls ranged from 1/8 to 1/4 of an inch and can be observed in Figure 48. The TCC Taconite Mix had the highest freeze thaw durability.

Figure 48: TCC taconite mix compressive, freeze-thaw, flexural and pull out specimens

Product Comparisons

A listing of the products with their corresponding ranking for each of the following tests; 3 hour compressive strength, 28 day compressive strength, modulus of rupture, durability factor, shrinkage in air and expansion in water (Table 14). These rankings are based on actual data collected during the ASTM C928 standard specification tests. All items not listed as failed meet or exceed the ASTM C928 specifications.

Table 14: Ranking of the performance for the tested patching materials

Product	Rank Based on Testing Results					
	Short Term Compressive Strength (3 Hr.)	Compressive Strength (28 Day)	Modulus of Rupture	Durability Factor	Shrinkage	Expansion in H_2O
3U18	Fails C928	7	12	11	8	7
3U18M	Fails C928	5	13	6	12	5
Akona	9	11	11	13	3	11
District 3 mix 1	Fails C928	2	9	9	9	10
District 3 mix 2	Fails C928	1	10	5	11	2
Five star	1	9	1	12	4	4
Futura 15	3	4	2	8	10	1
Futura 45	2	6	4	3	7	3
Mono Patch	Fails C928	8	7	4	2	Fails C928
Pavemend SL	5	3	3	10	5	6
Pavemend SLQ	6	12	6	2	1	8
Rapid Set Concrete Mix	4	10	5	7	6	9
TCC Taconite	Fails C928	Fails C928	8	1	Fails C928	12

Chapter 5:
Phase Two Testing Results and Discussion (Task 3 and Task 4)

Coefficient of Thermal Expansion (CoTE)

The CoTE was measured on two separate samples of Portland cement concrete (PCC) for comparison purposes. One of those controls contained limestone based aggregate from the southern region of Minnesota and the other contained granite based aggregate. In order to minimize the stress in the patch and surrounding pavement during temperature changes, the patch and base concrete should have similar CoTE values. The results of the test show that the materials are moderately close to one another (Figure 49). A box and whisker plot is presented in Figure 50 which shows the variability of the measurements that were taken of the four replicate samples for each product. The minimum and maximum values that were recorded are indicated by the whiskers in the plots. Subsequent measurements are represented by the top and bottom of the boxes while the center line in the box indicates the average value of the replicate samples that was reported as the CoTE.

The results indicate that 3U18M has as CoTE that is nearly the same as the normal PCC samples. The Futura 45 has the lowest CoTE of the group that was tested, with a value significantly below that of both PPC samples. This could be a detrimental factor for patches of large size due to the fact that CoTE is on a scale of length change per length for each degree of temperature change. Rapid Set had the largest CoTE at 1.05E-5 mm/mm/ °C, though it is close to the CoTE of the PCC sample with limestone aggregate.

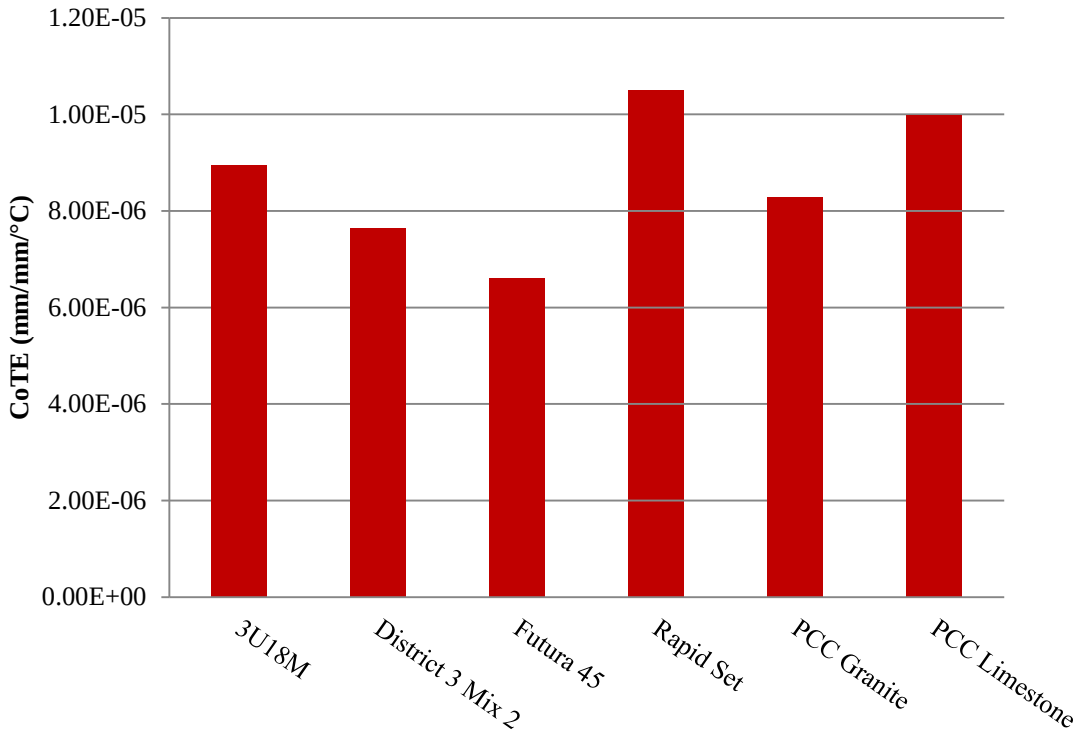

Figure 49: Coefficient of thermal expansion.

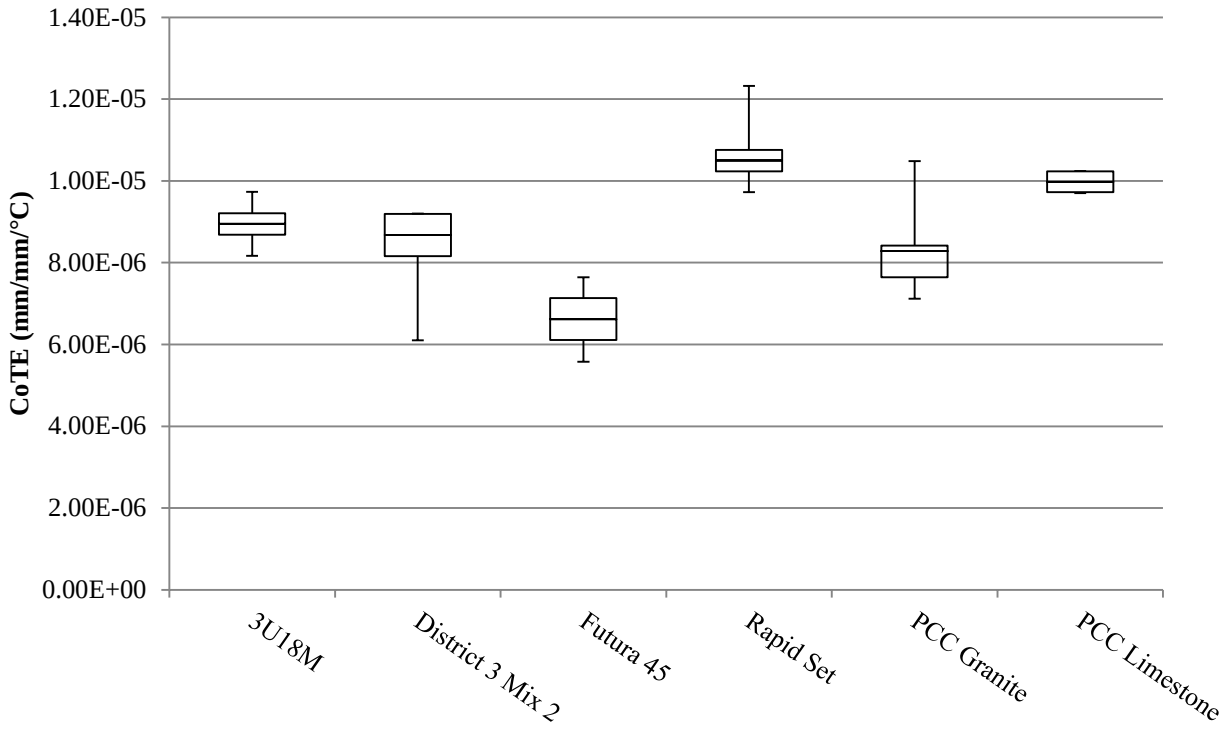

Figure 50: Box and whisker plot for coefficient of thermal expansion.

Modulus of Elasticity

The two control mixes of PCC mentioned in the CoTE were also used for this test. Both of the control mixes exhibited values that are typical of normal concrete. Unexpectedly the granite based aggregate concrete had a lower stiffness than the softer limestone based aggregate. This is most likely due to the size of the aggregates used; gradation of the crushed limestone was considerably larger than the crushed granite.

The 3U18M elastic modulus value is similar to normal concrete; a comparable trend was realized in the results for the District 3 mix. This is expected because both of them are Portland cement based products. However this is also unexpected because typically the elastic modulus increases as compressive strength increases, and both the 3U18M and the District 3 mix have more than double the compressive strength of the PCC concrete. A reason for this may be the size of the aggregate used in these two patching mixes, larger aggregate typically results in a higher elastic modulus and these products contain aggregate that does not exceed 3/8 of an inch whereas the normal concrete samples contained aggregate sizes exceeding one inch.

The elastic modulus of Futura 45 falls between the elastic modulus values of the PCC granite and the PCC limestone, both are representative of a typical pavement mix concrete. This data suggests that the Futura 45 matches the stiffness of normal pavement concrete.

Rapid Set has the lowest elastic modulus of any of the materials tested during this portion of the research. The results show that Rapid Set has only slightly more than half the modulus of the other products (Figure 51).

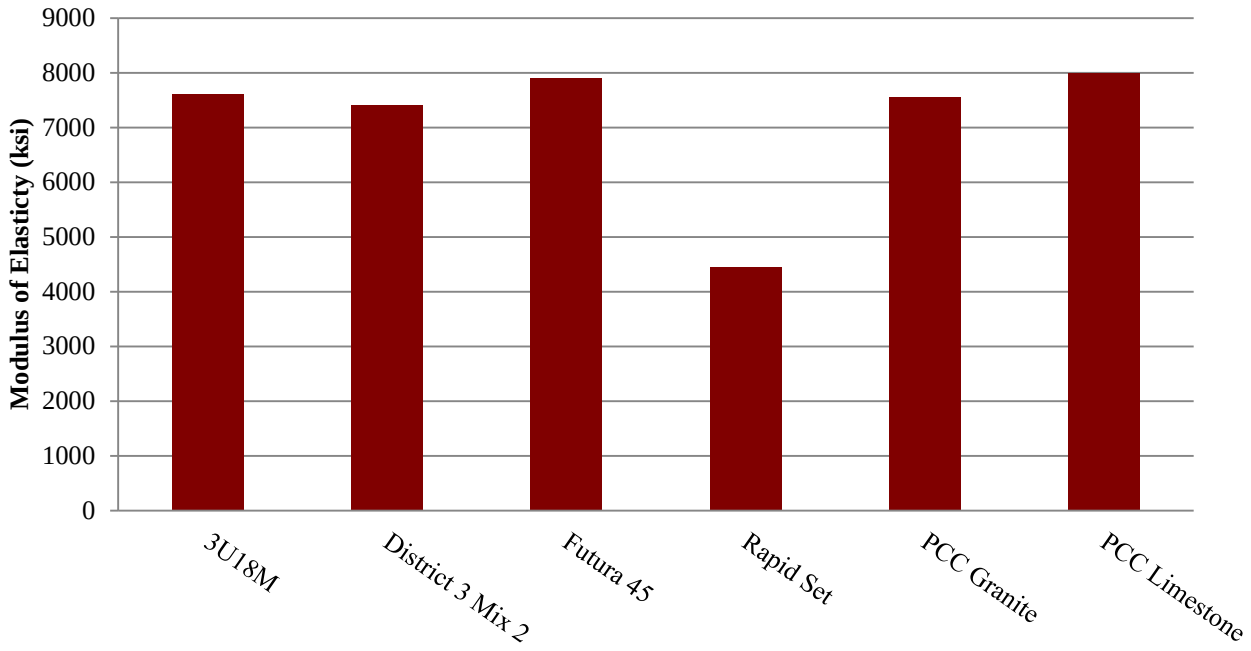

Figure 51: Modulus of elasticity results.

A comparison was also made between the elastic modulus findings and the dynamic modulus results from the freeze thaw tests performed in task 2. There is no apparent correlation between the two different test results (Figure 52). This was performed with a very limited group of specimens and should be investigated further.

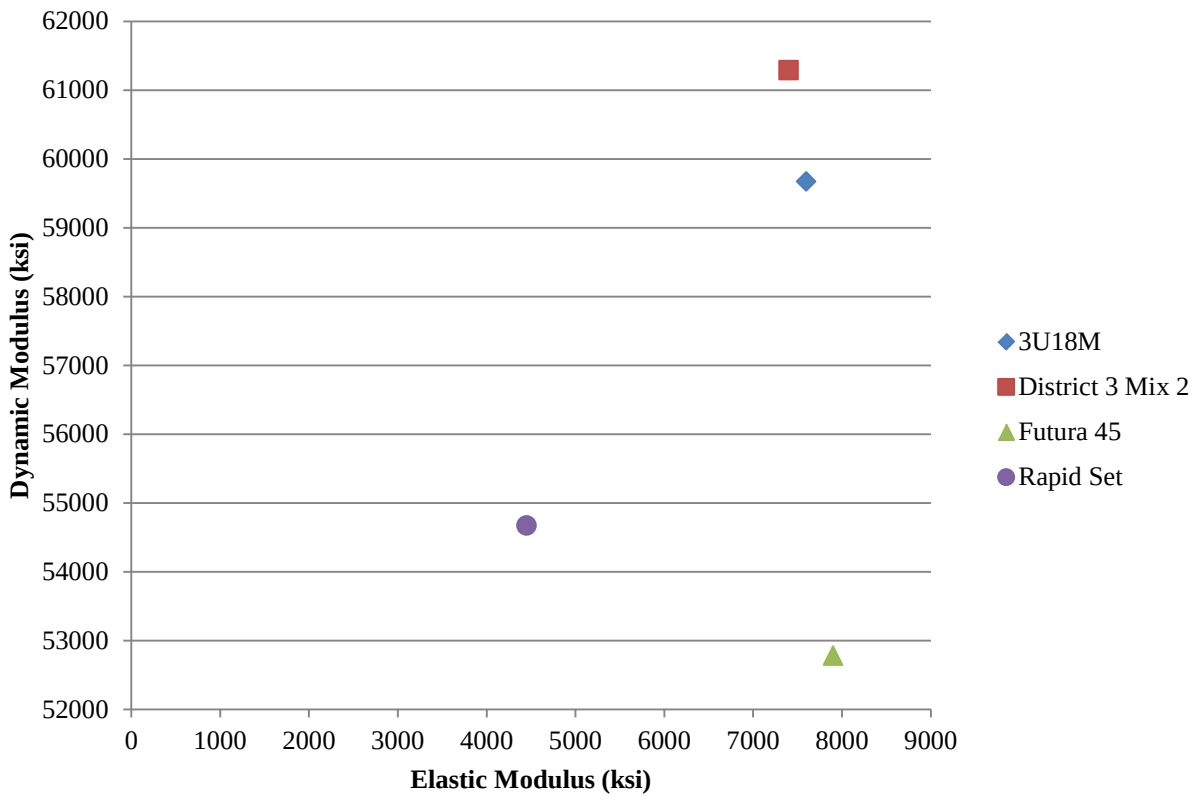

Figure 52: Dynamic modulus versus modulus of elasticity.

Another comparison of mechanical properties was performed to check for correlations. Modulus of elasticity was plotted against CoTE (Figure 53). The plot shows that there is a reverse correlation between the stiffness of a material and the rate at which it expands and contracts with temperature. Rapid Set had the lowest modulus of elasticity but showed the largest CoTE.

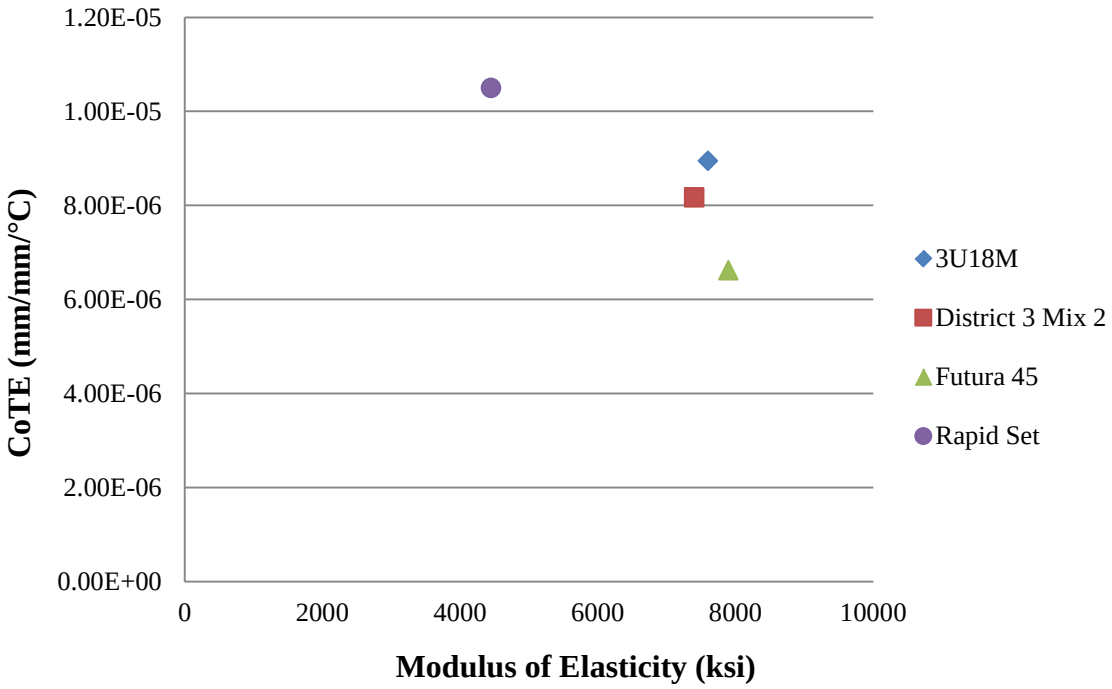

Figure 53: CoTE versus modulus of elasticity.

Abrasion Resistance

The abrasion coefficient is an empirical measurement used to rate a material's aversion to being worn due to direct physical contact. A lower abrasion coefficient indicates more resistance to abrasion.

The results show that the PCC with limestone aggregate abraded more readily than the PCC with granite aggregate. This was expected because some of the abraded area contains aggregate and the limestone is softer than granite.

The rapid set materials did show variability amongst the group (Figure 54). 3U18M, District 3 Mix 2 and Futura 45 had abrasion coefficients that are within ten percent of one another. The Rapid Set was above the rest of the group, sixty percent higher than the closest patching material.

When comparing the abrasion coefficient with the modulus of elasticity there is a correlation between how stiff a material is and how well it resists abrading. The data in Figure 55 shows that Rapid Set which had the lowest modulus of elasticity also displayed the highest abrasion coefficient. The outlier in the plot is the PCC with limestone aggregate, the softer aggregate actually abraded along with the PCC paste, resulting in a larger volume of material being removed.

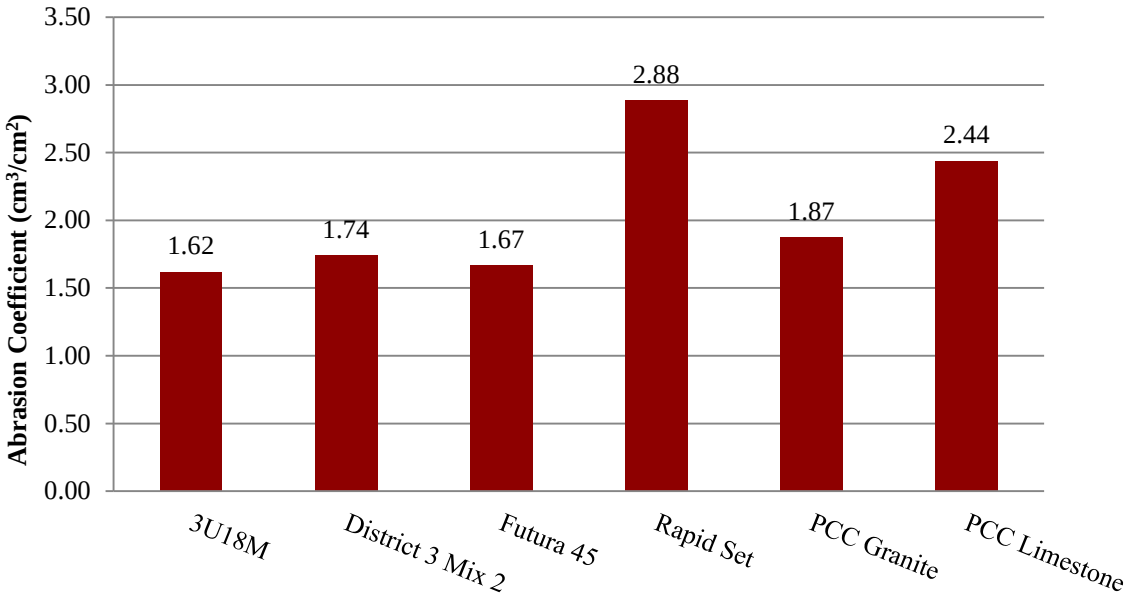

Figure 54: Abrasion coefficient results.

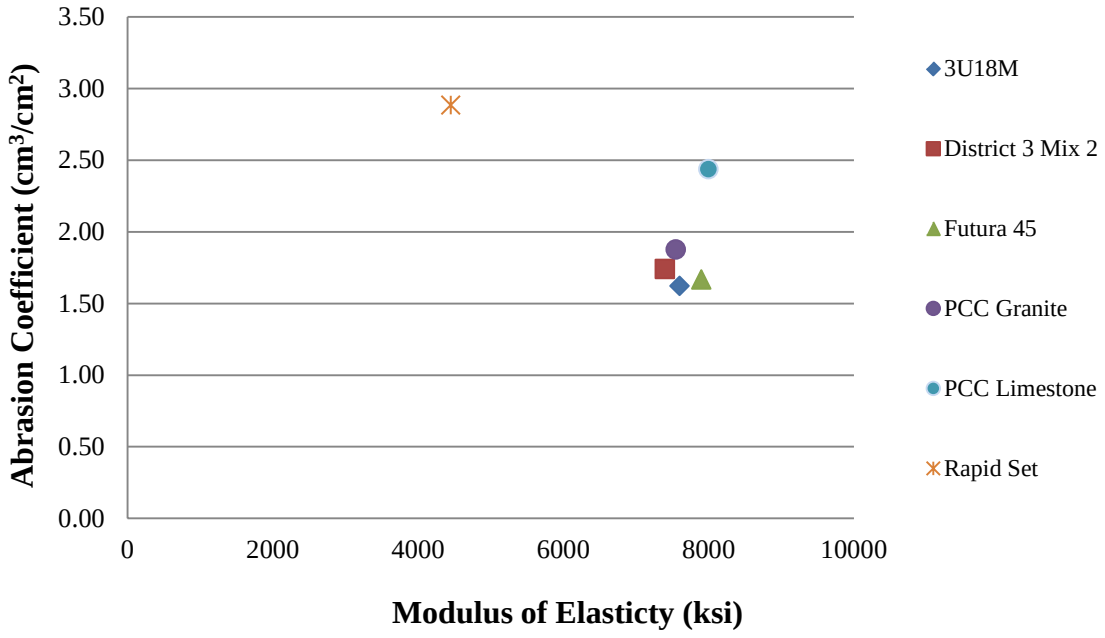

Figure 55: Abrasion coefficient versus modulus of elasticity.

The specimens are shown after the test was conducted in Figure 56. The specimen marked PCCS has the limestone aggregate; note the smoothness of the abraded area. The opposite can be seen on the PCCL sample; the aggregate in the abraded area is intact.

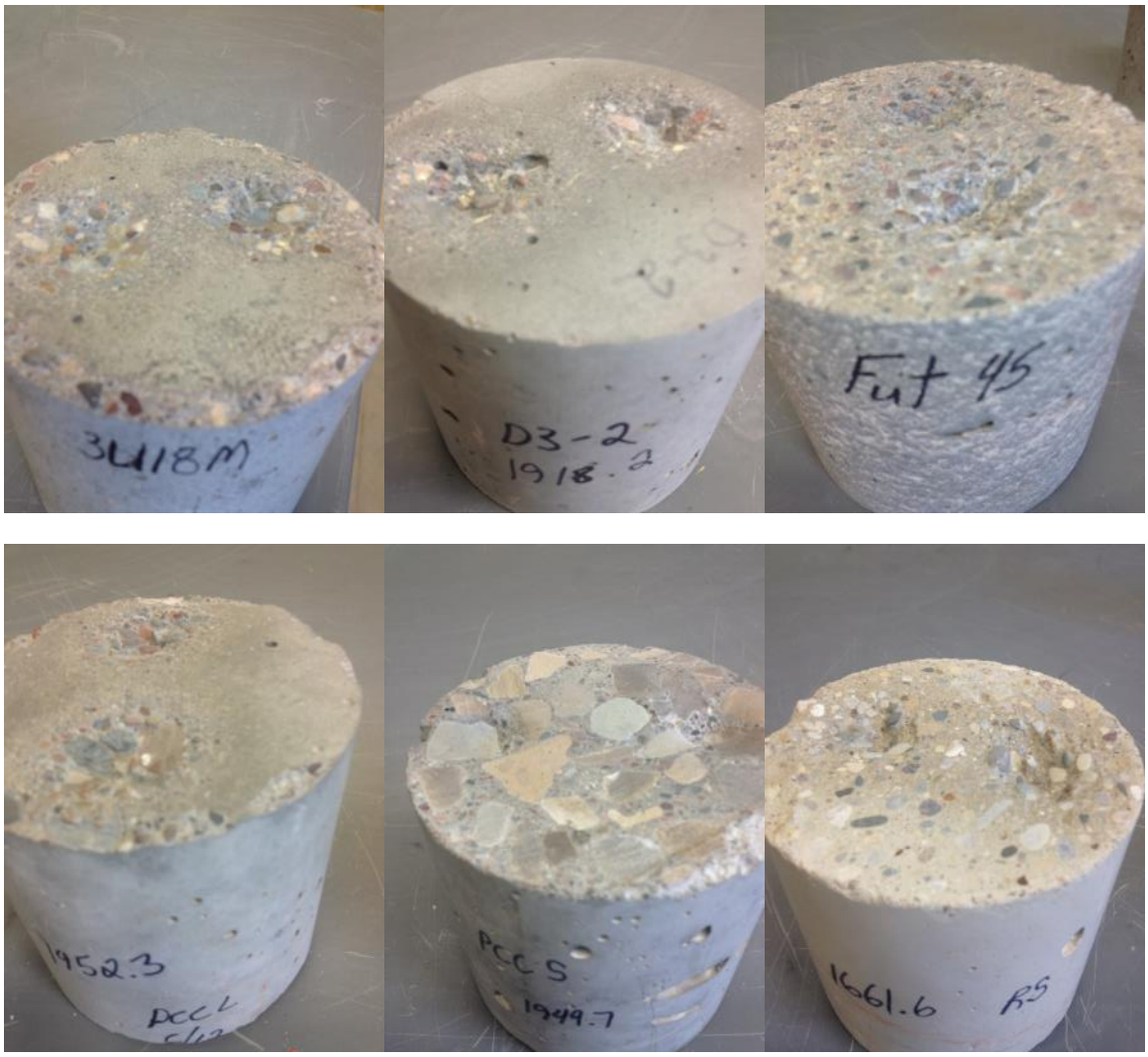

Figure 56: Abrasion test specimens.

Length Change in Sulfate

This test was run for the required fifteen weeks indicated by the ASTM C1012 specification. The length change in sulfate data exhibited unexpected results. Every sample expanded throughout the testing time frame. The condition of the specimens remained unchanged for the duration; no scaling or softening occurred. The amount of expansion exhibited during this test was minimal; the largest gain occurred in the PCC limestone samples at 0.075% (Figure 57).

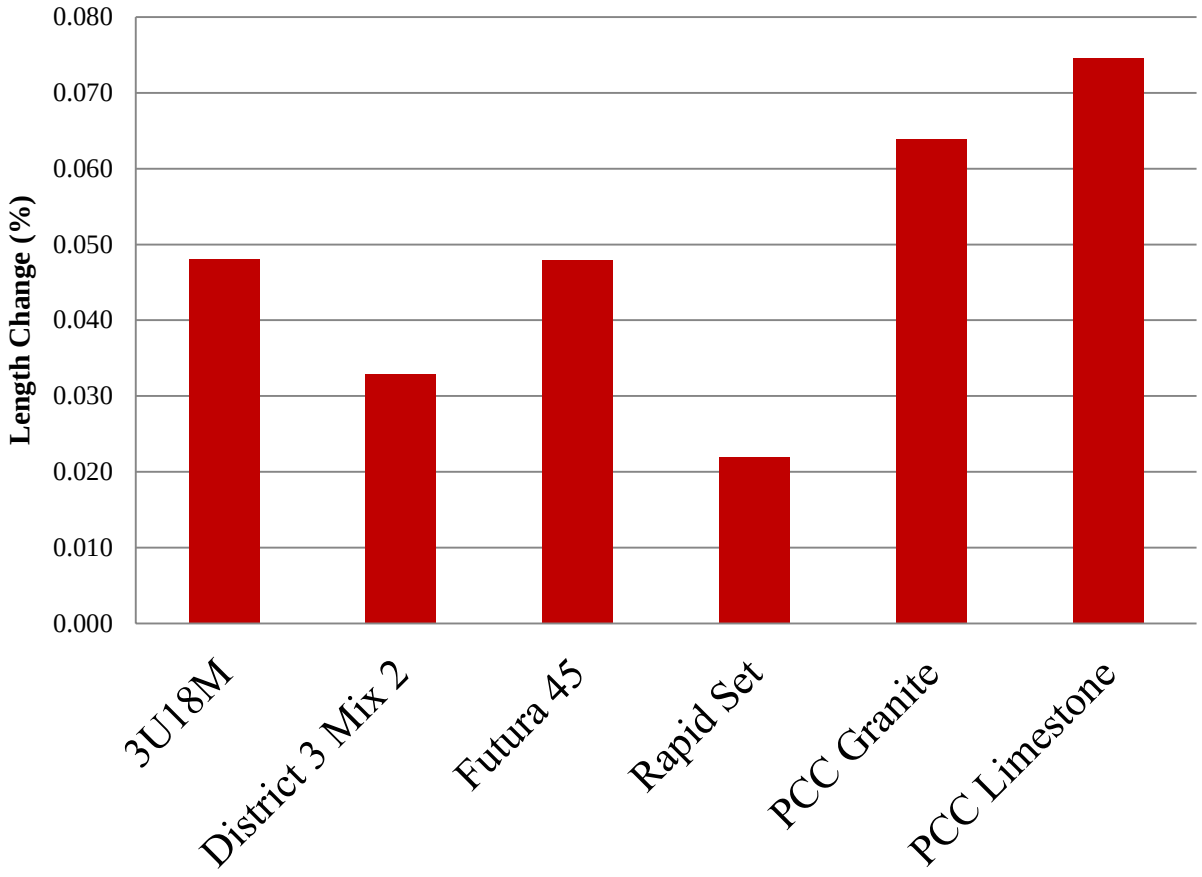

Figure 57: Average length change in sulfate.

Scaling Resistance to Deicing Chemicals

The scaling resistance test was done for fifty cycles as per the ASTM C672 specification. The duration of the test is longer than fifty days due to the samples being held in freezing conditions on some weekends. This is the prescribed method when the samples cannot be attended to on a daily basis. The Rapid Set Concrete Mix and The Futura 45 did not show any signs of scaling throughout the entire process. The District 3 Mix 2 patching material did exhibit signs of scaling, the larger aggregate was showing at the end of fifty cycles. The largest amount of scaling occurred on the 3U18M; the surface had some instances of large aggregate that was missing entirely. Results of the scaling resistance test are based on a visual interpretation of the surface (Table 15).

Table 15: Scaling resistance of concrete surfaces exposed to deicing chemicals.

	Sample#	3-Oct	9-Oct	14-Oct	19-Oct	28-Oct	5-Nov	2-Dec
Cycles		0	5	10	15	20	25	50
Rapid Set	1	0	0	0	0	0	0	0
	2	0	0	0	0	0	0	0
3U18M	1	0	0	1	2	3	3	4
	2	0	0	1	2	3	3	4
District 3 Mix 2	1	0	0	1	1	2	3	3
	2	0	0	1	1	2	3	3
Futura 45	1	0	0	0	0	0	0	0
	2	0	0	0	0	0	0	0

Note: The scale for scaling resistance is as follows.

- Zero – No scaling
- 1 – Very slight scaling, no coarse aggregate visible
- 2 – Slight to moderate scaling
- 3 – Moderate scaling, some coarse aggregate visible
- 4 – Moderate to severe scaling
- 5 – Severe scaling, coarse aggregate visible over the entire surface

Mass loss was also recorded for all samples included in the scaling resistance testing. The data showed that all of the products except Futura 45 lost mass during the process. The Futura 45 actually gained mass, indicated by the green data bar in Figure 58. This is not surprising as the Futura 45 showed no signs of scaling after fifty cycles. The Rapid Set also had no signs of scaling, however the edges of the sample were quite deteriorated which accounts for the mass loss.

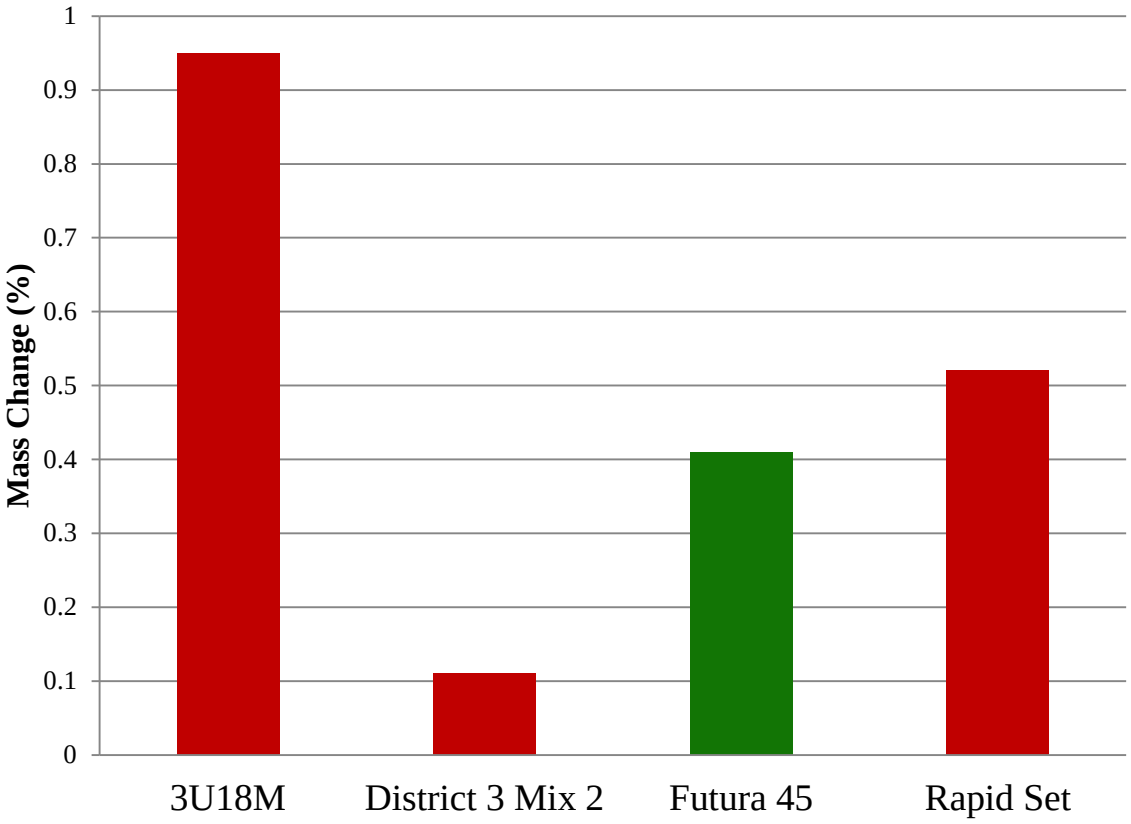

Figure 58: Percent mass change during scaling resistance.

Slant Shear Bond Test

The results for the slant shear bond test were obtained from testing that was conducted at Villanova University. Eric Musselman and Matthew Panzitta performed the slant shear test on two products; Futura 45 and 3U18M. The testing format they used involved two different surface preparations. The first only used water as a bonding agent; this was done by wetting the pre-cast face prior to placing the patching material. The other method utilized a cement paste mixture. The mixture consisted of only water and cement. This paste was placed on the pre-cast face prior to placement of the patching material. Results from the testing are in Table 16.

Table 16: Results from slant shear bond test.

	Maximum Shear Stress (psi)	Minimum Shear Stress (psi)	Average Shear Stress (psi)
Futura 45			
Water/wet	2794.8	2151.5	2435.9
Cement Paste	651.1	496.1	577.5
3U18M			
Water/wet	2064.4	936.3	1431.4
Cement Paste	914.4	635.5	720.8

The specimens required that a half cylinder be cast at a 30° angle creating the shear face (Figure 59).

Figure 59: Half mortar cylinder.

The cement paste bonding agent was placed on the half cylinder's exposed face (Figure 60). Once applied the half cylinder is then returned to a mold awaiting the placement of a patching mix.

Figure 60: Mortar paste on the half cylinder prior to patching mix placement.

After seven days the composite cylinders were removed from the molds and tested. The bond interface can be clearly seen in the photo (Figure 61).

Figure 61: Cylinder ready for testing.

All of the cylinders broke along the 30° plane. The photos in Figure 62 show samples from both products.

Figure 62: 3U18M on the left and Futura 45 to the right, both having slant faces intact.

Pop-out Flexural Test

University of Minnesota Duluth Results

Results from the flexure testing of the half slabs indicated that the bond of the patching material to the original pavement is of little concern. Each of the slabs containing the patching material displayed a modulus of rupture (MOR) very similar to a solid block of concrete. Deflection data was recording during the testing process, however because neoprene pads were used at the supports the deflection data was considered inconclusive.

Load data remained consistent to within 500 pounds for the twelve half slabs cast at room temperature. The exception to this was the specimens that were cast and cured at a reduced temperature of 50° F; these required a greater amount of load to reach failure. The replicate sample data is represented as a high, a low and the average load at failure (Figure 63).

The use of only water as a bonding agent shows a slightly higher load to failure trend than the cement grout bonding agent. Because of the small number of specimens sampled this would not indicate that the use of water is better than cement grout; however the results do indicate that the use of water alone is more than sufficient as a bonding agent.

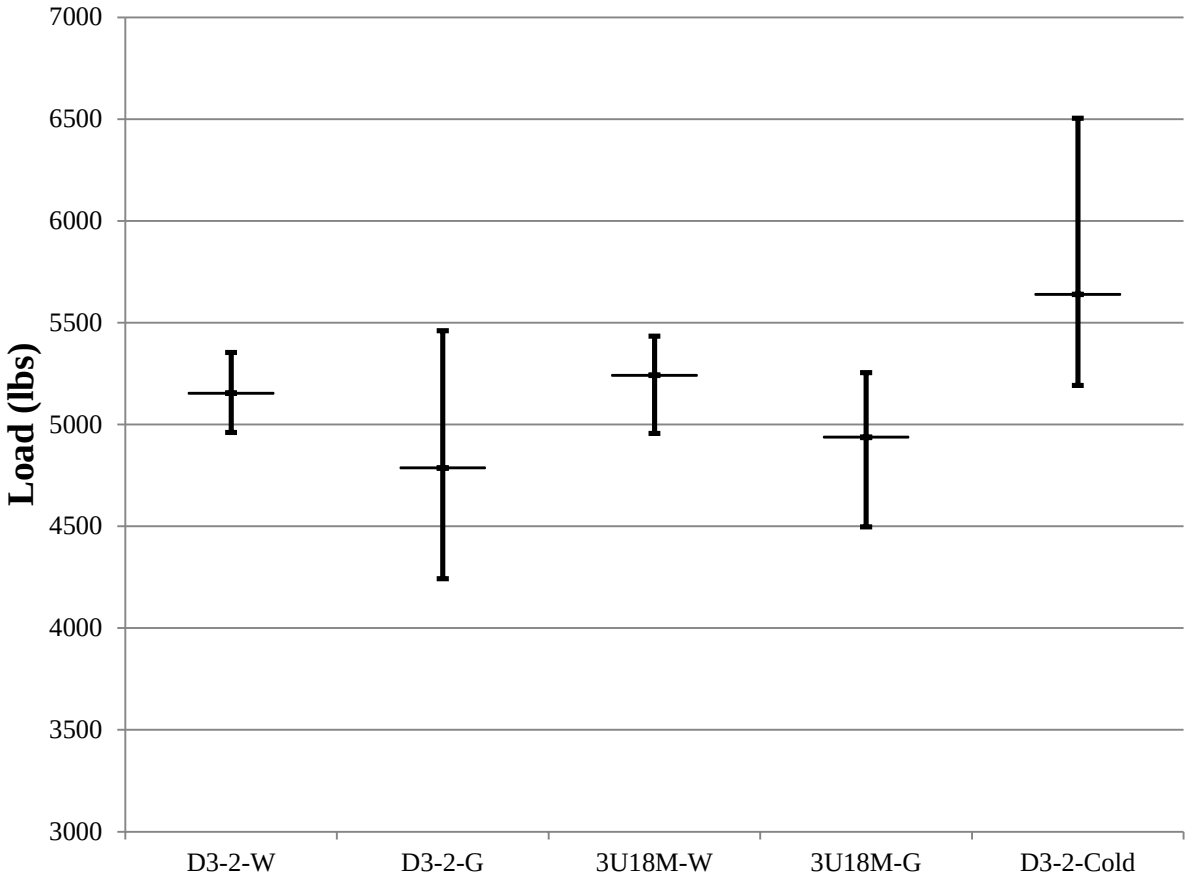

Figure 63: Load recorded at failure for half slab specimens (3 replicates).

The location of the crack propagation in the majority of the test specimens was directly through the center of the slab and the patch (Figure 64). A few of the slabs started to crack around the edge of the patching material at the surface of the patch, all of the cracks eventually propagated through the slab (Figure 65). The important information is that the slab still cracked and failed with the patch bond intact.

Figure 64: Specimen “A” (D3-2-W) exhibiting central crack propagation.

Figure 65: Specimen “D” (D3-2-G) started cracking at the edge of the patch, the bond held and the slab failed in two locations.

The bond does not seem to be an area of concern as the MOR of these half slabs is consistent with the MOR of a solid slab of concrete. The concrete used for the slabs had a compressive strength of ~4,000 psi. When the MOR estimation formula ($M_R = k\sqrt{f'c}$) is used for MOR the resulting range for a solid concrete slab with no patch is 474-570 psi. The calculated MOR values for the slabs containing the patching material exhibit values close to this range (Figure 66). Again the data is presented as a high value, a low value and the average value.

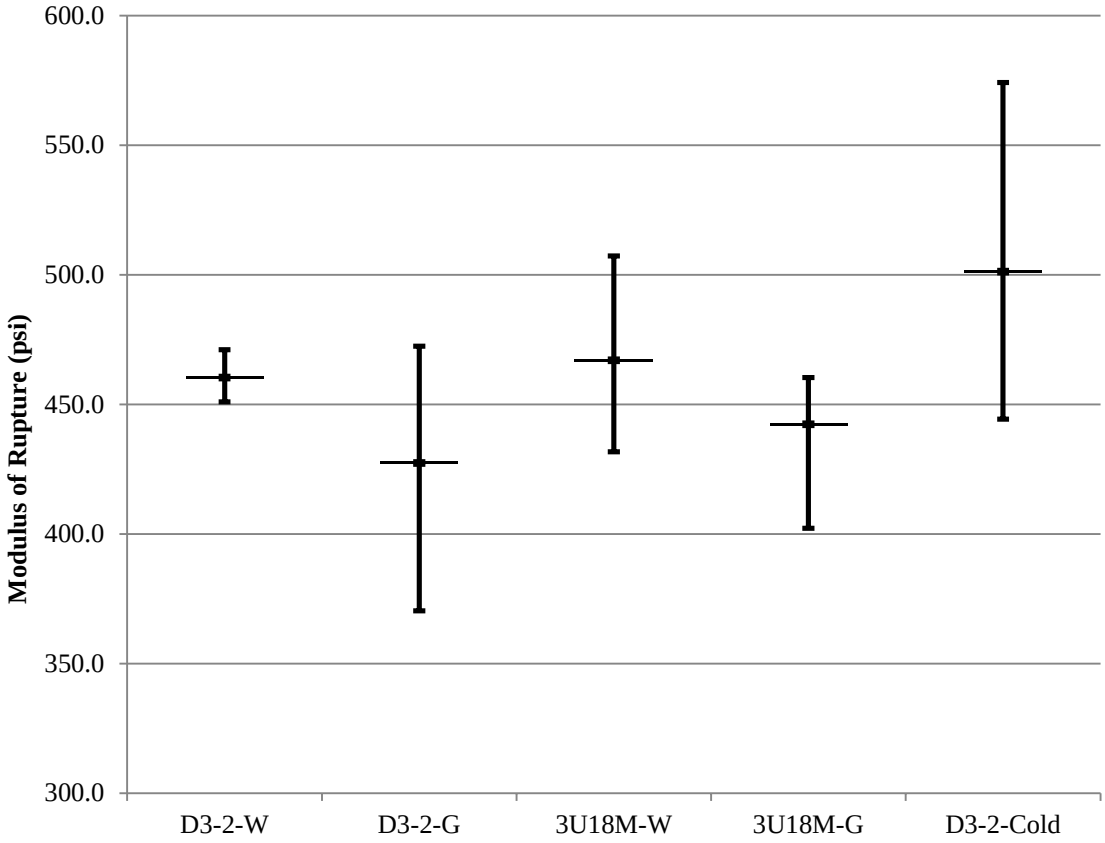

Figure 66: Measured MOR of half slabs containing patching material.

The cold samples showed an increased load and subsequently a larger MOR. The difference was not significant enough to draw any hard conclusions about cool casting being advantageous. However the results do show that performing partial-depth repairs in concrete is possible at 50° F.

It should also be noted that the patching material used for the “cold” test was District 3 Mix 2. Because of the low workability of the original mix design an additional 10% of water was added to the mix. The result of this addition was a mix that achieved a more acceptable level of workability. A side by side comparison of the two variations of the mix can be seen in Figure 67.

Figure 67: D3-2 mixed as per specified and mixed with 10% additional water.

The additional workability made consolidation into the patch area more thorough. The patch area must be in complete contact with the patching material in order to ensure the greatest amount of bond.

There was a full slab test performed on four specimens. The only bonding agent used for the full slab tests was water. The patching material was allowed to cure for twenty eight days prior to testing. The results are consistent among the individual patching materials (Figure 68). Once again none of the patches displayed any de-bonding or signs of patch failure.

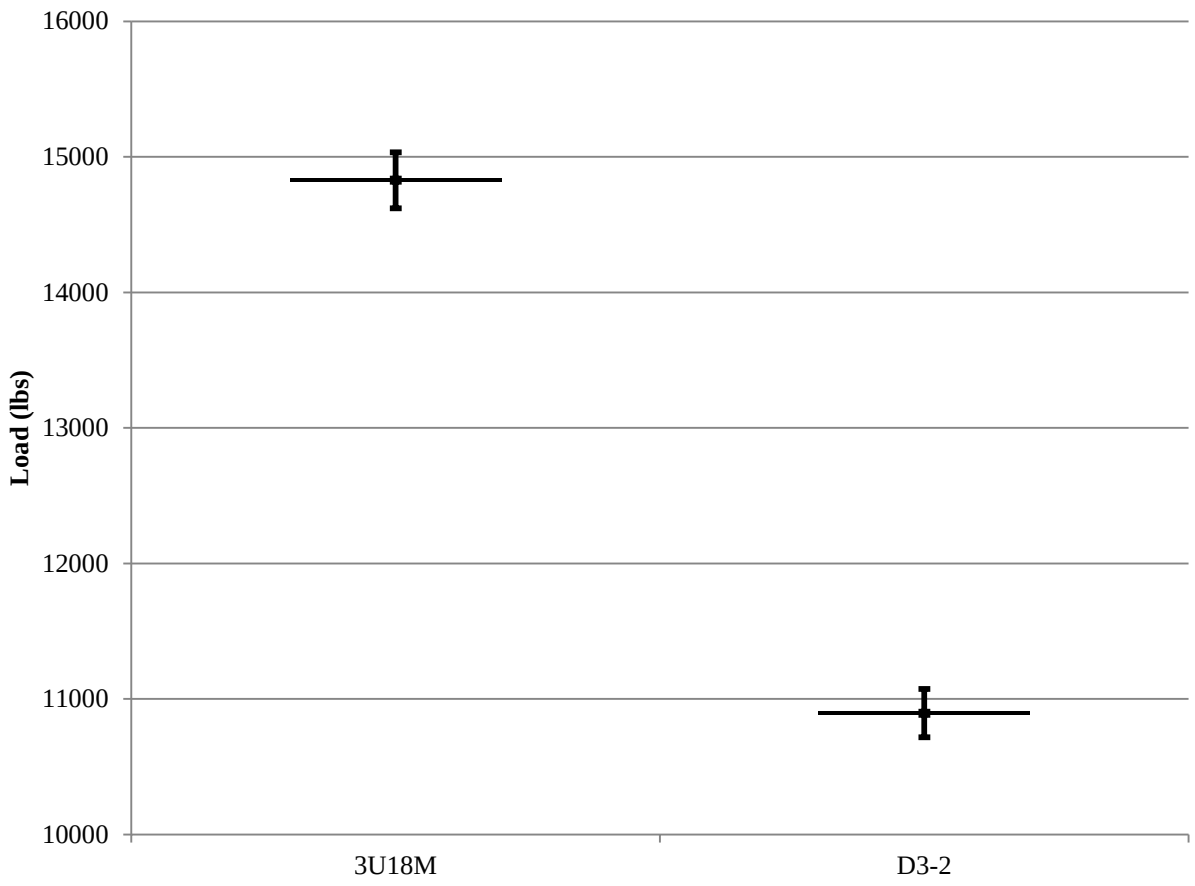

Figure 68: Load at failure for the full slab tests

Villanova Testing Results

The testing conducted at Villanova University included patch slabs exposed to both static and cyclical loading. The results from the load deflection data for the static tests did not seem to be a good indicator of bond performance. As shown in Figure 69, the variable that correlated to the load-deflection data is the type of patch. The milled slabs (shown in red in the figure) typically exhibited higher loads for a given displacement than the saw cut and chipped patches (shown in blue). This information is not critical to the issue of bond strength as it is primarily an indication of the section loss of the slab with the different patching methods.

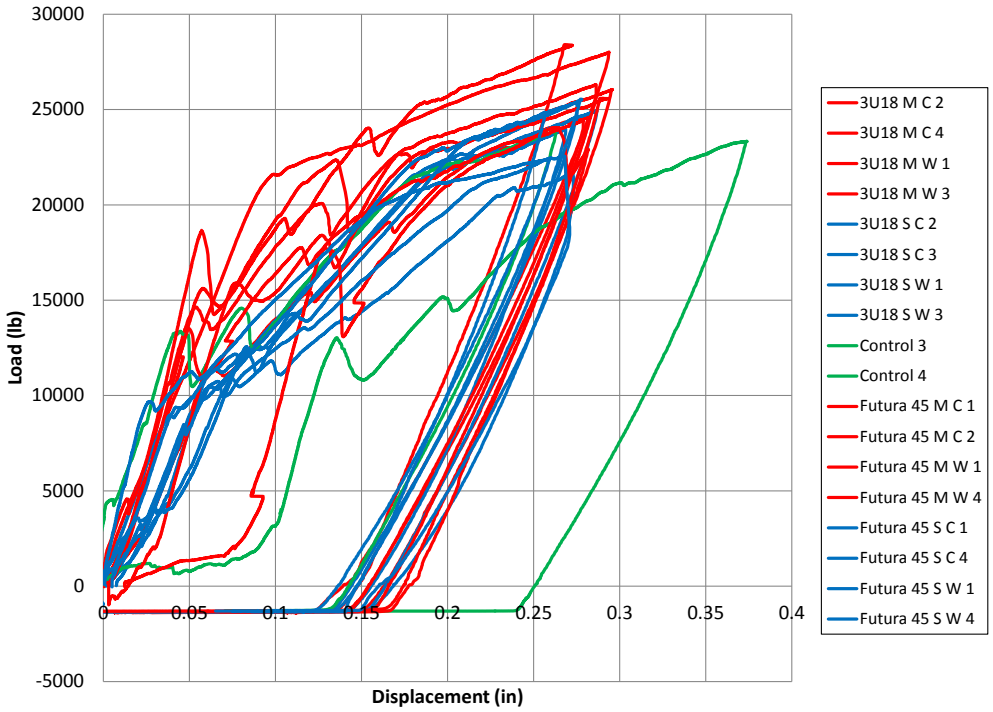

Figure 69: Static load displacement plot for different patch preparation methods.

A summary for the results of visual observations of the static bending slabs can be seen in Table 17. It clearly shows that the best performing patches were the Futura 45 material in milled (M) patches with either cement paste (C) or water (W) as the surface preparation. The 3U18 material did not perform well in the milled patches in our study with all samples de-bonding from the base concrete. Figure 70 shows one such sample before and after testing. The visual observations obtained during the cyclical testing were very similar to those shown in Table 17.

Table 17: Visual observations for static slab bending tests

Visual Observations		
	Cracking	*Bond*
3U18 M C 2		
3U18 M C 4		
3U18 M W 1		
3U18 M W 3		
3U18 S C 2		
3U18 S C 3		
3U18 S W 1		
3U18 S W 3		
Futura-45 M C 1		
Futura-45 M C 2		
Futura-45 M W 1		
Futura-45 M W 4		
Futura-45 S C 1		
Futura-45 S C 4		
Futura-45 S W 1		
Futura-45 S W 4		

Key

Cracking

= crackng through patch

= cracking around patch

= cracking under patch

Bond

= patch did not debond from base concrete

= patch debonded from base concrete

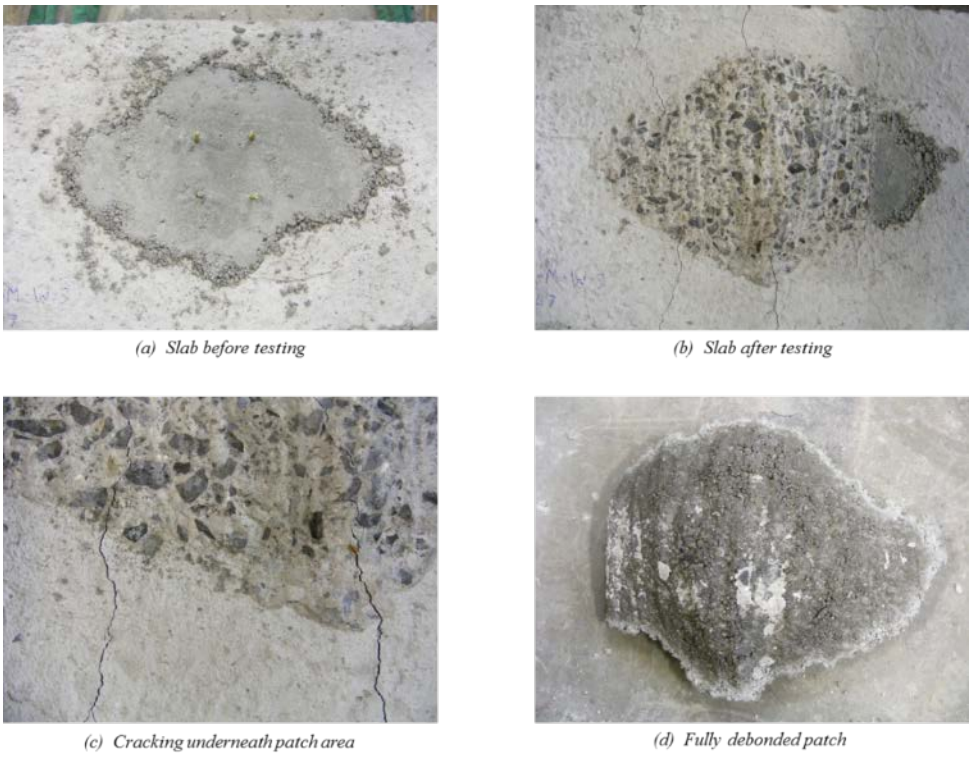

(a) Slab before testing

(b) Slab after testing

(c) Cracking underneath patch area

(d) Fully debonded patch

Figure 70: Photos of 3U18 Milled, Water Bonding Agent

The strain gages attached to the cyclical samples provided useful data as well. Figure 71 shows a typical result. The graph shows the strain for the first and last 20 cycles of each displacement range. As the

figure clearly shows, a dramatic drop in recorded strain occurred during the cycles with amplitude of 0.2 inches. This indicates it was sometime during this group of cycles that the patch de-bonded. Information provided in Table 18 summarizes the results for each of the samples testing under cyclical loads.

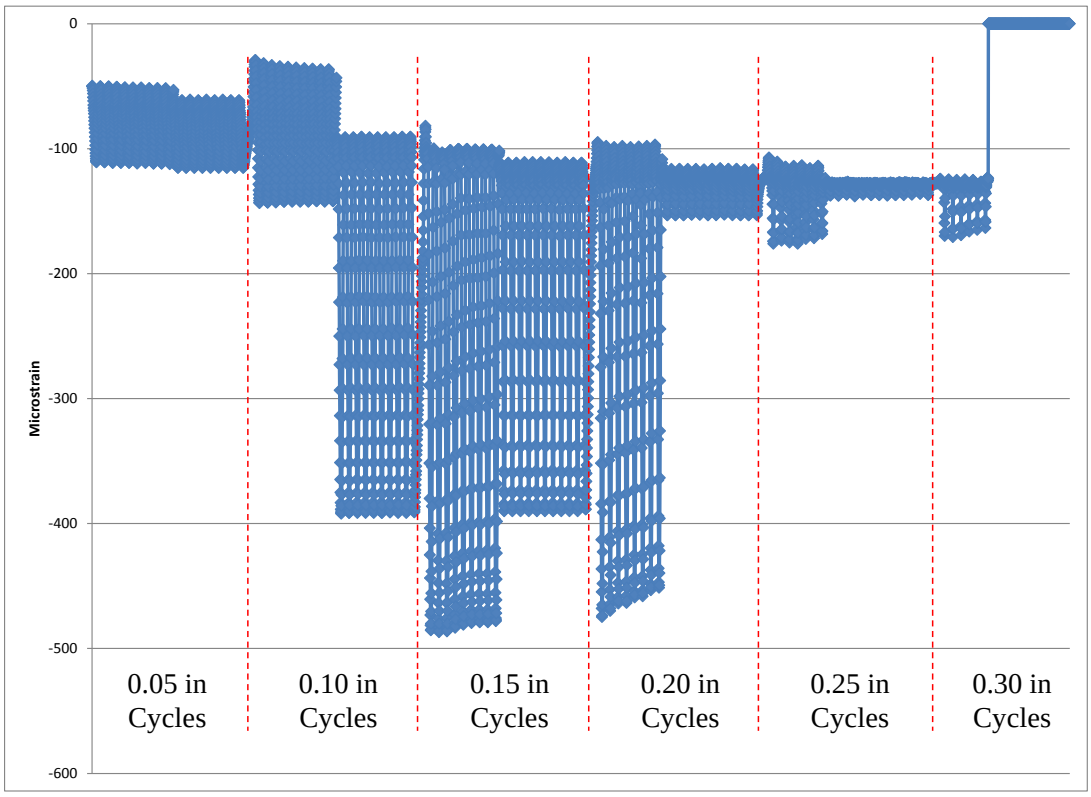

Figure 71: 3U18 M C 3 cyclic slab bending beginning and end cycles on strain gage 1

Table 18: Strain observations

Strain Observations		
	Indications of Bond Failure	*Details*
3U18 M C 1	Complete	Complete debonding during cracking phase
3U18 M C 3	Complete	Complete debonding at 5200 cycles; tension strain loss in 0.10" cycles; compression strain loss in 0.02" cycles
3U18 M W 2	Complete	Complete debonding at 250 cycles
3U18 M W 4	Complete	Complete debonding at 2100 cycles
3U18 S C 1	Moderate	Decrease in tensile strain over entire test; decrease in compressive strain w/o decrease in load in 0.25" cycles
3U18 S C 4	Few	Small decrease in tensile strain over entire test; small decrease in compressive strain w/o decrease in load in 0.25" cycles
3U18 S W 2	Few	Small decrease in tensile strain over entire test; small decrease in compressive strain w/o decrease in load in 0.25" cycles
3U18 S W 4	Few	Small decrease in tensile strain over 0.15" cycles and beyond; small decrease in compressive strain w/o decrease in load in 0.25" cycles
Futura-45 M C 3	None	
Futura-45 M C 4	Few	Small decrease in tensile strain over entire test; small decrease in compressive strain w/o decrease in load in 0.20" cycles
Futura-45 M W 2	Few	Decrease in tensile strain over entire test
Futura-45 M W 3	Moderate	Decrease in tensile strain over entire test; decrease in compressive strain w/o decrease in load in 0.25" cycles
Futura-45 S C 2	Moderate	Decrease in tensile strain over entire test; decrease in compressive strain w/o decrease in load in 0.25" cycles
Futura-45 S C 3	Few	Small decrease in tensile strain over entire test
Futura-45 S W 2	Few	Small decrease in tensile strain over entire test
Futura-45 S W 3	None	

Chapter 6: Recommendations for Acceptance Testing

Recommended Testing Procedure for Acceptance of Partial-Depth Patching Mortars and Concretes

The recommendations listed are based on laboratory testing that was conducted throughout the entire project. Consideration was also given to information that was gathered during field observations on site visits to partial-depth repair areas. Testing for acceptance of patching materials

While each of the properties tested are important to partial-depth patching in cold climate regions, some may be obtained indirectly through correlation. Consideration must be given to each test and to what condition in the field each of them represent. The data collected was gathered from a small test group and the following is based on that data. Future studies on additional materials would provide further confirmation and they are strongly recommended.

Acceptance testing should include the following:

- Compressive strength measurements can be reduced to only recording the 24 hour and 28 day values.
    - The exception to this would be any materials used for emergency spot repairs.
        - For this special case the 3 hour compressive strength should also be tested.
- Shrinkage testing is required.
- Freeze-thaw testing is required.
    - Mass loss should also be reported for the duration of the testing.
- Modulus of elasticity of patch material should be measured and compared to the modulus of elasticity of PCC used for pavement construction.
    - The exact range of acceptable variation had not been investigated thoroughly enough to make a recommendation.
- Abrasion resistance should be performed on products containing softer aggregates that may be susceptible to polishing.
- Air entrainment strongly recommended for patching materials.
- Setting times should be recorded and reported.
- Scaling resistance to de-icing chemicals should be performed on all patching materials.
    - Mass loss during this test should be recorded as a way to measure the overall durability of the product.
        - An example would be the Rapid Set; it showed no scaling but did exhibit mass loss due to mechanistic failure around the edge of the samples.

Acceptance testing that can be eliminated includes:

- Coefficient of Thermal Expansion can be eliminated from testing when considering PCC based products.

    - The correlation with stiffness is sufficient in determining the validity of a PCC based material for a thermal property match.
    - There were not enough products represented in this testing to eliminate this test completely for other materials that are not PCC based.
- Length change in sulfate solution does not need to be included in the testing regimen for the acceptance of patching materials.
- Flexural strength can be removed from the testing regimen.

Chapter 7:
Summary, Conclusions and Recommendations

Summary

Several states and some Canadian provinces have specifications for partial-depth repair. These specifications mainly involve patch area preparation and construction techniques. An extensive review of previous research found projects with a broad range of objectives. Some of the previous work focused on material types such as polymer modified cements and magnesium phosphate based cementitious materials. Previous research studies on patching included field studies, which were used to rate individual products. The search revealed little information about the acceptance criteria for rapid set materials for partial-depth patching in cold climate regions.

Throughout the project many tests were conducted on various patching materials. The current acceptance criterion, the ASTM C928 specification, was included in the testing protocol. Additional tests were added to the project based upon previous research and discussions with the technical advisory panel. The additional tests were chosen and developed to provide a broader spectrum of information about patching materials.

Conclusions and Recommendations

ASTM C928 tests

- The setting time of the materials is a good indicator of working time.
- Compressive strength gain varied greatly among the products tested. Materials that gained strength quickly exhibited ultimate compressive strengths that were lower than the materials that gained strength at a slower rate.
- The modulus of rupture was tested at four hours. This material property can be accurately estimated from the ultimate compressive strength.
- Length change in air and water provided some unique results. Most products did contract while exposed to air and expanded when stored in water.
    - Two products, Pavemend SLQ and Monopatch, expanded in air as well as in water.
    - The TCC Rapid Patch shrank in both air and water.
- The freeze-thaw durability test revealed the need for air entrainment in PCC-based patching materials.
- Slant shear bond testing was performed at Villanova University. Results were obtained while using water or a thick cement paste as a bonding material. With careful sample preparation, usable data can be obtained from the slant shear test. Although the standard deviation is typically high for this test, the results correlate well with those from more complex tests.
- The scaling resistance to deicing chemicals test had a greater effect on PCC-based materials.
- Length change in a sulfate solution showed very minimal results.

Additional tests

- Modified pull-out bond strength test showed that the chemical bond of the materials is of little concern.
- The modulus of elasticity results showed a correlation to the ultimate compressive strength. High compressive strength materials also had higher stiffness values.
- The abrasion resistance test results correlated well to the modulus of elasticity of a material. The stiffer a material was the more abrasion resistance it possessed.
- The coefficient of thermal expansion results for all the materials tested, including PCC, were within 4.00 E-06 (mm/mm/°C) of each other.

Pop-out bond test

The bond testing conducted using representative pavement slabs was performed to simulate field conditions as closely as possible. The results from that testing provided some useful information about bond strength, the use of bonding agents, and current construction techniques.

- Bond strength seems to be of little concern regarding the failure of patches.
    - None of the patches de-bonded during the testing conducted at UMD.
    - The match in MOR is evidence of this.
- The use of water as a bonding agent is acceptable.

Recommended Construction Techniques

The current methods of partial-depth patch construction used and specified by MnDOT may be considered to be optimal. That decision is based on the results of the pop-out bond test in conjunction with previous testing. The milling and feathering method of patch preparation requires less time to complete than saw cutting the edges. Saw cutting also requires more patching material to fill the repair area once the preparation is complete. The added cost of time and material can be considered enough evidence to no longer consider saw cutting as an option.

Partial-depth patch preparation should include the following:

- Milling
- Feathering the sides of the patch with a lightweight jackhammer to an angle between 30 and 60 degrees
- Clearing of debris with compressed air
- The patch contact area should be sandblasted to create a micro-texture on the bond surface
- Placement of bond breakers along all joints
- The application of a bonding agent
    - Water/cement grout (current MnDOT practice)
    - Water alone IS an acceptable bonding agent

    - A viscous cement paste bonding agent (used in the Villanova testing regimen) should NOT be used in field applications. The application of the paste actually decreases the bond strength between the patching material and the concrete.
- Placement of the patching material
    - Consolidation of the patching material
    - Finishing of the patching material
- Application of a curing compound on the surface of the patching material

Note
The bonding agent that was used during the University of Villanova testing procedure was a thickened paste of cement and water; it was not readily flowable like a grout mixture. Therefore it is not recommended for use as a bonding agent.
The bonding agents tested at the University of Minnesota Duluth were representative of the current cement/water grout mixture that MnDOT currently employs. This grout mixture and the use of water alone are both recommended as bonding agents for partial-depth patches.

References

ASTM. (2006). *Standard Test Method for Bond Strength of Hardened Concrete.* Philadelphia: American Society for Testing and Materials.

ASTM. (2009). *Standard Specification for Pachaged, Dry, Rapid-Hardening Cementitious Materials for Concrete Repairs, ASTM C928/C928M.* Philadelphia: American Society of Testing and Materials.

ASTM. (2012). *Standard Test Method for Bond Strength of Epoxy-Resin Systems Used With Concrete By Slant Shear.* Philadelphia: American Society for Testing and Materials.

Cervo, N. M., & Schokker, A. J. (2008). *Bridge Deck Patching Materials.* University Park: Pennsylvania Transportation Institute.

Chen, D., Won, M., Zhang, Q., & Scullion, T. (2009). Field Evaluations of the Patch Materials for Partial-Depth Rerairs. *JOURNAL OF MATERIALS IN CIVIL ENGINEERING,* Vol. 21, No. 9, pp. 518-522.

FHWA. (2006). *Freeze-Thaw Resistance of Concrete With Marginal Air Content.* Retrieved 2012, from http//:www.fhwa.dot.gov/publications/research/infrastructure/pavements/pccp/06117/

Interntional Grooving and Grinding Association (IGGA). (2011). *Partial Depth Repair Keeps Highways and Urban Roads Intact.* West Coxsackie: IGGA.

Mamlouk, M. S., & Zaniewski, J. P. (2011). *MATERIALS FOR CIVIL AND CONSTRUCTION ENGINEERS (Third Edition).* Upper Saddle River: Pearson Education.

Masten, M. A. (2011). *2011 Concrete Pavement Rehabilitation (CPR) Standards and Special Provisions.* Minnesota Department of Transportation.

MnDOT. (2012). *2011 Pavement Condition Annual Report.* Retrieved 2012, from http://www.dot.mn.us/materials/pvmntmgmdocs/annualreport_2011.pdf

MnDOT. (2012). *Approved/Qualified Prodcts.* Retrieved 2012, from http://www.dot.state.mn.us/products/concrete/pacheddryrapidhardeningcementitiousmaterials.html

MnDOT. (2012). *MnDOT Standard Specifications for Construction.* Retrieved 2012, from http://www.dot.state.mn.us/pre-letting/spec/2005/3101-3491.pdf

Mojab, C. A., Patel, A. J., & Romine, A. R. (1993). *Innovative Materials Development Testing, Volume 5: Partial Depth Spall Repair in Jointed Concrete Pavements.* Washington D.C.: Strategic Highway Research Program.

Panzitta, M., & Musselman, E. (2013). *EXAMINATION OF BOND STRENGTH OF PARTIAL DEPTH PATCHES USED IN RIGID PAVEMENTS.* Villanova: Pennsylvania Transportation Institute.

Pattnaik, R. R. (2006). *Investigation into Compatibility Between Repair Material and Substrate Concrete Using Experimental and Finite Element Methods.* Clemson: Clemson University.

Platte, K., Young, B., Beightel, C., Galarza, P., & Nelson, R. (2009). *Two Year Report of Field Performance and Laboratory Evaluations of Rapid Setting Patching Materials for Portland Cement Concrete.* Washington: AASHTO.

Swanlund, M., & Tyson, S. (2010). *Impact of Temperature Curling and Moisture Warping on Jointed Concrete Pavement Performance.* Federal Highway Administration.

Symons, M. (1999). *Portland Cement Concrete (PCC) Partial-Depth Spall Repair.* Fedral Highway Administration.

Trevino, M., McCullough, B. F., & Fowler, D. W. (2003). *Techniques and Procedures for Bonded Concrete Overlays.* Austin: Center for Transportation Research.

Ziegler, F. G., & Levi, G. (2008). *Standard Specifications for Road and Bridge Construction Volume 1 of 2.* Bismark, ND.: North Dakota Department of Transportation.

Appendix-A: Typical Partial-Depth Repair Schematics

There are two types of partial-depth repair that are common. The first is a failure that involves only one side of a joint in the pavement (Figure 72). This repair requires special care not to disturb the pavement on the side of the joint that is not affected by spalling. The second type of failure that requires repair is when both sides of a joint are spalled (Figure 73). For the double sided repair the grinder can simply follow the spalled area until all necessary material has been removed. Both of these repairs require that the existing joint be maintained through the use of a bond breaker.

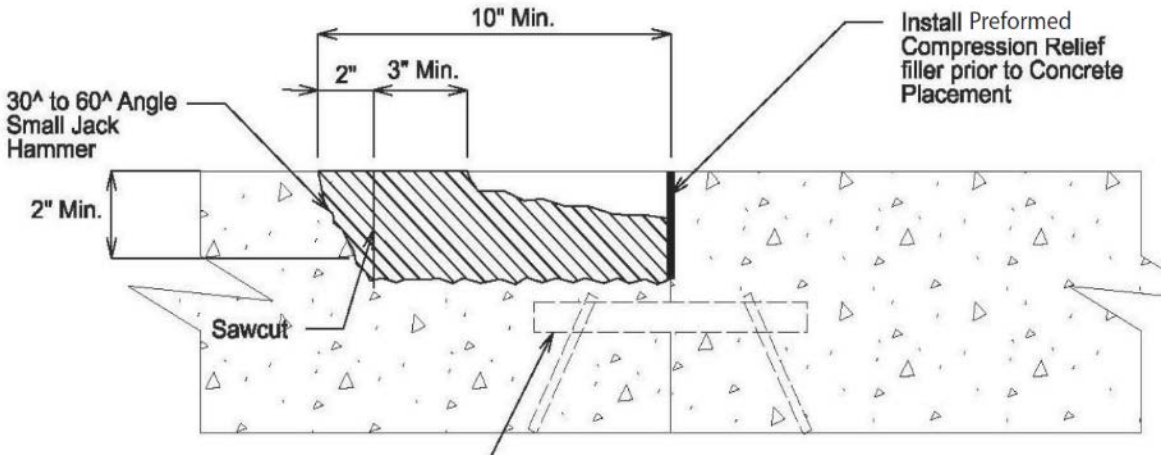

Figure 72: Single side partial-depth repair schematic

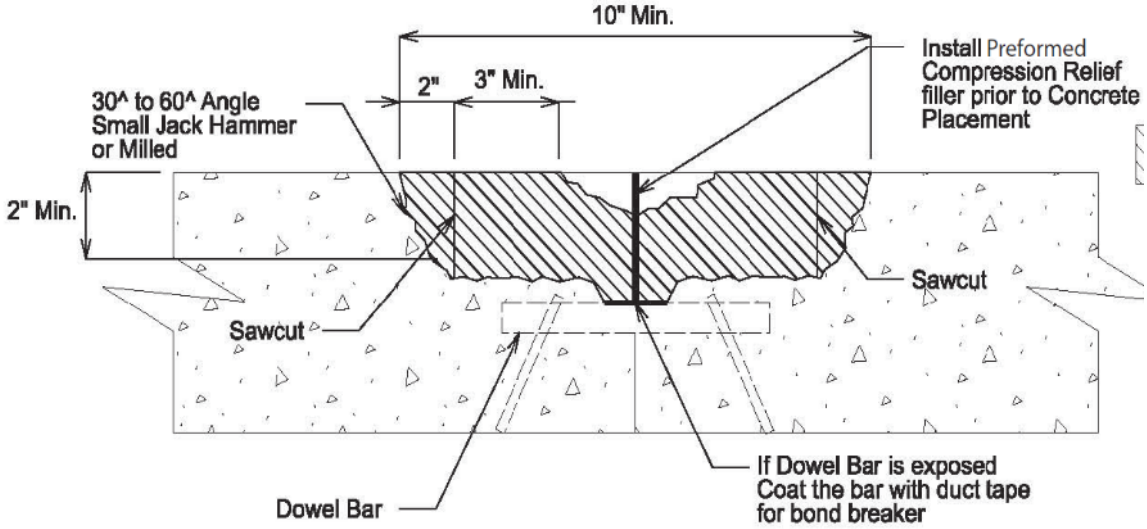

Figure 73: Two side partial-depth repair schematic

Appendix-B:

Best Practices

Methods

There are different approaches to installing partial-depth patches in PCC pavements. The way that a patch area is prepared is critical to the success of any patch. There are two widely accepted methods for preparing the area to be patched. The first is the saw cut and removal method; this creates a vertical edge at the border of the patch (Figure 74). The second is the grinding and chipping procedure which utilizes a light weight jack hammer to taper the edges of the patch area; the taper angle can vary from 30 to 60 degrees (Figure 75).

Figure 74: Saw-cut edge of a patch area, vertical face

Figure 75: Tapered edges of two opposing corner partial-depth repairs

The saw-cut method results in a smooth face for the patching material to bond with. The result is that the only bond available is a chemical bond between the patch and the substrate. Without the presence of any mechanical bond, aggregate interlock, the chemical bond alone is susceptible to any shrinkage that may occur (Figure 76).

Figure 76: Edge de-bonding due to shrinkage along a saw-cut patch area

The grinding and chipping method leaves a rough surface for the patching material to adhere with. This provides the patch material a greater surface area and develops a continuous mechanical bond at the patch/substrate interface. Once the edges have been prepared the patch area must be thoroughly cleaned so that no loose material or dust remains, compressed air is often used for this purpose.

After the patch area has been prepared it is ready to have patching material placed. A common approach to increase the bond that is developed is to place a thin layer of cement slurry to the patch surface. The patching material must be placed onto the slurry while it is still wet.

Another component of patching is to maintain all existing joints that are in the pavement. There are two materials commonly used for the purpose of preserving working joints in pavements. The first is a wax covered cardboard which is quite stiff and retains its shape during the placement of patching material. The wax provides a moisture barrier so that the patching material cannot leach through to eliminate the joint. The second is a manufactured fiber board that can be cut to size easily and also retains its shape (Figure 88). A measure that can be employed after the material has set is to saw-cut a new joint where the previous joint was located. This method is less than ideal but can be used if a joint was missed or if the joint maintaining materials fail.

Rapid set cementitious materials, as the name suggests, set up quickly. The finishing and curing of the filled patch is also of importance for the success of partial-depth patches. Two common types of curing procedures include the use of a curing compound or wetting the surface with water and covering with

plastic. A finished patch with a commercial curing compound can be seen in Figure 87. Curing with water and plastic can yield good results (Figure 77). Patches that receive no curing method of any kind, simply exposed to the air, tend to dry out rapidly and experience surface shrinkage cracking (Figure 78).

Figure 77: Wetted and covered curing method result

Figure 78: Cracked patch that was placed with no curing

Minnesota Concrete Patch Repair Process (Field Visit Summary)

A field visit was made in August of 2012 to observe the current practices of partial-depth patching in Minnesota. The location was on Cedar Avenue south of the Mall of America in Eagan MN. The following is a comprehensive photo essay explaining the processes of partial-depth repair as mandated

by the Minnesota Department of Transportation construction specifications (Figure 79 through Figure 88).

Figure 79: Milling machine grinding a spalled section of concrete

Figure 80: Chipping the edges to meet MnDOT specifications

Figure 81: Air blasting the hole to remove excess loose material

Figure 82: Sandblasting the patch area prior to being filled

Figure 83: Truck loaded with the pre-bagged rapid set cementitious material

Figure 84: The mixing operation

Figure 85: Applying the concrete slurry that provides adhesion for the patch material

Figure 86: Placement, consolidation and finishing

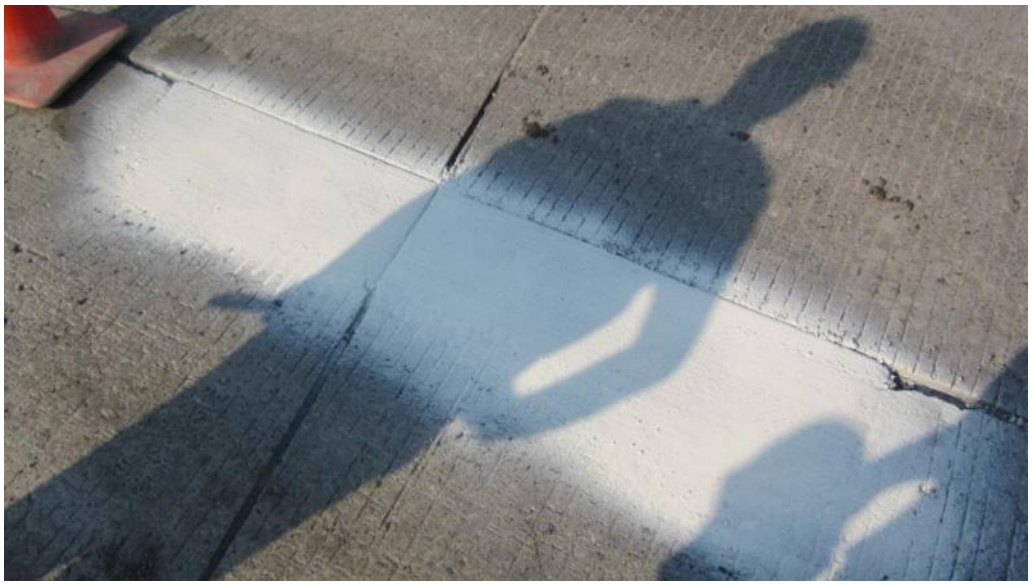

Figure 87: Finished patch with curing compound applied

Figure 88: A finished patch with fiber board inserted to maintain a working joint

Appendix-C:

Raw Data

Phase 1 (task 2)

Product	3 Hour Comp (psi)
Five star	4527
Futura 45	4333
Futura 15	4179
Rapid Set Concrete Mix	3965
Pavemend SL	3929
Pavemend SLQ	2402
Mono Patch	2392
TCC Taconite	1639
Akona	354
District 3 mix 1	0
3U18M	0
District 3 mix 2	0
3U18	0

Product	1 Day Comp (psi)
District 3 mix 2	6608
District 3 mix 1	6388
Pavemend SL	5811
Futura 45	5650
Five star	5299
Futura 15	5127
Mono Patch	4568
Rapid Set Concrete Mix	4526
3U18	4233
3U18M	3886
Pavemend SLQ	3725
TCC Taconite	2765
Akona	1720

Product	7 Day Comp (psi)
District 3 mix 2	9571
District 3 mix 1	9038
Futura 15	8083
Futura 45	7449
Pavemend SL	7437
3U18M	7327
3U18	7162
Five star	5835
Rapid Set Concrete Mix	5638
Mono Patch	5555
Pavemend SLQ	4285
Akona	3946
TCC Taconite	3020

Product	28 Day Comp (psi)
District 3 mix 2	11236
District 3 mix 1	9677
Pavemend SL	9172
Futura 15	8838
3U18M	8610
Futura 45	8509
3U18	8463
Mono Patch	8126
Five star	6518
Rapid Set Concrete Mix	6488
Akona	5454
Pavemend SLQ	4985
TCC Taconite	1852

Product	Modulus of Rupture - 4 hour flex (psi)
3U18	13
3U18M	2
Akona	160
District 3 mix 1	268
District 3 mix 2	175
Five star	606
Futura 15	606
Futura 45	466
Mono Patch	417
Pavemend SL	592
Pavemend SLQ	418
Rapid Set Concrete Mix	426
TCC Taconite Mix	306

Product	Length Change (%)	
	Air	Water
Rapid Set Concrete Mix	-0.04	0.032
Pavemend SLQ	0.018	0.026
Pavemend SL	-0.034	0.024
Mono Patch	0.006	0.364
Futura 45	-0.049	0.02
Futura 15	-0.08	0.002
Five star	-0.034	0.021
District 3 mix 2	-0.084	0.017
District 3 mix 1	-0.08	0.053
Akona	-0.025	0.07
3U18M	-0.085	0.021
3U18	-0.055	0.024
TCC Taconite	Un-measurable	-0.03

Product	Durability Factor DF
3U18	14.4
3U18M	23.59
Akona	2.87
District 3 mix 2	28.44
District3 mix 1	17.5
Five Star	4.57
Futura 15	17.9
Futura 45	100.17
Monopatch	96.23
Pavemend SL	16.78
Pavemend SLQ	117.23
Rapid Set Concrete Mix	18.2
TCC Taconite	121.66
Normal Concrete	95

Product	Set time (min)	
	initial	Final
3U18	174	230
3U18M	183	210
Akona	75	150
District 3 mix 2	180	230
District3 mix 1	180	230
Five star	11	12
Futura 15	25	34
Futura 45	47	72
Monopatch	33	44
Pavemend SL	11	20
Pavemend SLQ	4	6
Rapid Set Concrete Mix	18	27
TCC Taconite Mix	24	32

Product	Slump (inches)
3U18	0.75
3U18M	2
Akona	Self-leveling
District 3 Mix 1	7.5
District 3 Mix 2	2.5
Five Star	Self-leveling
Futura 15	Self-leveling
Futura 45	9
Mono Patch	7.75
Pavemend SL	Self-leveling
Pavemend SLQ	Self-leveling
Rapid Set	Self-leveling
TCC Taconite Mix	Not Available

Concrete for the pop out test					Avg.
	1	2	3	4	
Load (lbs.)	62970	74300	78930	76180	
Area (in^2)	12.566	12.566	12.566	12.566	
28 day comp (psi)	5011.00	5912.61	6281.06	6062.22	5816.7
Failure Type	5	5	5	5	
Air content (%)	5.30				
Slump (in.)	2.375				

Phase 2 (task3)

CoTE	mm/mm/°C
3U18M	8.95E-06
District 3 Mix 2	7.65E-06
Futura 45	6.62E-06
Rapid Set	1.05E-05
PCC Granite	8.28E-06
PCC Limestone	9.97E-06

Elastic Modulus Values	(ksi)
3U18M	7600
District 3 Mix 2	7400
Futura 45	7900
Rapid Set	4450
PCC Granite	7550
PCC Limestone	8000

Abrasion Resistance test	Abraded Volume (cm^3)	Abraded Area (cm^2)	Abrasion Coefficient
3U18M	10.45	6.45	1.62
District 3 Mix 2	11.21	6.45	1.74
Futura 45	10.75	6.45	1.67
Rapid Set	18.60	6.45	2.88
PCC Granite	12.09	6.45	1.87
PCC Limestone	15.72	6.45	2.44

Box Plots for Elastic Modulus and CoTE

The variability amongst the four replicate samples for both the elastic modulus and the coefficient of thermal expansion are displayed in the following box and whisker plots (Figure 89 and Figure 90). The

minimum and maximum values that were recorded are indicated by the error bars in the plots. Subsequent measurements are represented by the top and bottom of the boxes while the average value of the four replicates lies where the green box meets the red box.

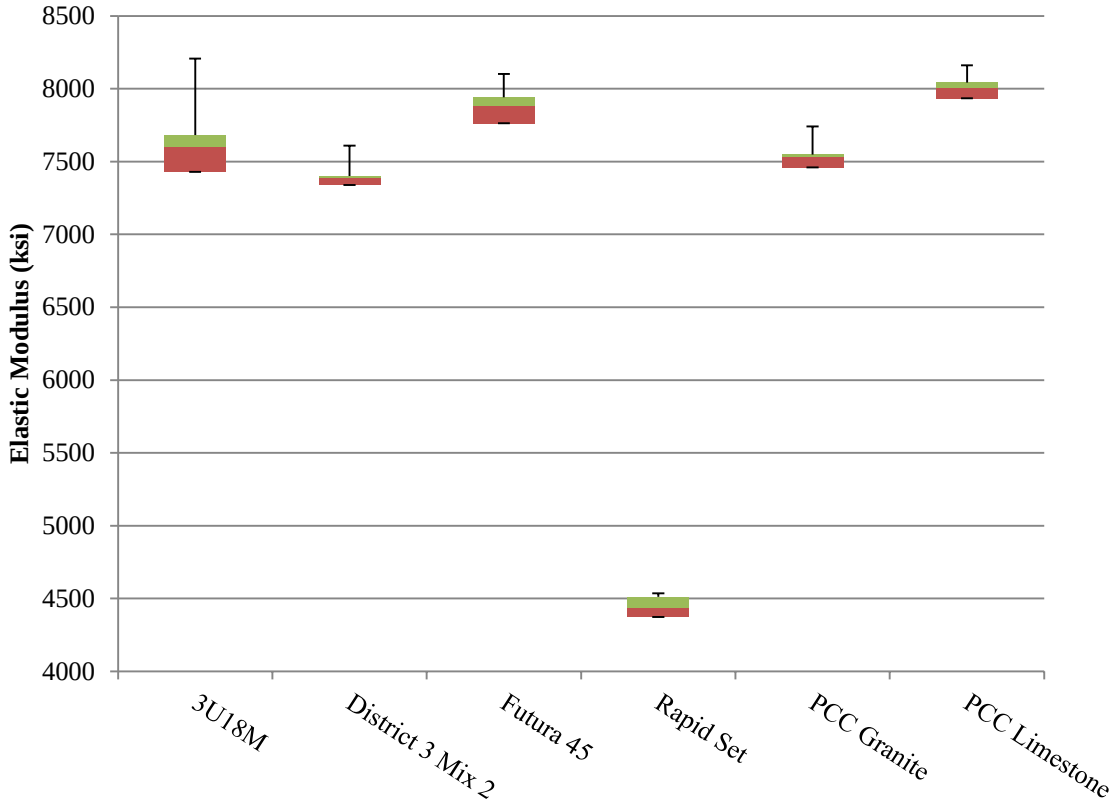

Figure 89: Box and whisker plot for the elastic modulus

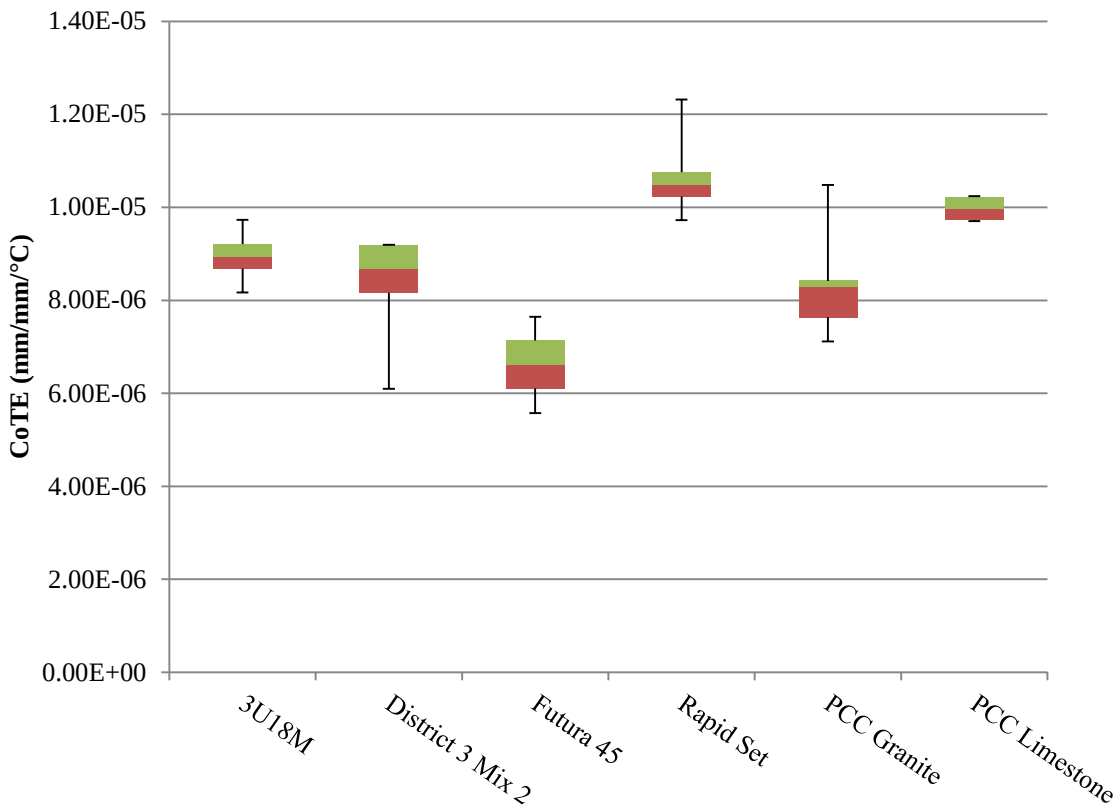

Figure 90: Box and whisker plot for coefficient of thermal expansion

Phase 3 (task 4)

Peak values @ initial failure				
			P (lbs)	δ (in)
D3-2-A	Water	A-W	4961	0.08926
D3-2-B	Water	B-W	5345	0.0833
D3-2-C	Water	C-W	5147	0.077028
D3-2-D	Grout	D-G	4718	0.074422
D3-2-E	Grout	E-G	4243	0.075685
D3-2-F	Grout	F-G	5391	0.089378
3U18M-I	Water	I-W	5461	0.097539
3U18M-J	Water	J-W	5271	0.097498
3U18M-K	Water	K-W	4987	0.105005
3U18M-L	Grout	L-G	4977	0.091221
3U18M-M	Grout	M-G	5291	0.086386
3U18M-N	Grout	N-G	4538	0.082735
D3-2-G	Cold	G-C	5192	0.089195
D3-2-H	Cold	H-C	6499	0.086447
D3-2-O	Cold	O-C	5647	0.084879
D3-2-P	Cold	P-C	5209	0.071643
3U18M-W	FULL		15009.67	0.211967
3U18M-X	FULL		14620.68	0.253842
D3-2-Y	FULL		11048.45	0.150739
D3-2-Z	FULL		10716.58	0.138438

Averages			
	LOAD (lbs)	δ (in)	MOR (psi)
D3-2-ABC-W	5151.233	0.0832	459.8
D3-2-DEF-G	4784.083	0.0798	426.9
3U18M-IJK-W	5239.507	0.1000	466.5
3U18M-LMN-G	4935.333	0.0868	441.8
D3-2-COLD	5636.535	0.0830	500.7
3U18M-FULL	14815.18	0.2329	538.1
D3-2-FULL	10882.52	0.1446	395.3

Appendix-D:

Villanova Testing

EXAMINATION OF BOND STRENGTH OF PARTIAL DEPTH PATCHES USED IN RIGID PAVEMENTS

By

Matthew Joseph Panzitta

Thesis
Submitted to Department of Civil and Environmental Engineering
College of Engineering
Villanova University
in partial fulfillment of the requirements
for the degree of

MASTER OF SCIENCE

In

Civil Engineering

September, 2013

Villanova, Pennsylvania

EXAMINATION OF BOND STRENGTH OF PARTIAL DEPTH PATCHES USED IN RIGID PAVEMENTS

By

Matthew Joseph Panzitta

Approved: _____

Eric S. Musselman, PhD
Assistant Professor, Department of Civil and Environmental Engineering
Faculty Advisor

Approved: _____

Shawn P. Gross, PhD
Associate Professor, Department of Civil and Environmental Engineering
Faculty Reader

Approved: _____

Ronald A. Chadderton, PhD
Department Chairman, Department of Civil and Environmental Engineering

Approved: _____

Gary Gabriele, PhD
Dean of the College of Engineering

STATEMENT BY AUTHOR

This dissertation has been submitted in partial fulfillment of requirements for an advanced degree at the Villanova University and is deposited in the University Library to be made available to borrowers under rules of the Library.

Brief quotations from this dissertation are allowable without special permission, provided that accurate acknowledgment of source is made. Requests for permission for extended quotation from or reproduction of this manuscript in whole or in part may be granted by the head of the major department or the Associate Dean for Graduate Studies and Research of the College of Engineering when in his or her judgment the proposed use of the material is in the interests of scholarship. In all other instances, however, permission must be obtained from the author.

ACKNOWLEDGEMENTS

First, I would like to thank my parents, Joseph and Paula, and my brother, Andrew, for all the love and support that they have given me, especially over my 5 years at Villanova University.

I would like to give special thanks my advisor, Dr. Eric Musselman, for allowing me to work alongside him on this project and for all that he has taught me along the way. I would also like to thank Dr. David Dinehart, Dr. Shawn Gross, Dr. Joseph Yost, Dr. Frank Hampton, Mr. Zeyn Uzman, and all the rest of the Civil and Environmental faculty for all that they have taught me, both engineering and not, over my undergraduate and graduate career.

I would like to thank Linda DeAngelis, George Pappas, and Jeff Cook for all that they do. If it weren't for the three of them going above and beyond in their jobs, nothing would go nearly as smoothly as it does around the lab.

Lastly, I would like to thank all of the other graduate and undergraduate students who have worked in the lab with me and were always willing to lend a hand on my project. I especially want to thank Dave Reichmann, Frankie Nagel, and Phil Reilly for their help over our entire college careers, Sergio Yáñez for showing me the ropes in the lab for the past 3 years, and Matt Mancini for all of his help during testing.

TABLE OF CONTENTS

TABLE OF FIGURES

LIST OF TABLES

ABSTRACT

There is a constant need to find an economically feasible method of repairing damaged roadways and reopening them to traffic quickly. Partial-depth patching poses a potential solution to this problem for deteriorating concrete found in rigid pavements, but evaluating the bond performance of partial-depth patching materials is crucial before they can be accepted for use in state roadways. The current ASTM standard for evaluating bond strength of patching materials is the slant shear test, but prior research shows that this test can sometimes yield erratic results. More complex tests were performed to help determine the accuracy of current simplified testing methods in place, as well as to examine the effects of several variables on patching material-concrete substrate bond performance.

A series of four different tests were performed to evaluate bond strength. First was the slant shear test according to ASTM C 882. A pullout test using a concrete slab that had had 2” diameter cores removed and replaced with patching materials was also performed to obtain a quantitative measure of bond strength. Small concrete slabs were cast, prepared, and patched to simulate field installation of partial-depth patches and loaded in four point bending. Half of the slab specimens were loaded in static positive bending, while the remaining slabs were loaded cyclically in both positive and negative bending. Specimens were prepared using two different patching materials, Futura-45 and 3U18, for all tests, and a cement paste bonding agent was applied to half of all samples. The two common field preparation methods, milling vs. saw cutting and chipping, were examined in the slab bending tests. Load-displacement data, strain data, and visual observation were used to evaluate bond strength.

Results from the experiments showed that Furura-45 created better bond with base concrete than 3U18 did. The cement paste bonding agent actually served to weaken bond between patching material and substrate. Both types of patch preparation had advantages, but the best bond was found to occur in milled prepared patches patched with a material with a high volume of paste and little coarse aggregate. Slant shear, despite having a fairly large spread in results, was deemed sufficient for evaluating patching material bond strength when compared to more complex evaluation methods.

CHAPTER 1 INTRODUCTION

1.1 Overview

Roadway deterioration occurs over time due to vehicle traffic and exposure to the elements. In order to maintain rider comfort and structural stability of concrete roadways in a more cost effective manner than roadway replacement, state departments of transportation (DOTs) have turned to the use of both partial- and full-depth repair techniques of rigid pavements. Partial-depth repairs use an assortment of different materials and preparation methods to achieve this goal. Patch materials are placed on top of prepared base concrete in partial-depth repairs, making the bond between the surface of the patch material and that of the base concrete crucial to the effectiveness of the patch. Presently, little research exists to determine which materials and preparation methods are most effective for partial depth repairs, and nearly all of the literature that does examine patching materials does so in field observations rather than laboratory testing. Laboratory testing of materials and installation practices used in partial-depth patches is necessary to ensure the most efficient application of partial-depth patches used in concrete roadways and to minimize the risk of patch debonding failures.

1.2 Research Objectives

In accordance with the research needs in the area of bond strength evaluation for rigid pavement partial-depth patching materials, the goals of this research are as follows:

(1) To review current DOT and third party requirements and practices for rigid pavement roadway repairs;

(2) To review current ASTM standards used for the evaluation of bond strength of cementitious materials;

(3) To evaluate the effectiveness of several different laboratory tests used to determine bond strength of partial-depth patching materials;

(4) To compare the bond strength of two different patching materials used in industry;

(5) To evaluate the effects on bond strength of the two most common patch preparation methods used in partial-depth repairs;

(6) To evaluate the effectiveness of using a cement paste slurry as a bonding agent applied to the surface of the base concrete before the patching material; and

(7) To make recommendations on the material testing and preparation practices used for partial-depth repairs of concrete roadways.

1.3 Background

1.3.1 Materials

The patching materials used in patching applications for rigid pavements are cement-based materials conforming to ASTM C 928 (ASTM, 2009). These materials typically gain strength rapidly so as to minimize the construction impact of the patching process by reopening roadways to traffic as quickly as possible. Several manufacturers produce rapid strength gain materials for repair applications. These bag mixes can simply be mixed with water in an on-site mixer and applied directly to the prepared roadway in need of repair, as seen in Figure 1-1. Other patch materials can be mixed on site from raw materials as prescribed by appropriate regulating bodies. The specific materials used in this examination, 3U18M and Futura-45, are discussed in detail in Chapter 2.

Figure 1-1 Futura-45 bag mix being placed in the field (http://www.wrmeadows.com/futura-45-horizontal-repair-mortar/)

1.3.2 Uses

Rapid strength gain patching materials are used for repairs to damaged portions of concrete roadways. Partial-depth repairs and full-depth repairs constitute the primary uses of such materials. Partial-depth repairs involve the removal and replacement of deteriorated concrete to a depth no more than half of the total depth of the pavement layer (Frentress & Harrington, Guide for Partial-Depth Repair of Concrete Pavements, 2012). Damage of the base concrete may have been caused by a variety of factors, including but not limited to freeze-thaw damage, vehicle wear, snowplow damage, and the inclusion of incompressible solids into cracks (American Concrete Pavement Association, 2004). Full-depth repairs involve the cutting and removal of a section of the pavement layer in its entirety without disturbing the underlying base materials and replacing it with a rapid strength gaining material (PennDOT patching practice). This research focuses on the bond strength properties of patching materials; however, some of the conclusions of the testing program may be transferrable to full-depth repair applications.

1.3.3 Preparation Techniques

Two methods of partial-depth patch area preparation are currently accepted and used in the field: the milling method and the saw cut and jackhammer method. Milling requires the use of a milling machine attached to a piece of heavy construction equipment. The miller consists of a rotating metal drum with large teeth. The milling machine is lowered onto the surface to be prepared and the teeth remove the top of the base concrete, eliminating the deteriorated concrete and exposing a textured surface of sound concrete. Examples of milling machines are shown in Figure 1-2.

Figure 1-2 Examples of milling machines used to remove deteriorated concrete (Frentress & Harrington, Guide for Partial-Depth Repair of Concrete Pavements, 2012)

The second method has workers saw cutting the extents of the patch to the appropriate depth. A series of interior cuts are then made to aid in the removal of the deteriorated concrete. The interior concrete is removed by chipping with a jackhammer to the depth of the patch, leaving a square or rectangular void in the roadway. For both preparation methods, any loose material is removed from the voided area before the patching material is applied to promote the best bond. Figure 1-3 depicts the different methods of patch preparation in the field.

(a) Saw cut and chipped patch area *(b) Milled patch area*

Figure 1-3 Different methods of partial-depth patch preparation (Frentress & Harrington, Guide for Partial-Depth Repair of Concrete Pavements, 2012)

Before the patching material is applied to the surface of the base concrete, the base concrete needs to be either dampened with a light coat of water or have a bonding agent applied. Some patching materials recommend applying a cement mortar or a slurry created using the patching material itself to the surface of the base roadway before placing the patching material (Frentress & Harrington, Partial-Depth Repairs for Concrete Pavaments, 2011). The bonding agent is intended to promote a stronger bond between the base concrete and the patching material.

1.4 Organization of Report

The remainder of this report begins with a review of the existing literature on partial-depth patching materials and procedures set forth by different organizations. The literature review is followed by a test matrix and a description of the instrumentation, apparatus, and testing procedures used in this investigation. A summary of the results obtained from the series of four tests performed is presented. Finally, comparisons among and between the tests, a summary, conclusions addressing the research objectives, and recommendations for future research are offered at the close of the report.

CHAPTER 2 LITERATURE REVIEW

This chapter sets forth industry standards for partial-depth patches, examines relevant published research already performed, looks at the materials being used in this research, and reviews the current testing procedures used to evaluate bond strength.

2.1 Partial-Depth Patching

As discussed briefly in Section 1.3.2, partial-depth repairs are performed to rehabilitate rigid pavement roadways whose damage is restricted to the upper portion of the pavement. This section of the report discusses current practices used by the Pennsylvania and Minnesota Departments of Transportation (PennDOT and MnDOT, respectively), as well as guides set forth by other agencies and recommendations found in published literature based on field and laboratory research.

2.1.1 PennDOT Specifications

Because the research was conducted at Villanova University in southeastern Pennsylvania, construction practices for the Pennsylvania state DOT were examined. PennDOT Publication 408/2000 contains PennDOT's construction specifications for all projects performed by the organization. Section 500 is concerned with rigid pavements, with Section 516 specifically referring to concrete pavement patching. PennDOT practices specify only full-depth repairs in this portion of the document, which are not necessarily closely related to the focus of this research (Pennsylvania Department of Transportation, 2000).

However, Section 525 of the same document discusses the practices for spall repair in concrete pavements, which is effectively the same as partial-depth repair. Penn DOT allows for several types of patching materials to be used, including their specified road

mix concrete, a modification of that road mix using type III cement, a rapid strength gaining patching material from an approved outside manufacturer, a latex modified concrete, and a thin bonded portland cement concrete inlay (Pennsylvania Department of Transportation, 2000). A list of approved bag patching materials can be found in PennDOT Bulletin 15 (Pennsylvania Department of Transportation, 2004). In order to use a rapid strength gain patching material, the section of roadway to be patched must be saw cut in a rectangle extending at least 3 inches beyond the extents of the deteriorated concrete and to a depth of at least 1.5 inches. The deteriorated concrete is chipped using a small jackhammer to the appropriate depth. PennDOT requires the use of either a cement paste or epoxy bonding agent for concrete patched with PennDOT Class AA Cement Concrete or Class AA Cement Concrete modified with type III cement, but defers to the manufacturer's instructions for all bagged rapid set patching materials (Pennsylvania Department of Transportation, 2000).

2.1.2 MnDOT Specifications

One of the patching materials used in this investigation, 3U18, is a MnDOT custom blended material, so the construction practices associated specifically with this material were investigated. Additionally, much of the literature that exists concerning research in the area of partial-depth patching references MnDOT practices or is based on field observations that took place in Minnesota. The MnDOT Concrete Manual contains a section focusing on concrete pavement rehabilitation, and it covers four different types of repairs: partial-depth patching, full-depth patching, slab replacement, and joint/crack sealing. For partial-depth patching preparation, MnDOT allows for either milling or saw cutting and chipping of the deteriorated concrete, although milling is the preferred

practice. Depth of concrete removal for partial-depth repairs ranges from a minimum of 2 inches up to a maximum of half of the total slab depth. The patch area should be sand blasted and air blasted to remove any remaining loose material after milling or chipping to prepare the surface to bond with the patching material. A cement grout bonding agent is required per MnDOT specifications. MnDOT also specifies that 3U18 should be used as the patching concrete for all partial-depth repairs. (Minnesota Department of Transportation, 2003)

2.1.3 Other Partial-Depth Patching Guides

Frentress and Harrington, through the Iowa State University Institute of Transportation, published a guide for the preparation and installation of partial-depth patches in concrete roadways to be distributed throughout the United States. The guide separates partial-depth repairs into three categories. The first, spot repairs of joints, cracks, and spalls, refers to small, isolated areas of deterioration within the pavement slab. Spot repairs are typically shallow, requiring only about 2 inches of concrete removal to reach sound concrete, and are frequently prepared using the saw and chip method. Extended-length repairs, the second type of repair, are typically larger and deeper than spot repairs, typically extending to a length of over 6 feet along a joint or crack and to a depth of up to half the total pavement depth. It is generally more cost effective to mill extended-length repairs rather than to saw cut and jackhammer because of the large area. The final type of repairs are bottom-half spot repairs, which are essentially small, full-depth replacements at corners and edges of the pavement slab. Figure 2-1 shows a diagram of the different types of repairs outlined by Frentress and Harrington.

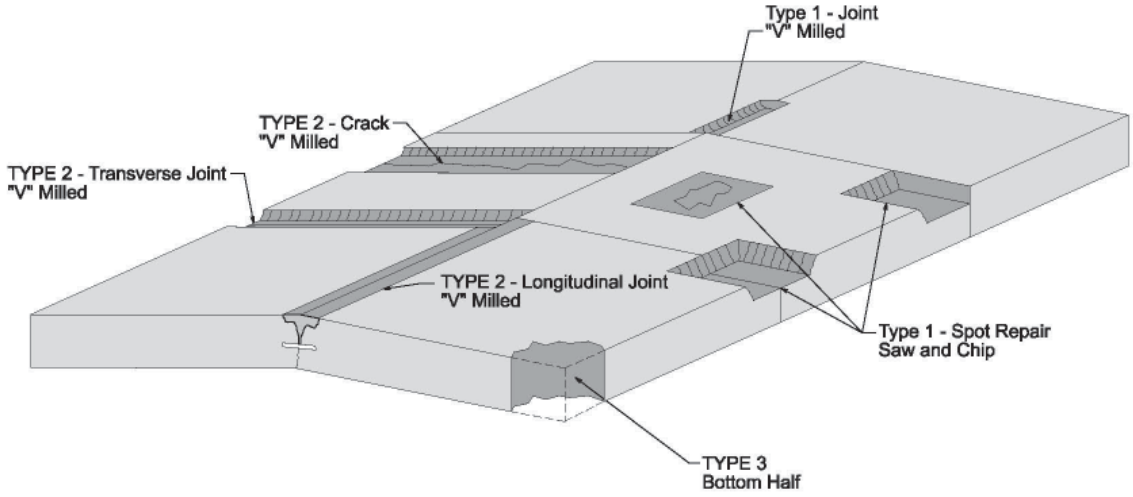

Figure 2-1 Different types of partial-depth spall/joint/crack repairs (Frentress & Harrington, Guide for Partial-Depth Repair of Concrete Pavements, 2012)

Frentress and Harrington offer suggestions for appropriate patching materials for partial depth repairs. They recommend the use of high quality concretes using type I, II, and III portland cement to repair concrete roadways. State DOTs have different strength requirements for patching materials before roadways can be reopened to traffic, so the rate of strength gain should be considered as a major factor when selecting a patching material. The authors cite MnDOT's success using the 3U18 mixture for their partial-depth patching projects for over 30 years, and they provide a mix design for the 3U18 concrete.

The patching guide also discusses the use of bonding agents for partial-depth patching to promote bond strength. Many states use a grout recipe that has proven sufficient to provide bond strength between the base concrete and the new patching material. The grout is comprised of 2 parts type I cement, 1 part sand, and 1 part water, and serves to fill in small spalls left behind from the deteriorated concrete removal process. Kansas DOT recommends a watery cement paste of 1 part type I cement to 3

parts water to wet the slab and prevent the patching material from absorbing moisture from the base concrete. Not all patching materials require the use of a bonding agent, and the manufacturer's instructions should be followed for each individual mix according to Frentress and Harrington.

Frentress and Harrington's guide also offers a suggestion for finishing to help promote better bond strength. Floating from the center of the patch to the outsides is recommended during finishing. This action causes the edges of the patch to become pinched to the base concrete pavement, helping to create a stronger bond between the two materials. (Frentress & Harrington, Guide for Partial-Depth Repair of Concrete Pavements, 2012)

2.1.4 Field Evaluations

Only a limited amount of research has been published on the topic of partial-depth patching because of the difficulty of performing laboratory testing that is representative of field conditions and the challenge of acquiring quantitative data from field observation.

2.1.4.1 Parker and Shoemaker

Parker and Shoemaker (1991) examined the performance of partial depth patches installed on two Alabama highways to observe the effects of different materials, ambient casting temperature, condition of surrounding concrete, patch preparation techniques, and the presence of an anchoring system. Patches were installed on I-59 and the more heavily trafficked I-85. Materials used to construct patches were a commercially available bag mix, Roadpatch II, and two portland cement concrete (PCC) mixtures made with type III cement, one with steel fibers and one without. Some patches were installed in the

summer heat, while others were poured in the cool of the winter months. Some patches contained an anchoring system comprised of a U-bent #4 reinforcing bar epoxied into holes drilled in the base concrete, with the remaining test sites receiving no anchors. A portion of the patches installed were saw cut to a depth of 1-2 inches before having the deteriorated concrete removed with a jackhammer. The remaining patches were jackhammered without first being cut. None of the patches had any further preparation or bonding agent application in order to maintain a construction time that could allow for the reopening of the highway within an 8-hour work shift.

All evaluations of patch grouping are based on periodic observations of the test sites with the final observation period occurring no more than 23 months after the patches were placed. Localized cracking and shallow spalling near joints and patch-slab boundaries were early indicators of deterioration. No patches displaced as a whole, so loss of bond was not viewed to be a serious problem, although Parker and Shoemaker suggested that loss of bond may have worsened cracking seen in the patches. A summary of patch deterioration based on the visual observation is shown in Figure 2-2. From the distress data, the authors reached several conclusions. Overall, the patches poured in warm weather fared better than those poured in the cooler weather. Fibrous PCC patching material performed better than the non-fibrous PCC or the Roadpatch II, having the most patches with no distress and the fewest with severe distress. Due to the higher volume of traffic and previously repaired base concrete roadway on I-85, the patches placed in I-59 saw less deterioration over the observation period. I-59 seemed to show a benefit to the inclusion of sawing patch areas before chipping out deteriorated concrete, while I-85 showed the opposite. Overall, however, the inclusion of the sawing step in

patch preparation showed improvement in patch performance. The inclusion of anchors in patches showed little difference in the durability of patches, indicating that loss of bond was less important to patch performance than originally believed by Parker and Shoemaker. (Parker Jr. & Shoemaker, 1991)

Variable (1)	Percent Patches in Distress Category		
	No distress (2)	Moderate distress (3)	Severe distress (4)
Warm (21)	67	24	9
Cool (22)	32	27	41
Type III (15)	33	27	40
Roadpatch (14)	36	36	28
Fibrous (14)	79	14	7
Unanchored (22)	41	32	27
Anchored (21)	57	19	24
Not sawed (10)	20	20	60
Sawed (33)	58	27	15
All patches (43)	49	26	25

Note: Numbers in parentheses indicate number of patches.

(a) I-59

Variable (1)	Percent Patches in Distress Category		
	No distress (2)	Moderate distress (3)	Severe distress (4)
Warm (25)	28	56	16
Cool (14)	14	29	57
Type III (14)	7	57	36
Roadpatch (13)	8	62	30
Fibrous (12)	58	17	25
Unanchored (20)	15	65	20
Anchored (19)	32	26	42
Not sawed (13)	23	54	23
Sawed (26)	23	42	35
All patches (39)	23	46	31

Note: Numbers in parentheses indicate number of patches.

(b) I-85

Figure 2-2 Parker and Shoemaker patch condition observations for (a) I-59 and (b) I-85

2.1.4.2 Chen, Won, Zhang, and Scullion

Chen, Won, Zhang, and Scullion (2009) presented a case study of the effectiveness of polymeric patching materials used to perform partial depth repairs on

three roadways in Texas. High traffic roadways showing signs of cracking and spalling were repaired using two different patching materials each containing a polymer resin (either polyurethane or epoxy based, in place of portland cement), aggregate (sand to 9.5 mm stone), and an initiator. Visual methods were used to measure the condition of the roadway before and after patching. Condition was based on a distress score, a measure of visible surface wear from traffic and environmental loading, and international roughness index (IRI), measured using high speed laser profilers to represent ride smoothness. The first site examined was SH6 in the Houston District. The polyurethane patch was used on SR6, and patched areas showed an improved distress score and a decrease in IRI over the 6-year period following the placement of the patches. The same patching material was used to make repairs to US290 in the Houston District. Overall, the patches on US290 prevented further deterioration of the roadway by substantially improving the distress score of the roadway and maintaining the IRI. The final roadway examined was US75 in the Paris District, which was repaired with an epoxy based patching material. The partial depth repair method with the epoxy based material was deemed much more cost effective than full depth repairs for slabs that are stable (no sign of settlement or slab movement).

The paper reached many helpful conclusions based on the results of the observations of the three roadways. Chip-and-patch methods worked as well as saw-and-patch methods of repair as long as all delaminated material was removed and was more cost effective than saw-and-patch. The polyurethane patching material was able to bridge cracks in the lower layers of the concrete pavement and showed a high resistance to the formation of new cracks and the propagation of existing cracks. Although this research dealt with polymeric patching materials, the response of pavements due to the presence of

a partial depth patch can be transferred to other materials. (Chen, Won, Zhang, & Scullion, 2009)

2.2 Materials Being Studied

This section provides available information on the two different patching materials being studied.

2.2.1 MnDOT 3U18 Modified

The Minnesota Department of Transportation has been using its custom blend, called 3U18, in partial depth repair applications for over 30 years (Frentress & Harrington, Guide for Partial-Depth Repair of Concrete Pavements, 2012). The complete mixture requirements for an acceptable 3U18 mix can be found in the Mn/DOT Standard Specifications for Construction (Minnesot Department of Transportation, 2005). Frentress and Harrington published a simplified mix design in their partial-depth repair guide which can be found below in Figure 2-3.

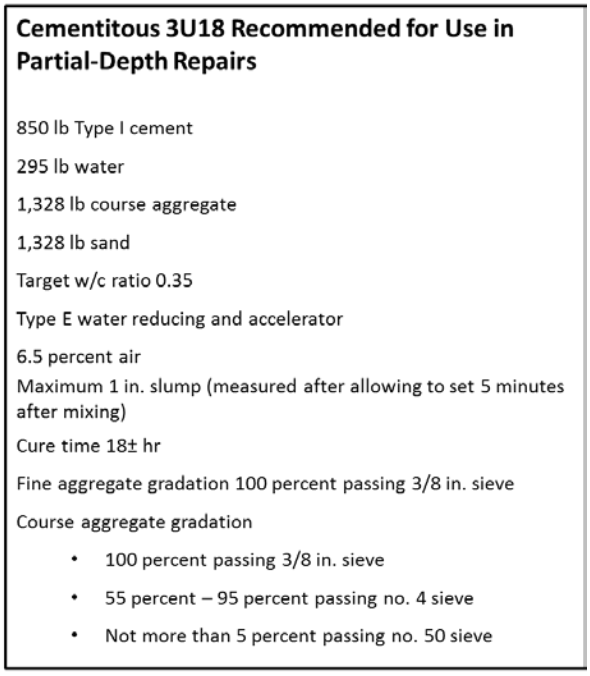

Figure 2-3 Mn/DOT 3U18 mix design reproduced from: (Frentress & Harrington, Guide for Partial-Depth Repair of Concrete Pavements, 2012)

The 3U18 mix achieves a compressive strength of over 3000 psi in an 18 hour cure time that can be shortened with appropriate admixtures if necessary. The 3U18 can be mixed by hand, in a small paddle mixer, or in a concrete mixing truck, depending on the quantity demand for a given repair. The mixture can also be purchased pre-blended in 75-lb bags for small projects (Frentress & Harrington, Guide for Partial-Depth Repair of Concrete Pavements, 2012).

For this project, a modified version of 3U18 is used, which includes supplementary admixtures in addition to the materials listed in Figure 2-3. The mixture was custom blended for Mn/DOT and shipped in 80-lb bags that needed to be supplemented with additional coarse aggregate.

2.2.2 Futura-45

Futura-45 is a commercially available bag mix produced by W. R. Meadows. This mix consists of cements, sands, and chemical admixtures, and can be extended by up to 50% by weight with coarse aggregate. The manufacturer data sheet indicates that Futura-45 obtains compressive strengths of 3500 psi in 3 hours, 5200 psi in 1 day, and 8500 psi in 28 days. High early strength allows for roadways patched with Futura-45 to be reopened within a short period of time, usually around 3 hours. One-day bond strengths of 1500 psi and 28-day strengths of 2500 psi are expected from the Futura-45 mix per ASTM C 882 (to be discussed in section 2.3.1). (W. R. Meadows, Inc., 2013)

2.3 Bond Testing

The following sections discusses the current methods used to evaluate the bond strength of patching materials used in partial-depth patching and previous research conducted on bond strength of such materials.

2.3.1 ASTM C 882 Standard Method for Bond Strength of Epoxy-Resin Systems Used with Concrete by Slant Shear

ASTM C 882 is currently the accepted standard for evaluating bond strength of materials such as those used for partial-depth patching (ASTM, 2012).

2.3.1.1 Procedure

ASTM C 882 requires that composite cylinders that are fabricated as two half-cylinders of the dimensions shown in Figure 2-4 be tested in compression to failure along the bonded plane. Mortar half-cylinders, comprised of type III cement, sand, and water, are cast at an angle of 30° from vertical. The mortar used must reach a compressive strength of at least 4500 psi at 28 days.

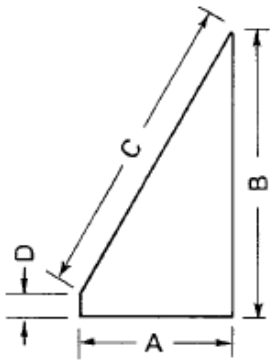

	Dimensions	
	mm	in.
A—Diameter	75±2	[3.000]
B—Height	140±2	[5.598]
C—Slant height	150±2	[6.000]
D—Base height	10±2	[0.402]

Figure 2-4 Half cylinder dimensions (ASTM, 2012)

The mortar half-sections should be soaked in water for 24 hours then placed on an absorbent material for 10 minutes prior to having the second material bonded to them. After applying a bonding agent (if necessary), the half-cylinders are placed into standard 3 in x 6 in cylinder molds. Each cylinder is held such that the shear plane is vertical so that a ½ in layer of the patching material can be applied. Cylinders are then turned upright, and the patching material is used to fill the cylinder in two layers, rodded 25 times each. After the curing period, composite specimens are tested in compression as composite cylinders in accordance with ASTM C 39/C 39M-12a. Bond strength is the shear stress between the two half-sections of each cylinder at failure, calculated as the total load carried by the cylinder divided by the bonded area. (ASTM, 2012)

2.3.1.2 Use of ASTM C 882

Because ASTM C 882 is the generally accepted standard for evaluating the bond strength of cementitious materials, many major agencies such as AASHTO use this assessment as part of their testing regimen for the acceptance of new materials.

AASHTO's National Transportation Product Evaluation Program (NTPEP) lists ASTM C 882 in its battery of tests for rapid-set concrete patching materials for portland cement concrete that it performs for manufacturers before recommending products for use in roadways by state departments (AASHTO, 2012).

Cervo and Schokker (2010) performed AASHTO's NTPEP testing regimen on a series of six bridge deck patching materials at Pennsylvania State University. The regimen included the ASTM C 882 Bond by slant shear testing. At the end of their paper, Cervo and Schokker proposed changes to the testing program. They concluded that ASTM C 882 should be omitted from the battery of tests to be performed on patching materials, citing high variability and the production of an unreliable set of data. (Cervo & Schokker, 2010)

2.3.2 ASTM C 1583 Standard Test Method for Tensile Strength of Concrete Surfaces and the Bond Strength or Tensile Strength of Concrete Repair and Overlay Materials by Direct Tension (Pull-off Method)

ASTM C 1583 is another ASTM standard test that can be used to examine the tension strength of concrete or the bond strength between a concrete substrate and another material attached to its surface.

2.3.2.1 Procedure for Bonded Specimens

A test area of base concrete is prepared and cleaned as is specified for bonding of an overlay or repair material in a field setting and the overlay or repair material is applied to a concrete substrate. A core rig with a 2" inside diameter diamond impregnated bit is used to create a circular cut extending to a depth of at least 0.5" into the base concrete beyond the bond interface. A steel disk with a 2" diameter and a minimum thickness of

1” that can be attached to a load application apparatus is bonded to the surface of the test specimen using an epoxy adhesive. The tensile loading device is attached to the steel plate and a tension force is applied to the specimen at a rate of 5 ± 2 psi/sec until failure. A schematic of assembled test setup for a bonded system is shown in Figure 2-5. At failure, both the failure load and the failure mode are recorded. Different modes of failure for this test can be observed in Figure 2-6.

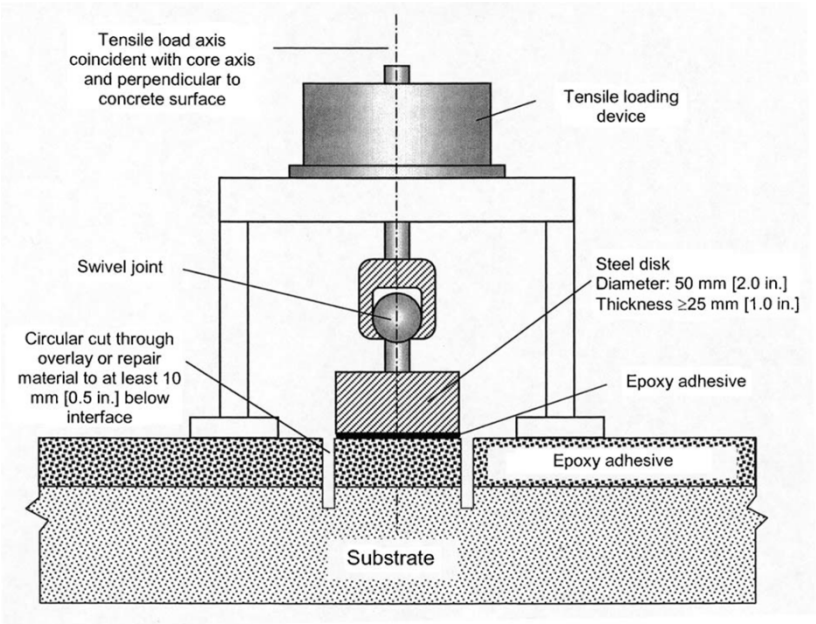

Figure 2-5 Schematic of setup to test material bonded to a concrete substrate

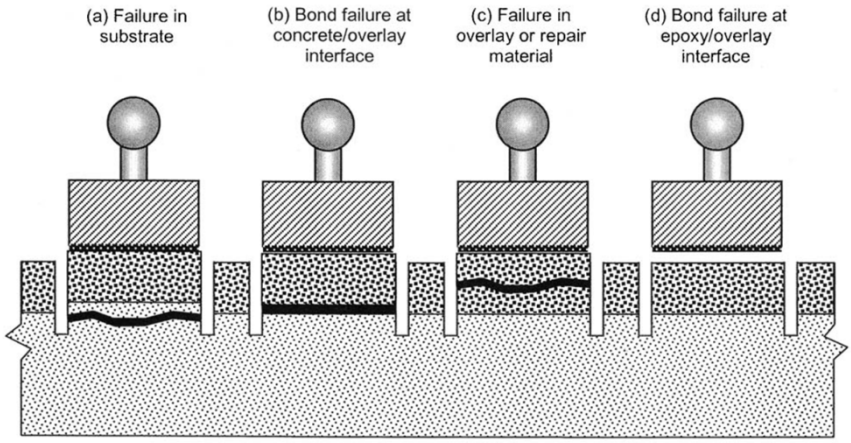

Figure 2-6 ASTM C 1583 failure modes

Test results should be disregarded if failure occurs at the bond between the steel disc and the overlay. Bond strength between the overlaid material and the concrete substrate can be calculated if the failure occurs in that bond area; material tensile strength can be calculated if the failure occurs within either of the material layers. Three failures of the same type must be recorded in order to reach any conclusion about the tensile or bond strength. Tensile or bond stress is calculated by dividing the tensile force at failure by the area of the specimen.

2.3.2.2 Use of ASTM C 1583

Carbonell Muñoz et al. (2013) found ASTM C 1583 to be somewhat effective in calculating bond strength between a normal-strength concrete substrate and an ultra-performance concrete repair material. Nearly all tests performed according to ASTM C 1583 failed by direct tensile rupture of the normal strength concrete. Because the bond was unbroken, an exact calculation of bond strength between the two materials could not be calculated, but the values obtained for the concrete rupture could be used to represent a minimum value for bond strength. However, a modulus of rupture calculation was also performed for the regular strength concrete based on the modulus of rupture equation presented in ACI 318-11. The observed rupture strength of the concrete was only about half of the calculated estimate, bringing forth some questions of the validity of the results obtained from the direct tensile tests. (Carbonell Muñoz, Harris, Ahlborn, & Froster, 2013)

Grace et al. (2013) performed a slightly modified version of ASTM C 1583 in an evaluation of shear key joints for a prestressed decked bulb T-beam bridge system. Ultra-high-performance concrete bonded to regular concrete was also used in this

investigation. Similarly to Carbonell Muñoz et al., Grace et al.'s results showed all specimens failing within the regular concrete portion of the test sample. This data also provided little data on the bond strength between the two materials beyond providing a minimum bond value. (Grace, Ushijima, Baah, & Bebawy, 2013)

2.3.3 Other Laboratory Testing

2.3.3.1 Patch Separation Test

As part of their bridge deck patching material study, Cervo and Schokker also developed a patch separation test. This test involved casting 8 ft x 4 ft slabs and casting a patch in them. The slabs were flipped such that the patches were on the bottom of the slab so the patch would be in the worst-case tension scenario and subjected to three-point bending by an actuator as seen in Figure 2-7. The slab was loaded to failure, stopping at 5 kip intervals to record load and deflection data.

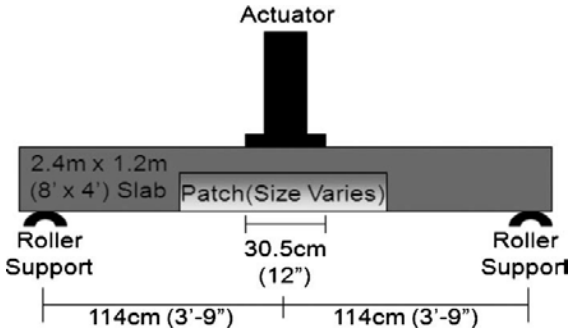

Figure 2-7 Three-point bending test schematic (Cervo & Schokker, 2010)

All slabs failed at a load higher than the calculated moment capacity of the slab. Cracking was visible at the interface between the patch and the base concrete. However, none of the 8 patches tested completely separated from the base concrete. Cervo and Schokker recommended the inclusion of the patch separation test as a part of a testing regimen for concrete patching materials because it demonstrates the ability of the patch

material to act as continuous with the concrete substrate and identifies weak points in the composite system. (Cervo & Schokker, 2010)

2.3.3.2 Patching Material Pullout Tests

ASTM D 4435 Standard Test Method for Rock Bolt Anchor Pull Test provides a schematic of a test setup for the rock bolt anchor pull, shown in Figure 2-8, that could easily be adapted to test the bond strength of patching materials. Such a test could be used to pull an anchor embedded in patching material bonded to prepared base concrete. The stress required to break the bond between the patching material and concrete substrate could be calculated by dividing load data acquired by the load cell by the bond area between the two concrete materials.

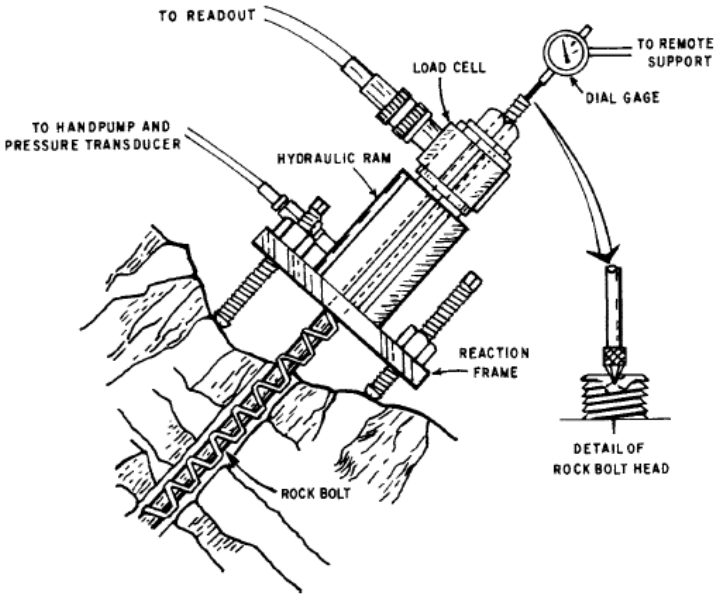

Figure 2-8 typical rock bolt pull test schematic (ASTM, 2008)

CHAPTER 3 EXPERIMENTAL PROGRAM

This chapter describes the specific methods and apparatus used in the experimental testing program. The following four tests were performed to examine the bond strength of patching materials:

- slant shear
- core pullout
- static slab bending and
- cyclic slab bending.

3.1 Test Matrix

Table 3-1 contains the test matrix for the testing program. The matrix describes the specimens that were examined in each test. The two materials tested were those discussed previously, Mn/DOT 3U18 modified and Futura-45. Bonding preparations included samples having a cement paste slurry used as a bonding agent and samples with water applied to produce a saturated surface dry base. For the slab bending tests, the methods of patch preparation were milled preparation and saw cut and jackhammer preparation, and the two methods of loading were static loading in positive bending and cyclic loading in both positive and negative bending. The specific details of each test are discussed throughout Chapter 3.

Table 3-1 Test Matrix

Test Matrix	
Variable	# Samples
Core Pullout	
Materials	2
Bonding Preparation	2
Duplicates	4
Total	**16**
Slant Shear	
Materials	2
Bonding Preparation	2
Duplicates	4
Total	**16**
Slab Bending	
Materials	2
Methods of Patch Preparation	2
Bonding Preparation	2
Load Cases	2
Duplicates	2
Total Test Samples	32
Controls	4
Total	**36**

3.2 Patching Material Mixing Procedure

The same procedure for mixing each patching material was followed for all test methods. A 3 cubic foot capacity electric mortar mixer, seen in Figure 3-1, was used to mix all patching material samples.

Figure 3-1 Mortar mixer used for mixing patching materials

3.2.1 3U18 Mixing Procedure

The mixture design and instructions, as well as the materials for the mixing of the 3U18 patching material were provided by Mn/DOT, except for water and 90% calcium chloride pellets used as an accelerator, as were directions for mixing. Mn/DOT provided pre-blended 3U18 cements and smaller aggregates in 80-lb bags, coarse aggregate (⅜" diameter crushed granite) to be added to extend the mix, and an unknown combination of water reducing and accelerating liquid admixtures. (include 3U18M mix design)

Mix water, liquid admixture, and calcium chloride pellets were measured to the appropriate quantities and added to the mixer. The mixer was run until all of the calcium chloride had dissolved. Half of the coarse aggregate and half of the bagged 3U18 cement/aggregate blend were then added to the mixer and mixed to a uniform consistency. The remainder of the bagged mix and aggregate were placed in the mixer, and all of the materials were mixed for approximately 4 minutes to a uniform consistency. The contents of the mixer were then transferred to a wheelbarrow for mobility within the laboratory to the location where the patching material was to be placed. Figure 3-2 shows fresh 3U18 in a wheelbarrow before being placed.

Figure 3-2 Fresh 3U18 patching material before placement

Table 3-2 shows the 7-day compressive strengths for the 3U18 concrete samples for the four days on which this patching material was cast. Standard 4 in x 8 in cylinders were used to calculate compressive strength. All cylinders were cast, prepared, and tested according to ASTM C 39. The average compressive strength of all 3U18 samples was 10,667 psi.

Table 3-2 3U18 compressive strengths

3U18 Samples (4x8 cylinders)		
6/13/2013		
Sample #	*Load (lb)*	*Stress (psi)*
1	128890	10257
2	129710	10322
3	139950	11137
Average	132850	**10572**
6/14/2013		
Sample #	*Load (lb)*	*Stress (psi)*
1	137260	10923
2	137480	10940
3	139770	11122
Average	138170	**10995**
6/17/2013		
Sample #	*Load (lb)*	*Stress (psi)*
1	142090	11307
2	141000	11221
3	139540	11105
Average	140877	**11211**
6/18/2013		
Sample #	*Load (lb)*	*Stress (psi)*
1	124740	9926
2	122180	9723
3	125940	10022
Average	124287	**9890**

3.2.2 Futura-45 Mixing Procedure

Dry Futura-45 patching material was provided by a local distributor of W. R. Meadows products in 50-lb bags. The prepackaged mix was simply placed in mixing drum with the amount of water recommended on the packaging and mixed for 3-5 minutes in the mixer. Because of the fluid consistency of the Futura-45 mix, which contained no coarse aggregates, the patching material was transferred from the drum to a

5-gallon bucket. Futura-45's fluid nature allowed for placement by pouring out of the bucket directly into the area to be patched. Figure 3-3 shows freshly mixed Futura-45 in a wheelbarrow before being placed.

Figure 3-3 Fresh Futura-45 patching material before placement

Standard 3 in x 6 in cylinders were used for the compressive strength tests. Compressive strengths measured at 7 days for the Furura-45 samples taken on casting days are found in Table 3-3. However, because an appropriate capping system was not available for the first three days of testing (dates in Table 3-3 marked with an asterisks), a 4 in neoprene cap was used to cap the samples. It is believed that the oversized neoprene expanded outward and caused a tensile splitting failure of the cylinders, resulting in observed failure strengths lower than the actual compressive strength of the material. Therefore, only the samples tested on June 5 are taken as representative of the actual strength of the Futura-45 patching material.

Table 3-3 Futura-45 compressive strengths

Futura Samples (3x6 cylinders)		
5/30/2013*		
Sample #	*Load (lb)*	*Stress (psi)*
1	31680	4482
2	27660	3913
3	29500	4173
Average	29613	**4189**
5/31/2013*		
Sample #	*Load (lb)*	*Stress (psi)*
1	33860	4791
2	39140	5537
3	27390	3875
Average	33463	**4734**
6/4/2013*		
Sample #	*Load (lb)*	*Stress (psi)*
1	33570	4749
2	35840	5071
3	33850	4789
Average	34420	**4870**
6/5/2013		
Sample #	*Load (lb)*	*Stress (psi)*
1	38990	5515
2	41370	5852
3	48270	6829
Average	42877	**6065**

3.3 Slant Shear

Bond of the two patching materials was calculated according to ASTM C 882 (see section 2.3.1), both with and without a cement paste bonding agent.

3.3.1 Sample Preparation

In order to cast several mortar sections at once, a frame was constructed to support a form setup. Leg supports were constructed from 2x4 lumber, and a sheet of plywood was attached to form the front face of the frame at a 30° angle from vertical. A sheet of plexiglass was fastened to the front of the plywood to provide a smooth surface against which the mortar half-sections could be cast. Sections of 3 inch inside diameter PVC tubing were cut at the appropriate angle using a radial arm saw and the appropriate length such that the inside dimensions of the pipe sections corresponded to the

dimensions shown in Figure 2-4. Lumber supports were screwed to the angled frame to hold the PVC sections in place such that the tops of the PVC was level. Figure 3-4 shows the assembled frame.

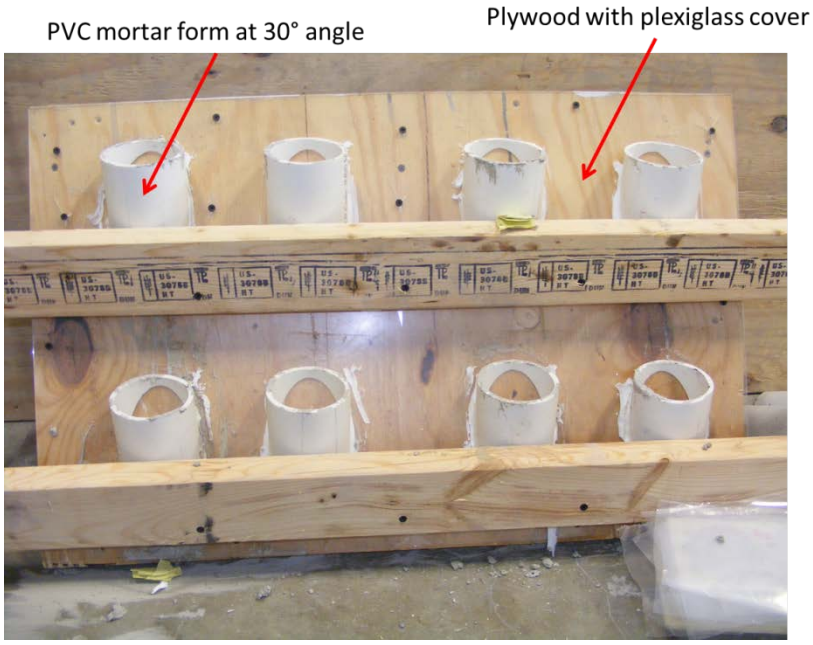

Figure 3-4 Mortar half-cylinder frame

Mortar samples were proportioned according to ASTM C 109, using type III cement per ASTM C 882 (ASTM, 2012). Mortar was placed into the PVC forms in the frame in three layers and rodded 25 times with a 3/8" steel rod in each layer. The half-sections were covered with plastic and allowed to cure for 2 days before being removed from the PVC. Mortar sections were then allowed to cure in the open air in the laboratory for a total of 28 days before testing. Figure 3-5 shows a mortar section after it was removed from the PVC form.

Figure 3-5 Mortar half-cylinder

The patching material portion of the slant shear cylinder was applied 33 days after the mortar half-section had been cast, such that the cylinder was be tested when the mortar half was 40 days old and the patching material half was 7 days old. Mortar half-sections were submerged in water for 24 hours, then allowed to sit on paper towels for 10 minutes prior to the application of the patching materials. The bond face of the mortar sections were wire brushed to remove any loose material and provide texture to promote improved bond between materials. The mortar half-sections were placed into 6 inch lengths of PVC to provide molds of the appropriate size to create the composite cylinders. Half of the mortar samples had a cement paste bonding agent applied to the bond surface before being placed in the PVC molds, as seen in Figure 3-6. Patching material was then mixed and used to fill the remainder of the PVC molds to create composite cylinders. Figure 3-7 shows one such cylinder. The patching material was applied in two lifts and each was rodded 25 times. Slant shear cylinders were demolded after 7 days and prepared for testing. It should be noted that, because of the small areas

in the mold into which the patching material had to flow, the larger coarse aggregate that was typically added to 3U18 mixes for other tests was not added to the mix for the slant shear samples.

Figure 3-6 Mortar half-cylinder with cement paste applied and placed in PVC mold

Figure 3-7 Mortar and 3U18 composite slant shear cylinder

3.3.2 Testing Procedure

Compression testing of the slant shear cylinders was carried out in accordance with ASTM C 39 (ASTM, 2012). Samples were capped with neoprene pads restrained

by steel caps. All tests were conducted in the laboratory's Forney compression testing machine, as seen in Figure 3-8. Samples were loaded at a rate of 250 ± 50 lb/sec, which complies with the ASTM C 39 required load rate of 35 ± 7 psi/sec for a 3 inch diameter cylindrical sample. Samples were loaded to failure, either by bond failure between the two half-cylinders or composite crushing of the entire cylinder. Maximum load was reported by the compressions testing machine and recorded. Bond stress was calculated for those samples that failed along the bond plane by dividing the maximum load on the cylinder by the area of the bonded surface as calculated from the dimensions given in Figure 2-4.

Figure 3-8 Slant shear specimen in Forney compression testing machine

3.4 Core Pullout

For this test, cores were removed from a concrete slab, and the voids were filled with patching material. A rod was installed in the patching material at casting and used to pull the patching material cores out of the slab.

3.4.1 Sample Preparation

Two 3 ft x 3 ft x 2½ in concrete slabs were formed and cast using concrete batched and mixed in the laboratory in a drum mixer. Curing compound was applied to the surface of the slabs with a sprayer immediately after the concrete had been placed in the forms. These slabs served as the base material for the core pullout tests. Table 3-4 contains the compressive strength of the base slabs used for the core pullout tests.

Table 3-4 Compressive strength of slab concrete for core pullout

28-Day Samples		
Cylinder#	*Load (lb)*	*Stress (psi)*
1	117160	9323
2	109830	8740
3	111880	8903
Average	112957	**8989**

After the base slabs had been allowed to cure, nine 3-inch diameter cores were drilled at approximately equal spacing in each slab, for a total of 18 usable sample areas. Each core hole was vacuumed and wire brushed to remove all loose material from the bond surface. A 1-inch hole was drilled in the bottom plywood form at the center of each core hole. The cement paste bonding agent was applied to 8 of the test sites. A 6-inch length of 3/8” diameter steel threaded rod with a washer and nut on one end was placed in the core hole with the nut resting on the laboratory floor in the hole in the plywood. Patching material was mixed using the usual methods, placed in each of the 16 test sites used in the slab, and compacted using a steel rod. Eight 3U18 samples and eight Furura-45 samples were cast, 4 of each material with the bonding agent and 4 without. Materials were tested at 7 days. Figure 3-9 displays one of the slabs after the cores had been filled with the patching materials.

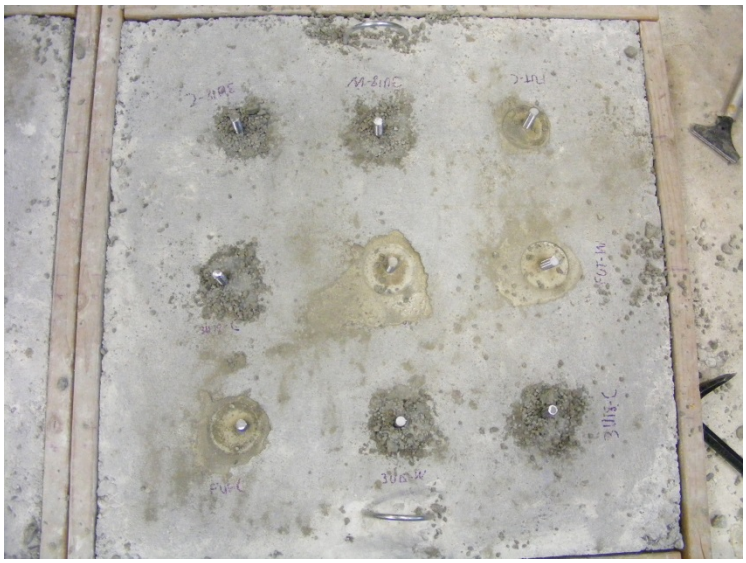

Figure 3-9 Pullout slab filled with core pullout specimens

3.4.2 Test Apparatus

A load application system resembling that shown in Figure 2-8 was assembled to pull the cores. A 9" x 7½" x 1" thick steel plate with a 9/16" diameter hole in the middle and 8 nuts welded to the perimeter of the bottom face served as a table to distribute the applied load to the area around the core. Before each test, the load table was leveled using thin steel shims. On top of the load table was a load cell with a hole in the middle. The load cell was wired to the data acquisition system to record the applied pullout load. A washer allowed the through ram piston to transfer force to the load cell. The piston was attached to a hydraulic hand pump. Through the piston and load cell was an 18-inch length of ⅜" diameter threaded rod with a coupler that attached to the rod exposed from the patching material sample. The rod also passed through a small piece of 1" thick plate that was bearing against the piston as it extended, which in turn was bearing against a nut on the threaded rod. This load path could be traced down to the nut and washer embedded in the patching material and was used to apply the force to pull the patching

material from the base concrete slab. A labeled photo of the load system for the pullout tests is shown in Figure 3-10.

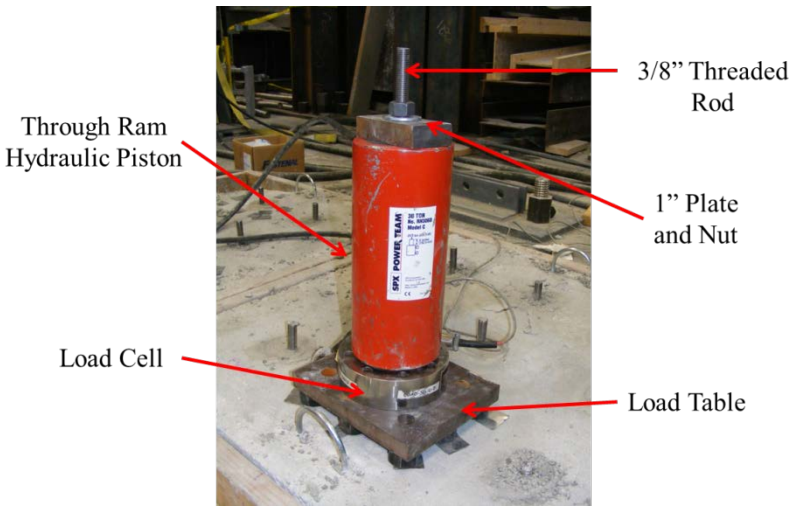

Figure 3-10 Core pullout load application system

3.4.3 Testing Procedure

After the extension portion of the threaded rod was attached to the base section extending from the patching material, the load table, load cell, hydraulic piston, and plate were all slipped over the top of the rod. The nut was brought into contact with the top plate so that the system could be loaded. Load was applied slowly using the hydraulic hand pump until patching material pullout became evident or a maximum load of 15,000 lb was reached. An upper load limit of 15,000 lb was chosen to prevent yielding of ⅜" threaded rod sections of the load application system. Load data was recorded at 10 Hz by the computerized data acquisition system so as not to miss the maximum load on the specimen before bond was broken and the sample pulled out of the base concrete.

3.5 Slab Bending

Two types of slab bending experiments were performed as a part of this investigation: static testing in positive bending and cyclic testing in both positive and negative bending. Because the sample preparation and testing apparatus for both of these tests are generally the same, they are discussed together. The procedure for each test is presented separately.

Figure 3-11 diagrams the nomenclature for all slab bending specimens.

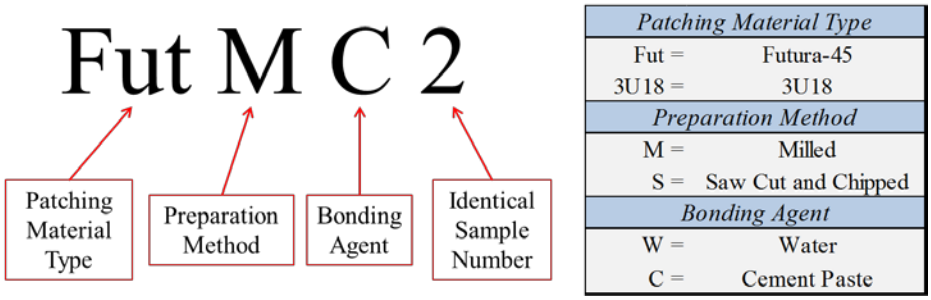

Figure 3-11 Slab bending specimen nomenclature

3.5.1 Specimen Preparation

A total of 36 specimens for the slab bending tests were cast. Each specimen was 47 inches long by 24 inches wide. A #4 steel reinforcing bar was placed in each corner of the specimens, as shown in Figure 3-12.

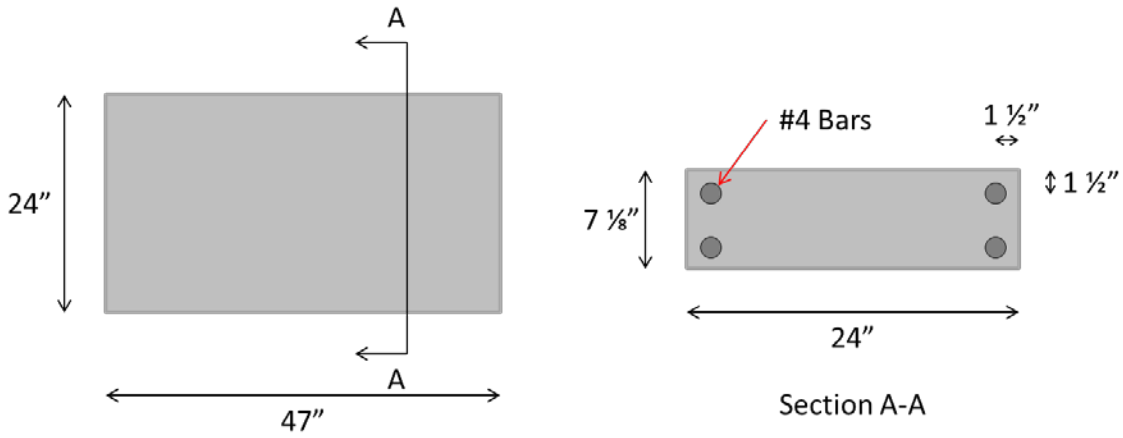

Figure 3-12 Slab bending specimen dimensions

Formwork for the slab bending specimens was constructed from a series of 2 x 8 planks and laid out in a grid on the laboratory floor, as seen in Figure 3-13. Holes were drilled to a depth of approximately ½" in the 2 x 8 planks to hold the 48" lengths of rebar in place. Rebar was installed in the formwork as it was assembled. The formwork was assembled on top of a plastic liner to protect the laboratory floor when concrete was poured.

Figure 3-13 Formwork for slab bending specimens

Concrete for the slab specimens was received from JDM Materials, a local ready mix plant. The mix used was representative of concrete that would be used in a typical rigid pavement roadway in Pennsylvania, meeting the requirements for PennDOT AA concrete mixes. Table 3-5 contains the 28-day compressive strengths of three 4 x 8 cylinder compressive tests, as well as three cylinder tests performed on the first day of slab testing to gain a more accurate assessment of the concrete strength at testing.

Table 3-5 JDM Materials concrete strengths

28-Day Samples		
Cylinder#	*Load (lb)*	*Stress (psi)*
1	81170	6459
2	82810	6590
3	82440	6560
Average	82140	**6536**
First Day of Slab Specimen Tests (5/30)		
Cylinder#	*Load (lb)*	*Stress (psi)*
1	88650	7054
2	92380	7351
3	88780	7065
Average	89937	**7157**

Slabs were cast within a period of 1 hour. A concrete bucket hung from an overhead crane was used to place concrete in the forms. Slab samples were compacted using a small stick vibrator, screeded with a 2 x 4, and finished by hand with a mag float. Two lifting hooks were installed in each slab to assist in moving the slabs around within the laboratory workspace. After the concrete had been allowed to set, a white curing compound was sprayed on all slab specimens. Figure 3-14 shows photographs of various stages of slab casting.

(a) Concrete placement

(b) Concrete vibration

(c) Concrete screeding

(d) Lifting hook placement

Figure 3-14 Concrete slab placement

3.5.1.1 Milled Slab Preparation

A milling machine as described in Section 1.3.3 was used to create an area to be patched in 16 slab samples similar to that which would be seen in a field condition. The milling machine used to prepare the specimens was mounted on the front of a Bobcat loader, as seen in Figure 3-15. Slabs were allowed to cure for at least 28 days before being prepared to be patched. The slabs to be milled were moved to a location where they could be braced against a stationary object before being milled. Because the 24" width of the miller was larger than the desired patch size, the milling drum was tilted to an angle approximately 15° from horizontal. After milling, the drum was tilted to 15° from horizontal in the other direction, and a second round of milling was performed, as shown in Figure 3-16. The final patch area had an oblong bowl shape with a textured surface and was approximately 3 inches in depth in the center. Milled patch areas were typically about 23" by 16" at their widest extents with a maximum variation of about 2" in each dimension. Figure 3-17 shows a milled slab sample.

(a) Miller attached to Bobcat loader

(b) Miller teeth

Figure 3-15 Milling machine used to prepare samples

Figure 3-16 Slab being milled

Figure 3-17 Milled slab

3.5.1.2 Saw Cut and Chipped Slab Preparation

The second set of 16 specimens was intended to represent the other common patch preparation method, saw cut and chipped. A 14" square was drawn centered on each of the slabs to provide a guide for the saw cuts. Cuts were made using an electric cut off saw with a 12" diamond blade for concrete cutting. An initial cut was made along the perimeter of the patch area at a depth of 1½", as well as two additional cuts evenly

spaced along the width of the patch area make the removal of the concrete during chipping easier. Second cuts were made for all slabs to the full depth of 3” before chipping was started. After all cuts were completed to full depth, a small electric jackhammer with a chisel tip was used to remove the concrete from the interior of the patch area. Concrete was removed by holding the jackhammer at a relatively small angle from the horizontal and chipping until material was removed down to a depth of 3” through the entire patch area. Figure 3-18 presents photographs of the saw and chip patch area preparation process.

(a) Sawing slab specimen

(b) Sawed outline before chipping

(c) Jackhammer used for chipping

(d) Cut and chipped patch area

Figure 3-18 Saw cut and chipped slab test preparation

3.5.1.3 Patching Material Placement

After slabs were cast and prepared, all loose debris was removed from the voids that were to be patched using a vacuum and a wire brush. When dust and debris had been removed, the patch areas were cleaned with compressed air to remove any other loose particles and vacuumed a second time. Patching materials were prepared as described in Section 3.2 and placed. Refer to 3.1 Test Matrix for details on quantities of each type of patch cast. All patching concrete was rod compacted in place and finished by hand using a small mag float. Immediately after patching material was placed, four bolts with washers were inserted in a square in the patch to allow for a patch pullout to be performed (discussed in Section 3.5.4.3). Liquid curing compound was applied to patch areas as soon as they had set sufficiently. Patches were allowed to cure for 7 days before testing.

3.5.2 Slab Bending Test Apparatus

The loading frame used to perform all slab bending tests was constructed from steel components. Both static loading and cyclic loading tests were four-point bending tests with supports spaced at 15", for a total span length of 45". Figure 3-19 shows a general side view schematic of the bending load apparatus with the span dimensions highlighted.

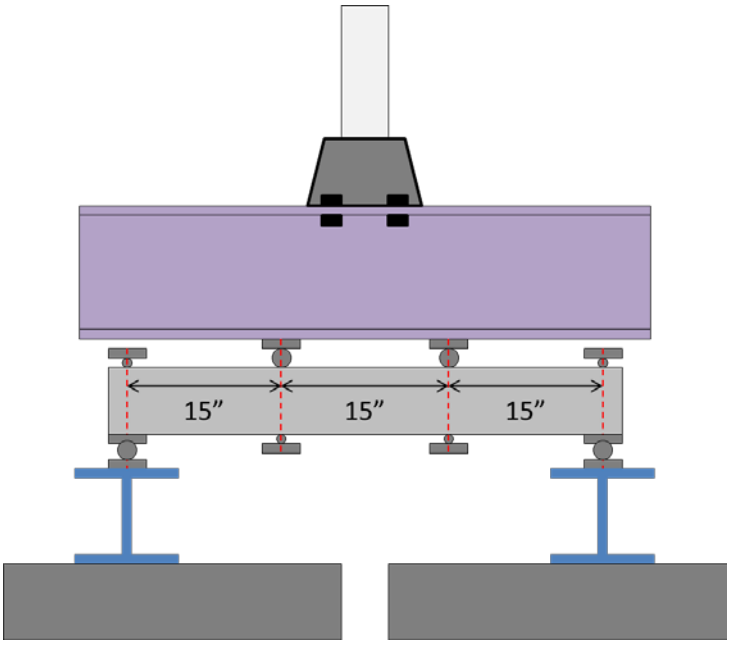

Figure 3-19 Slab bending load apparatus schematic

The 35 kip capacity hydraulic actuator shown in Figure 3-20 was hung from a reaction frame to apply load to the concrete slab specimens. An I-beam used as a distribution beam was bolted to the actuator head. Roller supports that acted as load points for positive bending were bolted across the width of the distribution beam 7½” from the center of the beam, for a total span distance between load points of 15 inches. Because the rollers extended to a total width of 24” to contact the full width of the slab specimens and the distribution beam was only 12” in width, the rollers were bolted in place within C-channels to provide additional stiffness to resist flexural deflection in the overhanging roller sections. Negative moment load points were created from 4” wide 1” thick plate with an additional piece of 1½” wide 1” thick plate welded to them to contact the specimen. The contact plates extended 4” in from the edge of the slab on each side such that the contact points did not cross the patched portion of the slab. This allowed for the patch to fall out if full debonding should occur between the patch and concrete

substrate during testing. Each plate with the negative moment load points was held in place by a length of ⅝" diameter threaded rod extending from overhanging portions of the stiffening C-channel from the positive moment load points down to the negative moment support plate on each side of the specimen.

Figure 3-20 35-kip capacity hydraulic actuator, fully extended

Positive bending end supports were spaced at 45 inches. Each roller support was bolted to a 10" deep W-section, which in turn was bolted across two 6 x 8 rectangular HSS sections. The HSS sections were attached to the laboratory's 3-foot thick reinforced concrete strong floor with 2" diameter bolts. Beveled plates were placed between the rollers and the specimen to prevent the slab from falling off of the support if it moved slightly during cyclic testing. Negative moment end supports were also rollers attached to 1" thick plate. Supports were placed on top of the specimen and tied to the support W-section with two ⅜" diameter threaded rods on each side of the support. A labeled photograph of the major components of the load apparatus can be seen in Figure 3-21.

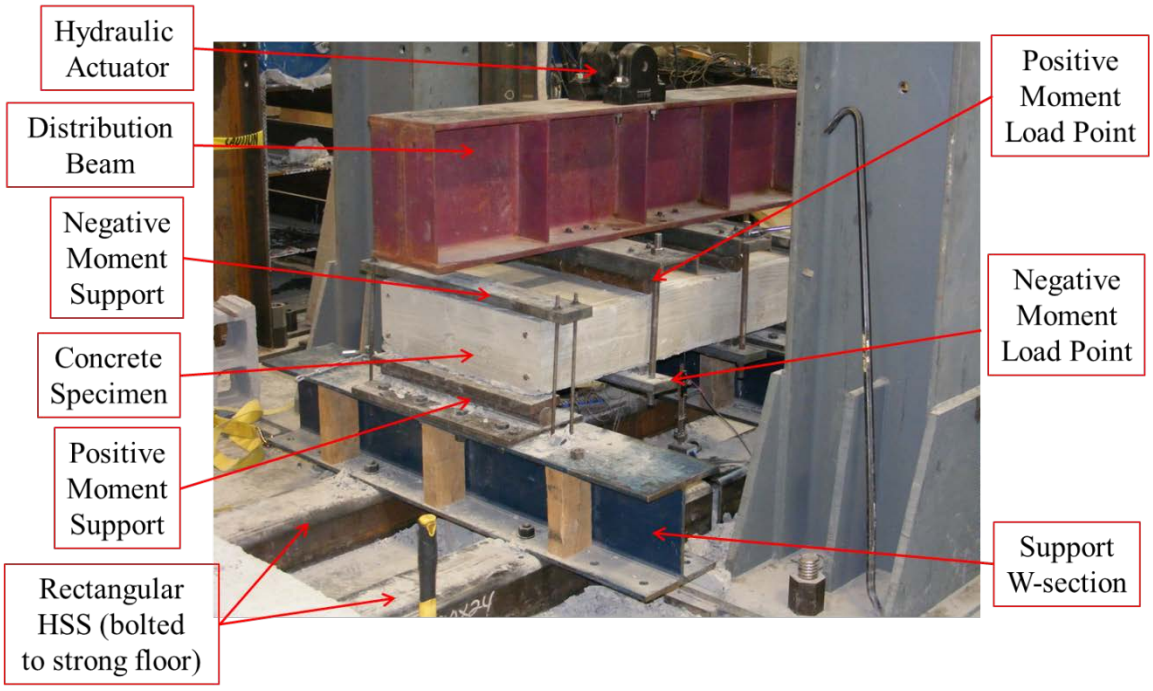

Figure 3-21 Components of slab bending load apparatus

The same apparatus was used for both the static and cyclic testing procedures. For static testing, which only loaded specimens in positive bending, the negative moment supports at the ends of the slab were not attached. The negative moment load points in the middle of the specimen were still attached but not tightened. These were left in place to catch the patch if it debonded completely as a unit and to lift the slab so that it could be seated appropriately before testing.

3.5.3 Data Acquisition

Two systems were used to obtain data from slab testing. One system recorded data directly from the hydraulic actuator and was run through the same computer system as the actuator controls. This system featured a load cell and displacement records for the actuator head. The second data acquisition system recorded data from outside sources using Strainsmart computer software. Potentiometers and strain gages were programmed

into the Strainsmart system. Figure 3-22 shows a potentiometer and a strain gage used to acquire displacement and strain data.

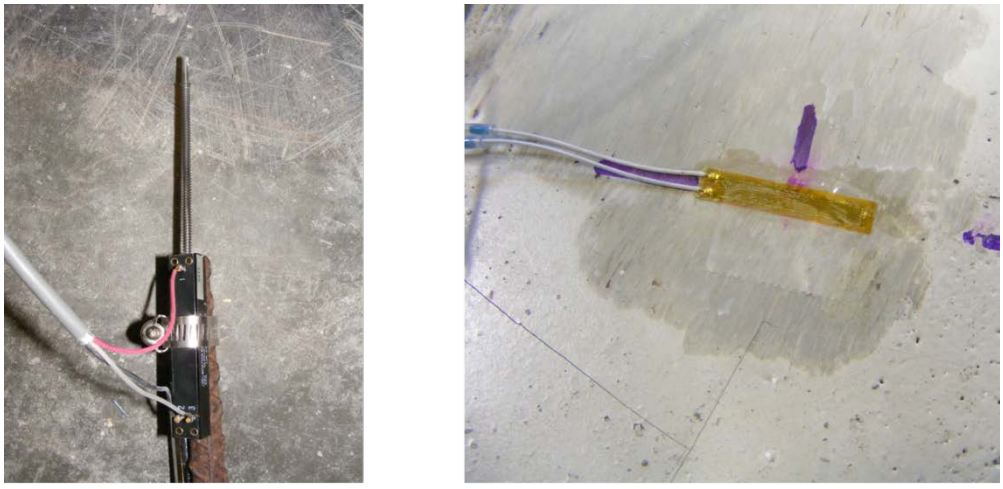

(a) Potentiometer *(b) Strain gage*

Figure 3-22 External data acquisition equipment

Two potentiometers were used to obtain displacement data for each slab in both static and cyclic testing. One potentiometer was placed on each side of the specimen, as seen in Figure 3-23, to provide an average deflection for the entire slab and to offer some redundancy had one of the potentiometers malfunctioned during testing.

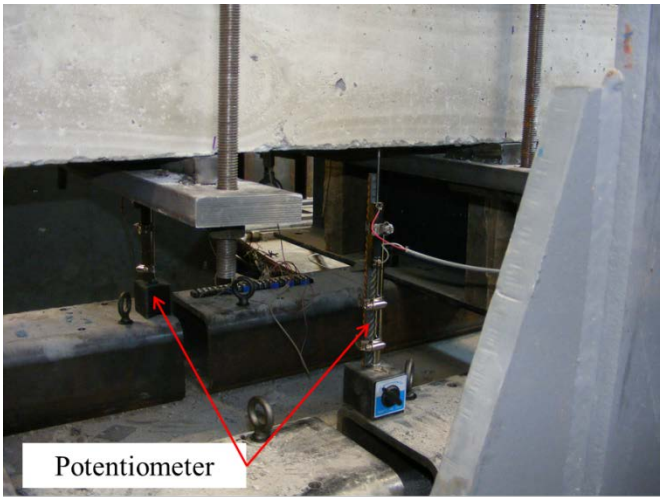

Figure 3-23 Potentiometers measuring slab deflection

Strain gages were applied only to cyclic test specimens. Preliminary tests showed that strain data from static tests provided little useful information. Cyclic test samples received three strain gages placed uniformly on all patches of the same type. Before gages were applied, the surface of the patching material where the gages were to be placed was ground smooth with an electric hand grinder and cleaned with compressed air. Strain gages were applied per the manufacturer's instructions using an adhesive compound purchased from the gage manufacturer. Strain gages of 1" length were attached to samples, rather than 2" length gages that are typical for concrete applications. The use of shorter gages was justified because the maximum aggregate size used in either of the patching materials was ⅜", so longer gages were not necessary to span large aggregate particles. Figure 3-24 shows a saw cut patch and a milled patch after strain gages had been attached.

(a) Saw cut and chipped patch with strain gages *(b) Milled patch with strain gages*

Figure 3-24 Patch areas with strain gages applied

3.5.4 Testing Procedure

After the patching material was allowed to cure for 7 days, all specimens were flipped such that the patched area was on the bottom and placed in the testing apparatus.

Separate procedures are offered for the static and cyclic slab bending tests. Testing method programs were created within the actuator control program for both types of tests. Preliminary testing determined that 0.30 inches of actuator displacement provided and appropriate maximum deflection in the slab.

3.5.4.1 Static Slab Bending

A program was written in the actuator control software that applied the bending load in a displacement controlled fashion. The actuator head displaced downward, placing the patch in tension, at a steady rate of 0.05 in/min for 6 minutes, ultimately reaching the maximum deflection of 0.30 in at the end of the loading phase. The actuator head then returned to the starting position over a 1-minute duration. During this test, load, actuator head displacement, and slab deflection were recorded at a rate of 10 Hz.

3.5.4.2 Cyclic Slab Bending

The program for the cyclic slab testing was separated into two distinct phases. The first phase was similar to the static loading test to cause the slab to crack before cycling. A static load was applied downward at a displacement rate of 0.05 in/min for 2 minutes, to a total displacement of 0.10 in. The actuator head was then moved upward at a rate of 0.05 in/min for 4 minutes, moving the actuator to a location 0.10 in above the starting point. It was then returned to the starting location at the same rate of movement, taking 2 minutes. This static movement in both directions allowed for the development of both positive and negative bending cracks before the beginning of the cyclic phase.

Once the slab had returned to the starting position, the cyclic portion of the test began. Each segment of the cyclic test lasted for 1000 cycles performed at a rate of 2 Hz. For the first 1000 cycles, the actuator head was displaced 0.05” from the starting position

in each direction. Actuator displacement increased by 0.05” for each 1000 cycle interval. The sequence terminated after the actuator had completed 1000 cycles at a displacement of 0.30” in each direction, having completed a total of 6000 cycles.

For all cyclic tests, load and actuator displacement were recorded at 10 Hz, as was done for the static tests, for the cracking portion of the test only. Potentiometer deflection data and strain data obtained from the three strain gages attached to each patch were recorded at 100 Hz for the duration of the testing procedure. Load and actuator displacement data was also recorded at each peak and valley during the cyclic portion of the test.

3.5.4.3 Patch Pullout

For specimens where the patch did not debond fully during the cyclic or static test, an attempt was made to measure the force required to achieve full debonding of the patch material from the base concrete. During casting, four ⅜” bolts were installed in each patch. A coupling nut with an eye hook attached to the other end was threaded onto each bolt. A second set of eye bolts was attached to the 6 x 8 HSS base of the test setup, and a turnbuckle was used to span between the eye bolts, anchoring the patch to the HSS. Another program was written for the actuator software that caused the actuator to pick up on the slab while the patching material was being held in place by the turnbuckles. A maximum load of 3000 lb as limited by turnbuckle and bolt strength was used to attempt to remove the patch.

CHAPTER 4 RESULTS AND DISCUSSION

This chapter presents and discusses the results of the four different tests and test specimens described in Chapter 3.

4.1 Slant Shear Results

All 16 slant shear specimens failed along the bond plane between the base mortar and the patching material, as shown in Figure 4-1. Table 4-1 contains the strengths at the time of testing for the materials used to create the slant shear specimens. Table 4-2 and Table 4-3 display the results of the slant shear tests performed as described in Section 3.3 for the Futura-45 samples and the 3U18 samples, respectively. Shear stress was calculated as outlined by ASTM C 882 by dividing the vertical failure load by the area of the bond surface, which was given as 14.13 in^2 in the standard.

(a) Cement paste bonded surface

(b) Bond surface with no bonding agent

(c) 3U18 material specimen

(d) Futura-45 material specimen

Figure 4-1 Photographs of slant shear specimens after failure

Table 4-1 Slant shear material strengths

Futura-45 Sample Materials		
Sample #	*Base Mortar (psi)*	*Patching Material (psi)*
1	5922	7778
2	5457	8044
3	5966	7796
Avg.	**5782**	**7873**
3U18 Sample Materials		
Sample #	*Base Mortar (psi)*	*Patching Material (psi)*
1	5053	10740
2	4686	10507
3	4927	10353
Avg.	**4889**	**10533**

Table 4-2 Futura-45 slant shear results

Futura-45 Slant Shear Specimens			
Surface Prep	*Load (lb)*	*Bond Area (in^2)*	*Shear Stress (psi)*
Water	30400	14.13	2151.5
Water	35020	14.13	2478.4
Water	32770	14.13	2319.2
Water	39490	14.13	2794.8
Cement	9200	14.13	651.1
Cement	7750	14.13	548.5
Cement	8680	14.13	614.3
Cement	7010	14.13	496.1

Table 4-3 3U18 slant shear results

3U18 Slant Shear Specimens			
Surface Prep	*Load (lb)*	*Bond Area (in^2)*	*Shear Stress (psi)*
Water	29170	14.13	2064.4
Water	20020	14.13	1416.8
Water	18480	14.13	1307.9
Water	13230	14.13	936.3
Cement	9820	14.13	695.0
Cement	9020	14.13	638.4
Cement	8980	14.13	635.5
Cement	12920	14.13	914.4

A plot of the average bond stress at failure with a standard deviation bar is shown in Figure 4-2 for each material and preparation combination.

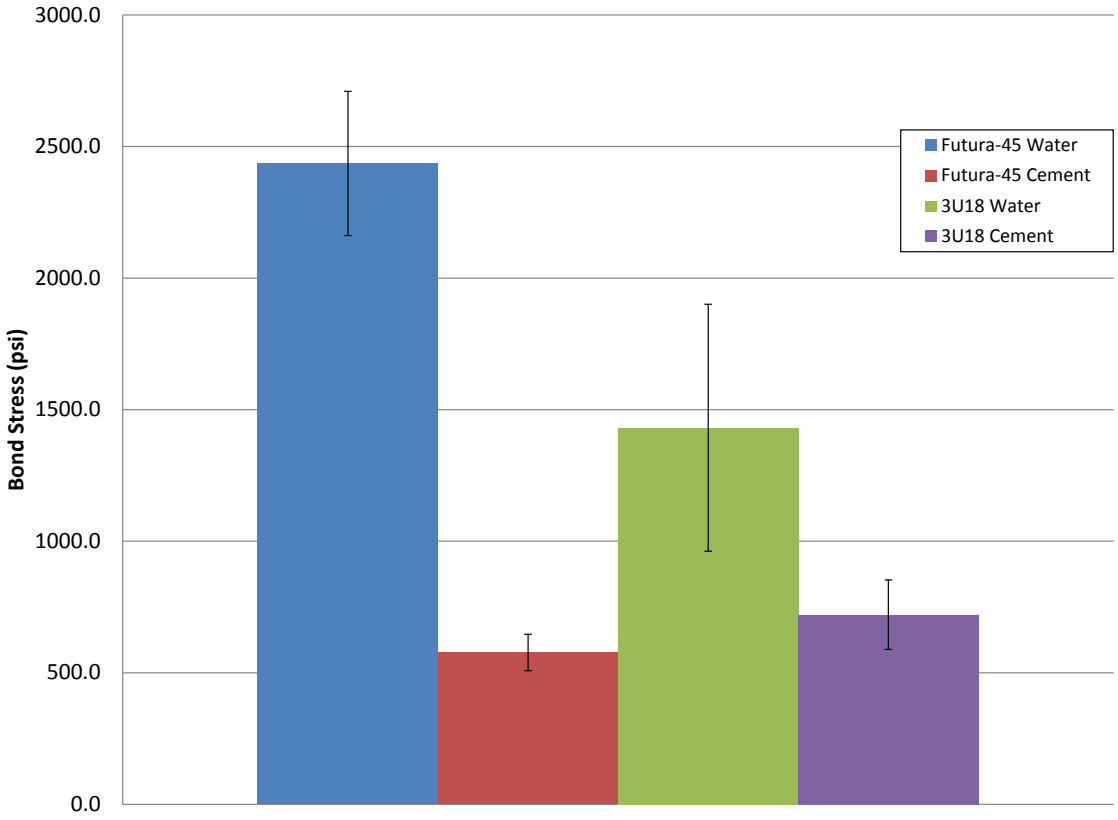

Figure 4-2 Average bond stresses at failure

It can be seen from the data that the samples that utilized the cement paste bonding agent exhibited much lower bond strength when compared to the samples where the patching material was bonded directly to the base mortar. In fact, all 8 samples prepared with the bonding agent failed at the bond surface at similar stresses. Failures occurring at similar stresses regardless of patching material indicated that the cement paste bonding agent governed the bond strength, which, as seen in Figure 4-2, was lower than that of either of the patching materials being examined.

The data from the slant shear also indicates that the bond created by Futura-45 was stronger than that of the 3U18. Futura-45 samples had an average bond stress of over 1000 psi greater than the bond strength of 3U18 samples, in addition to having a

smaller standard deviation, demonstrating more consistently high bond strength from Futura-45.

Additionally, the fairly large standard deviation bars from the specimens that were not bonded using cement paste, especially the 3U18 specimens, show a relatively large scatter in the measured bond strength. Large standard deviations suggest an inconsistency in the results of the test, a trend which has been seen in other research. Cervo and Schokker (2010) found high variability as a result of their testing program, and the additional scattered data seems to support their conclusions.

4.2 Core Pullout Results

Of the 16 specimens tested in the core pullout tests, only one specimen showed evidence of bond failure below the load limit of 15,000 lbs. One of the 3U18 specimens that had had the cement paste bonding agent applied to the bond surface debonded at a load of 9000.1 lb, which translates to a shear bond stress of:

$$\frac{P}{A_{bond}} = \frac{P}{\pi dh} = \frac{9000.1\ lb}{\pi * 3\ in * 3.5\ in} = 273\ psi$$

Upon bond failure, the patching material cylinder began to pull away from the base concrete slab, as shown in Figure 4-3.

Figure 4-3 Failed core pullout specimen

The remaining 15 specimens did not show any indications of bond failure between the patching material and the base concrete at an applied load of 15,000 lb. This indicates that the bond failure stress was greater than the strength of the ⅜" diameter threaded rod. The results of the test indicate that the 15 remaining samples possess a minimum bond stress of:

$$\frac{P}{A_{bond}} = \frac{P}{\pi dh} = \frac{15000\ lb}{\pi * 3\ in * 3.5\ in} = 455\ psi$$

Although an exact value of bond strength was not indicated for the majority of specimens, it is clear that the 15 samples that did not pull out of the base concrete exceed 455 psi shear bond strength.

4.3 Static Slab Bending Results

4.3.1 Load-Displacement Data

A total of 16 patched specimens and two control slabs were tested in static slab bending. Figure 4-4 displays load vs. displacement plots for all specimens tested in static

slab bending. All specimens seem to exhibit the same trend of multilinear behavior. The first branch extends up to a load of about 1200 lb and a deflection of approximately 0.06 in. It is at this location where initial cracking began, and a decrease in slab stiffness is observed. A decrease in resisted load is also observed at cracking in most of the slabs. The slope of the plot is slightly decreased and remains linear to about 2200 lb and 0.20 in of deflection. At 2200 lb and 0.20 in of deflection, the stiffness reduced again, and the load deflection plot remained linear for the remainder of loading up to 0.30 in of deflection. It is believed that this second decrease in stiffness occurred at the first yield of the reinforcing steel within each slab. An analysis using basic beam theory confirmed that the loads at which cracking and yielding occurred seem reasonable.

It should be noted that Control 4 appears to have had a malfunction with the potentiometer data. It exhibits the same behavior as all other specimens, but at deflections greater than those applied by the actuator.

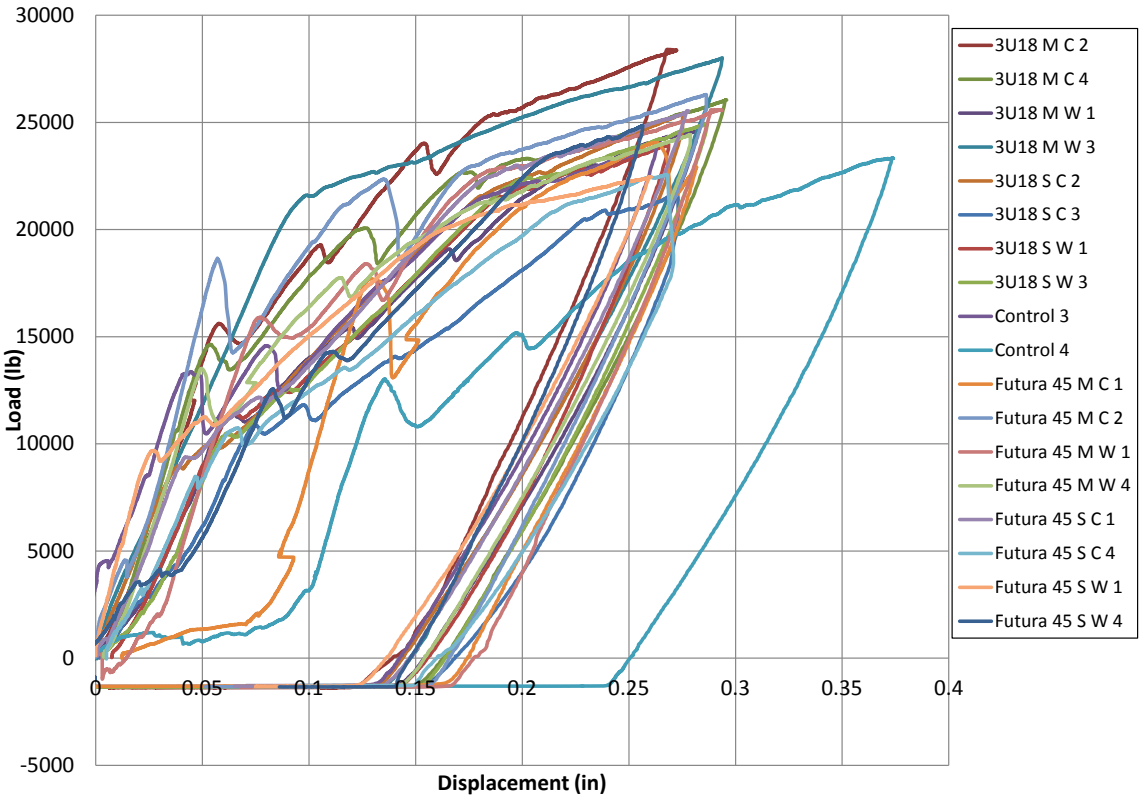

Figure 4-4 Load-displacement plot for all static slab bending specimens

After examining trends for different variables in the static bending slabs, only the patch preparation type seemed to show a difference in the load-displacement data. Figure 4-5 is a replication of Figure 4-4 with all milled prepared patches shown in red, all saw cut and chipped patches shown in blue, and the controls shown in green. It appears from the plot in Figure 4-5 that the milled prepared patches generally reach slightly higher loads than the saw cut and chipped prepared patches before first cracking. There are a few possible explanations for this behavior. This behavior may possibly result from the geometry of the removed concrete in each type of patch. The rectangular concrete removal in the saw cut and chipped patches likely results in an overall lower section modulus of the cross-section than that resulting from the bowl-shaped geometry of the

void in the milled slabs. This may also have been caused by a more composite behavior of the patch and base concrete resulting from a better bond between the materials. The most likely explanation, however, is that the saw cut edge of the patch area encouraged the development of a stress concentration at the corner of the patch, resulting in cracking of the slab at a lower load.

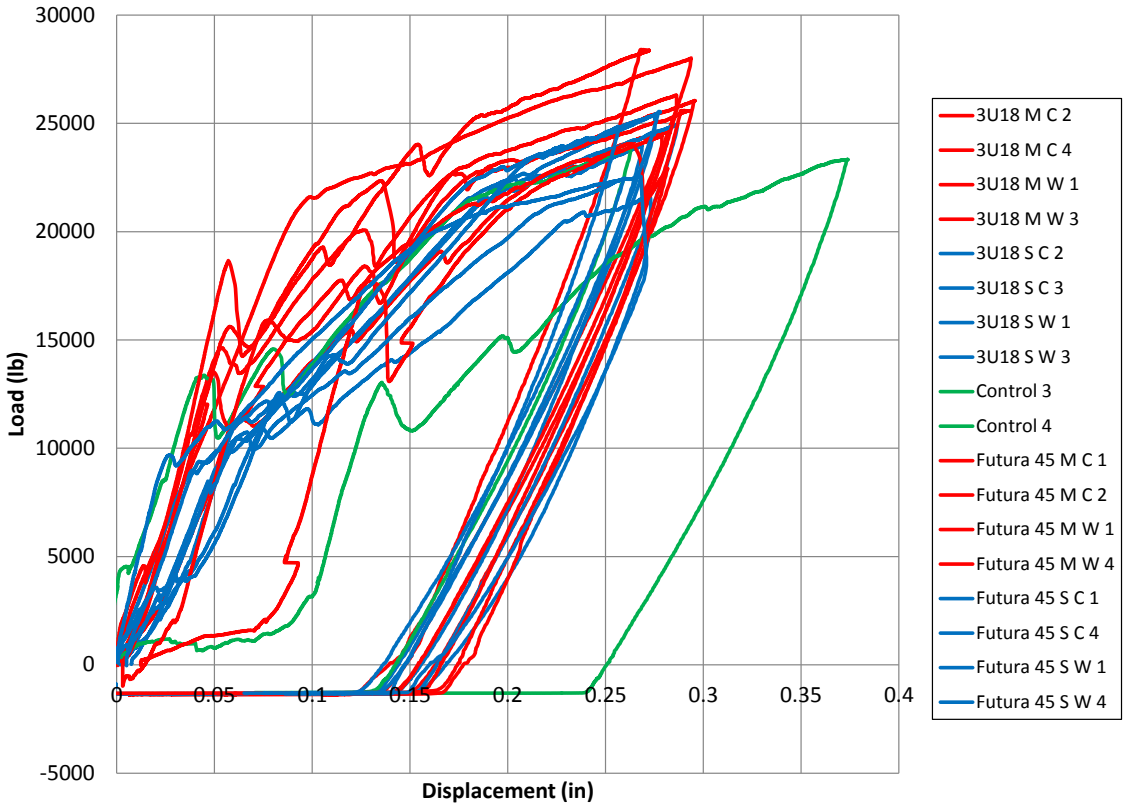

Figure 4-5 Static load displacement plot for different patch preparation methods

4.3.2 Visual Observations

In addition to the data acquired from the data acquisition systems, important qualitative data was obtained about patch behavior from the visual observations made of the patch specimens during and after testing. Observations were made and recorded for

cracking patterns in the patch area and the bond condition of the patching material at the end of testing. Cracking and bond observations are summarized in Table 4-4.

Table 4-4 Visual observations for static slab bending tests

Visual Observations		
	Cracking	*Bond*
3U18 M C 2		
3U18 M C 4		
3U18 M W 1		
3U18 M W 3		
3U18 S C 2		
3U18 S C 3		
3U18 S W 1		
3U18 S W 3		
Futura-45 M C 1		
Futura-45 M C 2		
Futura-45 M W 1		
Futura-45 M W 4		
Futura-45 S C 1		
Futura-45 S C 4		
Futura-45 S W 1		
Futura-45 S W 4		

Key

Cracking

= crackng through patch

= cracking around patch

= cracking under patch

Bond

= patch did not debond from base concrete

= patch debonded from base concrete

As is evident in Table 4-4, milled prepared areas patched with 3U18 exhibited the weakest bond. The patch material completely debonded from the concrete substrate for all four specimens with this combination, regardless of bonding agent. One of the four specimens, 3U18 M C 4, did not fully debond until the pullout portion of the test at a load of 678 lb, while the patches fully debonded from the remaining three milled 3U18 specimens during the static bending phase. Cracks formed in the slab during the static loading phase of the test propagated beneath the 3U18 patches for these samples, which is an additional indication of poor bond between substrate and patching material. Figure 4-6 shows 3U18 M W 3, one of the patches that debonded fully from the concrete slab. Cracks across the width of the slab can be seen through the middle of the patch area but not propagating through the patch itself. Only small areas of bonded base concrete are evident on the bond surface of the removed patch, indicating that the bond was likely

weak over the rest of the bond surface. Table 4-5 shows the time of full bond loss for those samples that debonded completely.

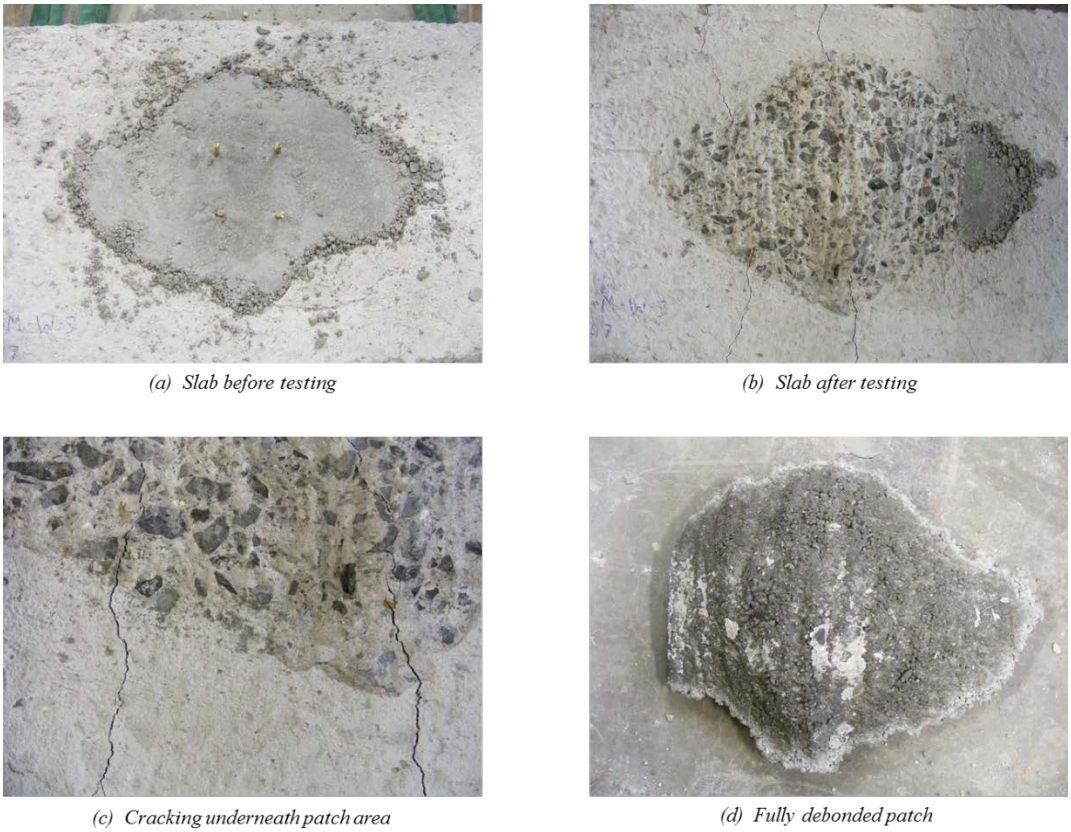

(a) Slab before testing

(b) Slab after testing

(c) Cracking underneath patch area

(d) Fully debonded patch

Figure 4-6 Photos of 3U18 M W 3

Table 4-5 Static test time of debonding for fully debonded patches

Fully Debonded Patches from Static Slab Bending Test		
Specimen	Status	Actuator Displacement (approx) (in)
3U18_M_C_2	Fully Debonded	0.30
3U18_M_C_4	Fully Debonded	Pullout
3U18_M_W_1	Fully Debonded	0.30
3U18_M_W_3	Fully Debonded	0.19

The milled slabs patched with Futura-45 appeared to exhibit the strongest bond behavior. All four of this type of specimen exhibited cracking through the patch during slab bending, indicating a strong bond by showing a unified response from the base concrete and patching material. Figure 4-7 shows photos of Fut M C 2, an example of

one of the samples that showed cracking through the patch. None of the four milled Futura-45 patches failed in the patch pullout test after the bending phase of the test protocol, signifying a remaining bond strength of at least 3000 lb over the patch.

(a) Slab before testing *(b) Slab after testing*

Figure 4-7 Photos of Fut M C 2

The remaining 8 slabs were the saw cut and chipped prepared slabs. All of these specimens behaved similarly, regardless of patching material or bonding agent. None of the specimens debonded fully, even after the application of 3,000 lb of tension in the pullout test. Each of the specimens exhibited similar patterns of cracking around the patch, as highlighted in Figure 4-8. Slabs with saw cut and chipped patches typically showed cracks or separation of the base concrete from the patching material at the sawed edges of the patch area, indicating poor bond along the smooth cut face of the patch area. However, the chipped surface of the middle of the patch provided adequate bond strength for both materials with and without the cement bonding agent to hold the patch in place because none of the 8 patches of this type debonded completely.

(a) Slab after testing with location of (b) indicated

(b) Crack propagating around patch

Figure 4-8 Photos of Fut S C 4

4.4 Cyclic Slab Bending Results

4.4.1 Load-Displacement Data for Static Cracking

As with the static slab bending test, 16 patched slabs and 2 unpatched control slabs were tested. Load vs. displacement plots for the static cracking portion of the cyclic test program are shown in Figure 4-9. Cyclic slabs were loaded to 0.10" of actuator deflection in both the positive and negative bending directions. In positive bending, all slabs appeared to behave linear-elastically until cracking, at which point the load carried by each slab decreased and the stiffness of each slab was reduced. The negative portion of each plot shows a similar trend of a reduction in stiffness at cracking, but without the drop in resisted load. The maximum displacement reached for negative flexure was less than that in positive bending despite the same amount of actuator head movement in each direction. However, the loads resisted by the slab at similar magnitudes of displacement in each direction appeared to correlate well, indicating that the slab was acting as a composite member. The static cracking portion of the cyclic samples displayed bi-linear behavior, as opposed to the tri-linear behavior seen in the static bending tests. This

change in behavior can be explained by the reduction in actuator displacement from 0.30” for the static tests to 0.10” for the static portion of the cyclic tests.

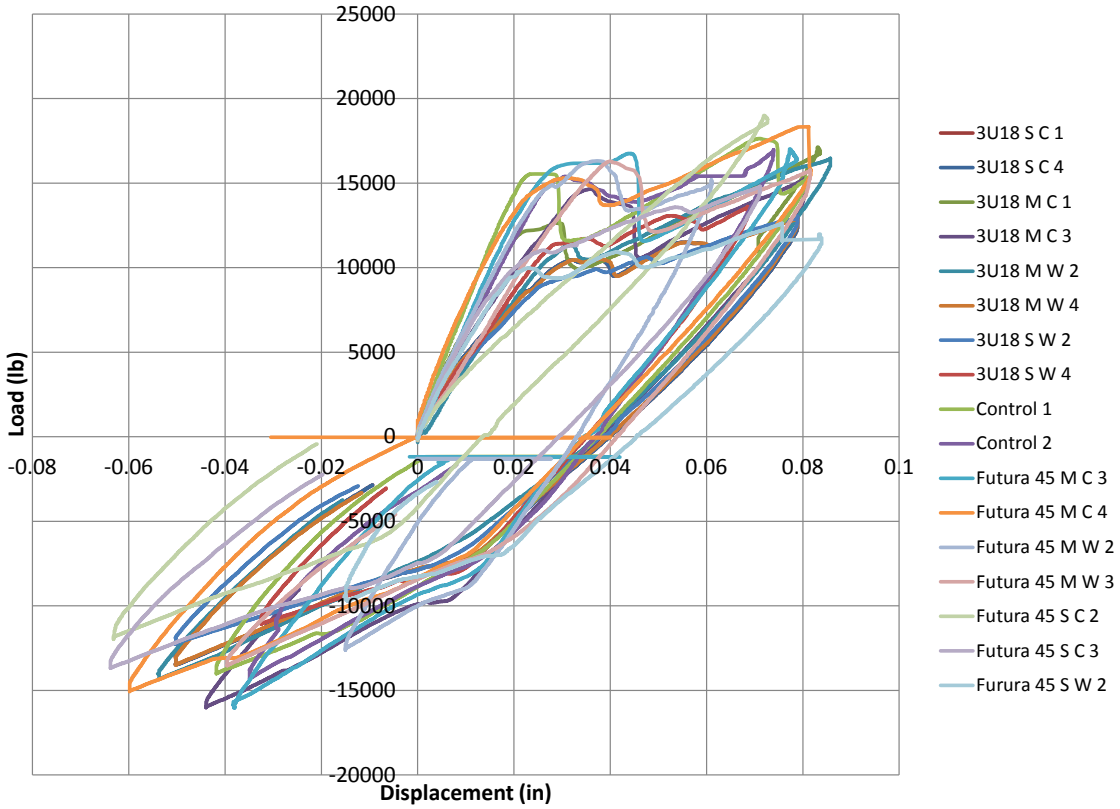

Figure 4-9 Load-displacement plot for all cyclic slab bending specimens during cracking phase

A similar trend to that seen in the cracking loads was seen in the cyclic slabs as was seen in the static slabs. The milled slab specimens typically had a higher cracking load than the saw cut and chipped prepared slabs, both for positive and negative bending crack formation.

The Futura-45 S W 3 sample behavior seems to be an outlier from the rest of the data. It is believed that the sample was not seated and the load on the specimen was not zeroed properly prior to the beginning of the test procedure. During the cyclic portion of the Futura-45 S W 3 procedure, the test had to be stopped to readjust the specimen, which

had moved within the test apparatus and was rubbing against a threaded rod. For clarity, Fut S W 3 was not included in the plot.

4.4.2 Peak-Valley Data

Peak-valley data was recorded for all cyclic specimens for the cyclic portion of the test program by the data acquisition system. The peak-valley data provided absolute maximum loads on each slab in both bending directions, the peak values providing maximum load in the positive bending direction and the valley values providing minimum load in the negative bending direction. Average maximum and minimum loads were calculated for each set of 1000 cycles corresponding to actuator displacement values from 0.10 in to 0.30 in, shown in Table 4-6 and Table 4-7, respectively.

Table 4-6 Average Maximum Load for Each Cycle

Average Maximum Load for Each Cycle					
Cycle Displacement (in) / ***Specimen***	0.1	0.15	0.2	0.25	0.3
Cyclic Control 1	9840.06	14229.26	18220.38	17797.78	1969.96
Cyclic Control 2	12021.04	15668.13	19877.35	9546.22	4579.50
Fut_M_C_3	11582.69	15380.88	16482.51	17688.35	17442.97
Fut_M_C_4	12632.13	17661.92	19729.27	17553.82	8438.587
Fut_M_W_2	8412.72	13156.83	18163.51	19282.07	12409.51
Fut_M_W_3	7090.84	12873.59	17130.12	18904.46	18586.35
Fut_S_C_2	14560.89	19630.78	21799.82	20238.23	11775.53
Fut_S_C_4	7346.123	13373.66	16847.95	18901.2	11674.46
Fut_S_W_2	8969.859	14654.02	18843.66	19021.45	17654.62
Fut_S_W_3	-1404.05	1993.084	8428.733	19404.32	10659.55
3U18_M_C_1	Patch debonded during cracking phase				
3U18_M_C_3	8492.565	14917.65	19123.73	19921.66	5028.332
3U18_M_W_2	16469.32	Patch debonded			
3U18_M_W_4	7346.123	13373.66	16847.95	18901.2	11674.46
3U18_S_C_1	12251.41	17878.48	20788.42	21199.45	8232.445
3U18_S_C_4	8885.671	3131.406	Patch debonded		
3U18_S_W_2	9109.964	15016.22	19227.99	19112.63	13548.22
3U18_S_W_4	7130.272	11096.52	16422.93	19539.88	4314.729

Table 4-7 Average Minimum Loads for Each Cycle

Average Minimum Load for Each Cycle					
Cycle Displacement (in)	0.1	0.15	0.2	0.25	0.3
Specimen					
Cyclic Control 1	-13518.64	-16877.07	-20553.32	-15961.58	-2043.59
Cyclic Control 2	-15775.08	-18647.74	-16373.66	-2678.24	-1698.22
Fut_M_C_3	-14374.59	-18476.07	-21378.95	-19356.22	-16270.38
Fut_M_C_4	-14093.68	-17334.09	-17700.65	-10681.41	-8145.182
Fut_M_W_2	-15240.36	-17705.17	-19910.51	-17213.01	-12914.03
Fut_M_W_3	-16567.47	-19276.39	-20753.36	-18676.02	-12728.73
Fut_S_C_2	-11464.01	-14042.17	-16541.89	-17584.57	-7084.101
Fut_S_C_4	-12379.66	-17399.72	-19606.61	-19757.07	-10373.3
Fut_S_W_2	-11947.2	-15621.85	-17747.01	-18697.1	-17628.05
Fut_S_W_3	-16825.72	-19600.6	-20924.64	-17189.31	-13151.63
3U18_M_C_1	Patch debonded during cracking phase				
3U18_M_C_3	-16924.94	-19235.64	-18691.43	-17030.16	-3975.402
3U18_M_W_2	-14349.82	Patch debonded			
3U18_M_W_4	-12379.66	-17399.72	-19606.61	-19757.07	-10373.3
3U18_S_C_1	-13125.94	-17033.39	-19124.64	-17158.14	-14647.69
3U18_S_C_4	-14329.11	-3532.87	Patch debonded		
3U18_S_W_2	-11010.19	-13806.02	-16417.92	-17321.78	-13731.69
3U18_S_W_4	-12718.6	-16861.66	-18965.87	-16503.11	-2410.139

It was speculated before the tests that a relationship might exist between decreases in maximum and minimum loads and bond failure between the patches and concrete substrate, especially on the negative load when the patch area was in compression. However, the average maximum and minimum load values seem generally inconsistent, with significant variations due to the formation of cracks and settlement of the test setup. In addition, several of the specimens formed plastic hinges during the larger displacement cycles, and some saw fractured or debonded reinforcing bars. These situations caused substantial decreases in load resisted by the specimens, which could not be differentiated from a decrease in load caused by patch debonding. Therefore, the peak-valley data provided little useful information about bond strength.

4.4.3 Visual Observations

Visual observations were also made to obtain qualitative data from the cyclic slab bending tests, as with the static slab bending tests. Observations were made concerning

the nature of cracking with relation to the patched area and the status of the patch at the conclusion of the cyclic test.

Table 4-8 Visual observations for cyclic slab bending tests

Visual Observations		
	Cracking	*Bond*
3U18 M C 1		
3U18 M C 3		
3U18 M W 2		
3U18 M W 4		
3U18 S C 1		
3U18 S C 4		
3U18 S W 2		
3U18 S W 4		
Futura-45 M C 3		
Futura-45 M C 4		
Futura-45 M W 2		
Futura-45 M W 3		
Futura-45 S C 2		
Futura-45 S C 4		
Futura-45 S W 2		
Futura-45 S W 3		

Key

Cracking

= crackng through patch

= cracking around patch

= cracking under patch

Bond

= patch did not debond from base concrete

= portion of patch debonded from base concrete

= patch debonded from base concrete

As with the static bending tests, all of the cyclic milled 3U18 patches performed poorly. All four of these specimens exhibited poor bond by full bond failure between patching material and base concrete. Upon examination of the void left by the debonded patch, it was apparent that cracks had formed beneath the patch, indicating non-composite behavior of the two materials and a weakening bond. Figure 4-10 shows some photographs of a typical milled 3U18 specimen before and after being tested.

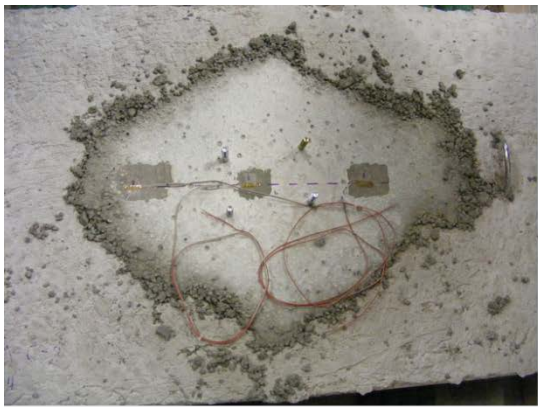

(a) Slab before testing

(b) Slab after testing

(c) Slab cracking under patch

(d) Bond surface of debonded patch

Figure 4-10 Photos of 3U18 M C 3

Table 4-9 Cyclic test time of debonding for fully debonded patches

Fully Debonded Patches from Cyclic Slab Bending Test		
Specimen	Status	Cycles (approx)
3U18_M_C_1	Fully Debonded	0
3U18_M_C_3	Fully Debonded	5200
3U18_M_W_2	Fully Debonded	250
3U18_M_W_4	Fully Debonded	2100

All four milled Futura-45 specimens cracked through the patch for the cyclic loading process, indicating a strong bond between substrate and patching material. However, some of milled Furura-45 specimens had pieces of patching material debond and break off of the remaining patch. Photos of a typical specimen of this type can be

seen in Figure 4-11. None of these four patches debonded during patch pullout, demonstrating some remaining bond strength after 6000 cycles of cyclic testing.

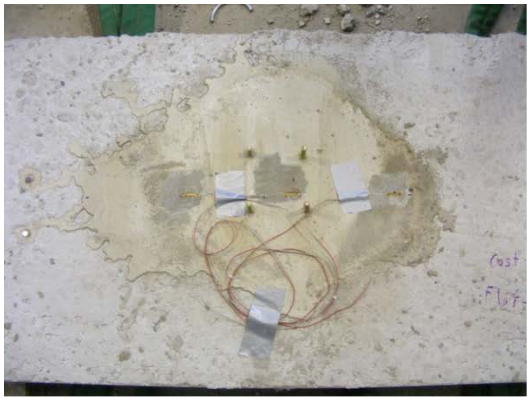

(a) Slab before testing

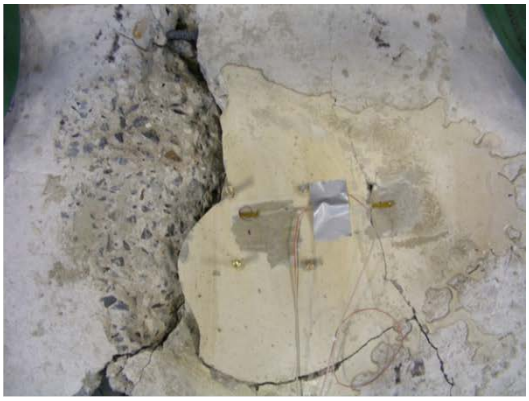

(b) Slab after testing

(c) Bond between remaining patch and substrate

(d) Bond surface on debonded portion of patch

Figure 4-11 Photos of Fut M C 4

Seven of the 8 remaining saw cut and chipped prepared patches displayed behavior generally similar to those tested under static loading. These specimens cracked around the patch area, showing poor bond at the extents of the patch area, with little or no cracking propagating across the corners of the patches. Typical saw cut and chipped cyclic patch behavior is pictured in Figure 4-12. The lone exception to this behavior was Fut S W 3, shown in Figure 4-13, which cracked through the patch. The lack of cracks around the edges of the patch area suggests that the bond along the saw cut edges of the

patch area was strong enough to allow the crack to propagate along its natural course through the patch rather than seeking a less resistive path around the patch.

(a) Slab before testing *(b) Slab after testing*

Figure 4-12 Photos of 3U18 S W 4

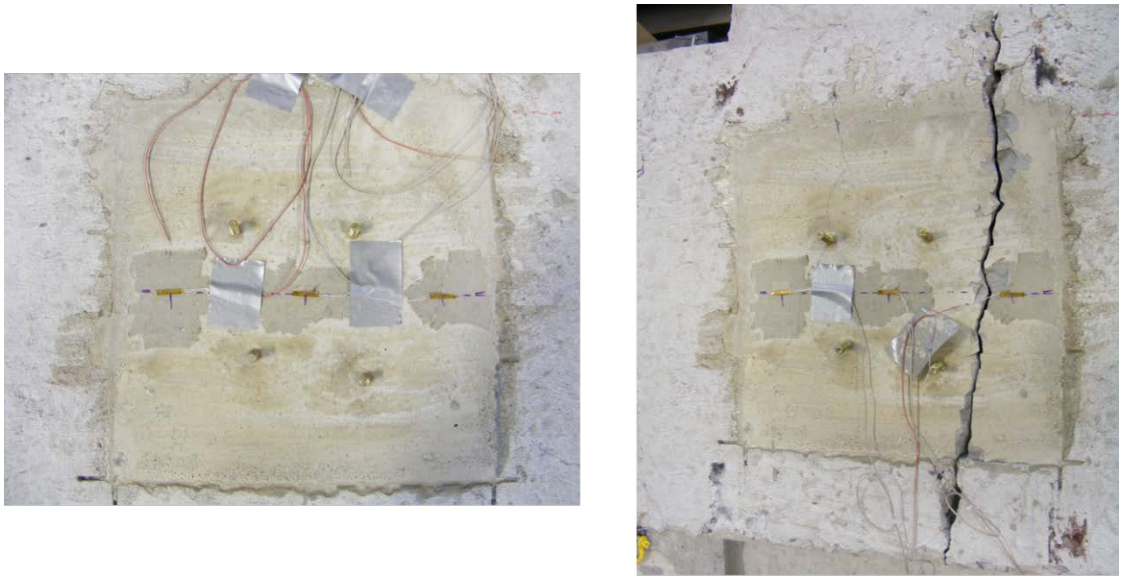

(a) Slab before testing *(b) Slab after testing*

Figure 4-13 Photos of Fut S W 3

4.4.4 Strain Data

Strain gages attached to the patched slabs provided strain data that was able to help determine debonding of the patches from the base concrete in some samples. It was believed that a decrease in strain would be seen as the bond between patching material

and concrete substrate was reduced. With the bond intact, the patch and the substrate should act as a single unit, similar to one of the unpatched control slabs tested in cyclic bending. Figure 4-14 shows a plot of the middle strain gage readings for one of the control stabs of ten cycles at the beginning and end for each set of 1000 cycles at each displacement magnitude. The important behavior to be observed from this strain data is the increase in tension strain (positive strain on the plot) as the displacement magnitudes increase. This behavior is consistent for the control specimen shown until the 0.25" displacement cycles. It is believed that the reinforcing steel bars yielded and formed a plastic hinge during these cycles. This belief is supported by the abrupt reduction in load observed in the peak/valley data.

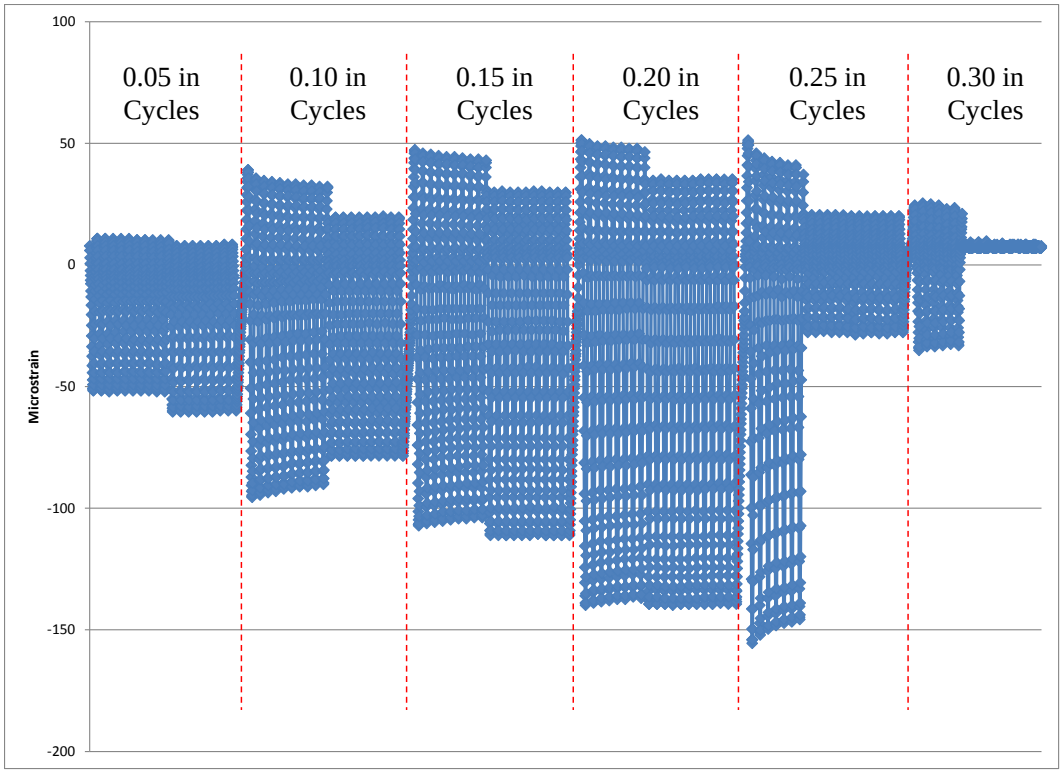

Figure 4-14 Control 1 cyclic slab bending beginning and end cycles on strain gage 2

A similar plot for the cyclic slab specimen 3U18 M C 3 is shown in Figure 4-15. The 3U18 M C 3 specimen was chosen as a representative sample because the strain data showed two clear indications of bond failure before the patch fully debonded from the concrete substrate. This specimen debonded fully at approximately 5200 cycles, during the actuator displacement cycles of 0.30 inches, indicating that some bond strength was retained for the majority of the test program. The plot indicates a decrease in tensile strain over the 1000 cycles at 0.10" of actuator displacement, indicating a loss of bond during these cycles resulting in little to no tensile force being applied to the patch for the remainder of the test. The specimen continues to apply considerable amounts of compression strain to the patch while less bond is present between the patch and base concrete due to the geometry of the patched area. However, further debonding is indicated by the substantial loss of compressive strain during the 0.20" actuator displacement cycles. This is not believed to be the result of the formation of a plastic hinge as was seen in the control specimen because the peak/valley data does not show a decrease in load on the slab corresponding to the decrease in strain.

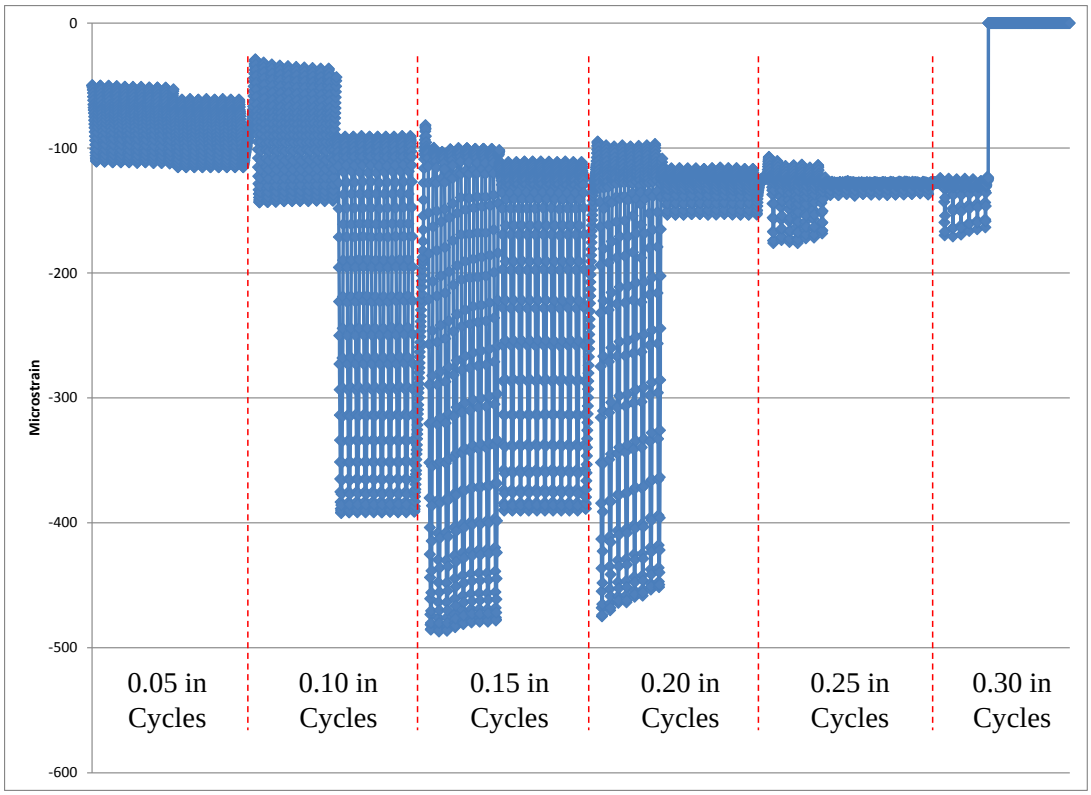

Figure 4-15 3U18 M C 3 cyclic slab bending beginning and end cycles on strain gage 1

Based on the comparisons made between the behaviors of 3U18 M C 3 and those of Control 1 under cyclic loading, observations were made about the bond in all other cyclic slab bending specimens based on strain data. Observations are summarized in Table 4-10. As is evident, nearly all specimens showed some indication of bond failure in the strain data. All 3U18 patches showed some indication of bond failure, including the 4 milled specimens that debonded completely from the base concrete slabs. In patches that did indicate some debonding, Futura-45 patched slabs showed fewer signs of bond failure than did 3U18 patched slabs.

Table 4-10 Strain observations

Strain Observations		
	Indications of Bond Failure	*Details*
3U18 M C 1	Complete	Complete debonding during cracking phase
3U18 M C 3	Complete	Complete debonding at 5200 cycles; tension strain loss in 0.10" cycles; compression strain loss in 0.02" cycles
3U18 M W 2	Complete	Complete debonding at 250 cycles
3U18 M W 4	Complete	Complete debonding at 2100 cycles
3U18 S C 1	Moderate	Decrease in tensile strain over entire test; decrease in compressive strain w/o decrease in load in 0.25" cycles
3U18 S C 4	Few	Small decrease in tensile strain over entire test; small decrease in compressive strain w/o decrease in load in 0.25" cycles
3U18 S W 2	Few	Small decrease in tensile strain over entire test; small decrease in compressive strain w/o decrease in load in 0.25" cycles
3U18 S W 4	Few	Small decrease in tensile strain over 0.15" cycles and beyond; small decrease in compressive strain w/o decrease in load in 0.25" cycles
Futura-45 M C 3	None	
Futura-45 M C 4	Few	Small decrease in tensile strain over entire test; small decrease in compressive strain w/o decrease in load in 0.20" cycles
Futura-45 M W 2	Few	Decrease in tensile strain over entire test
Futura-45 M W 3	Moderate	Decrease in tensile strain over entire test; decrease in compressive strain w/o decrease in load in 0.25" cycles
Futura-45 S C 2	Moderate	Decrease in tensile strain over entire test; decrease in compressive strain w/o decrease in load in 0.25" cycles
Futura-45 S C 4	Few	Small decrease in tensile strain over entire test
Futura-45 S W 2	Few	Small decrease in tensile strain over entire test
Futura-45 S W 3	None	

It can be noted that Futura-45 S W 3, which did not appear to show any indications of debonding in the strain data, was the only saw cut and chipped patch that cracked through the patch. Cracking through the patch was deemed an indication of very good bond between the patching material and concrete substrate. The clear agreement between the strain data and visual observations for this sample serves to reinforce the accuracy of the strain data.

CHAPTER 5 CONCLUSIONS AND RECOMMENDATIONS

5.1 3U18 vs. Futura-45

Nearly all of the data obtained from the testing program indicates that Futura-45 creates a stronger bond with a concrete substrate than does 3U18. The average bond stress as measured by the slant shear test without was about 1000 psi stronger for Futura-45 than for 3U18 (2436 psi vs. 1431 psi) and provided more consistent results. In milled prepared patches, all 3U18 samples debonded completely for both static and cyclic slab bending, where Futura-45 specimen performance indicated very good bond characteristics for the same circumstances. Strain data for the cyclic tests also seemed to indicate better bond performance from Futura-45 with fewer specimens showing signs of debonding. Futura-45 was also much easier to place into a patch area by pouring than the harsh, gravely 3U18 mix.

The poorer bond exhibited by the 3U18 is likely related to the high percentage of coarse aggregate in the mix and relatively small amount of paste. Excess paste is the part of the patching concrete that gets into the textured portions of a prepared concrete substrate. Figure 4-6 and Figure 4-10 show fully debonded 3U18 patches, which have only small areas that show remnants of paste from the patching material remaining on the base concrete after bond failure.

The high compressive strength of 3U18 may also be detrimental to the bond between 3U18 and a substrate. High compressive strength is also an indicator of high elastic modulus. Because the compressive strength of the 8U18 is much greater than that of the base concrete used in the tests performed as a part of this investigation, it follows that the elastic modulus is also much greater for the 3U18. This leads to a greater portion

of the applied load trying to reach the patch, resulting in a greater shear force across the bond surface.

5.2 Cement Paste Bonding Agent vs. No Bonding Agent

In general, test data seemed to indicate that the inclusion of a cement paste bonding agent before applying patching material actually weakened bond strength. Slant shear tests indicated a consistently low bond failure stress for specimens prepared with the cement paste bonding agent, with little difference between samples utilizing different patching materials. It is clear that the bonding agent is governing these failures and that the strength of the bonding agent is substantially less than the bond strength generated by the materials on their own.

The other tests confirm that the cement paste does nothing to improve the bond between substrate and patching material. The lone core pullout specimen to pull away from the base concrete was a cement paste prepared 3U18 specimen, which failed at a low bond stress of only 273 psi. Although the static slab bending tests showed little difference between specimens with or without the bonding agent, the cyclically tested specimens without cement paste performed slightly better than those that included the bonding agent.

5.3 Saw Cut and Chipped vs. Milled Patch Preparation

During the slab bending tests, mixed results were seen from the two patch preparation methods. Milled patches exhibited both the best bond behavior with Futura-45, as well as the worst bond with 3U18. It appeared as though the characteristics of the patching material being used interacted with the method of patch preparation to affect the overall bond strength of a patch.

Clearly, 3U18 patches installed in milled prepared slabs did not exhibit very strong bond with all specimens for both static and cyclic testing debonding completely, some at very small deflections or few cycles. The poor bond exhibited by 3U18 in milled patches may be due in part to the difficulty for the harsh mix to fill shallow portions of the patch area and be finished well.

However, milled prepared slabs patched with Furura-45 showed exceptional bond quality in both the static and cyclic slab bending tests. All specimens with this combination cracked through the patch, indicating that the slab and the patch were acting as a single, composite unit.

More labor intensive saw cut and chipped prepared patches behaved much better than milled patches when patched with 3U18. Overall, Futura-45 showed only slightly better bond strength in saw cut and chipped patches over 3U18. The most important features about saw cut and chipped prepared patches are the behaviors relating to cracking in slabs patched in this manner. Fifteen of the sixteen saw cut and chipped patches cracked along the edges of the patches, indicating that the bond between patch and substrate at the saw cut edge is not very strong. Also, recall that a trend of lower loads was required to crack saw cut and chipped slabs near the saw cut edge when compared to cracking loads for milled slabs. Combining poor edge bond with the lower cracking loads introduces a route for water and other contaminants to infiltrate a roadway slab and cause damage. Such damage could shorten the lifespan of the repair, or potentially even create need for a full-depth repair later.

5.4 Slant Shear vs. Core Pullout vs. Static Slab Bending vs. Cyclic Slab Bending

Clearly, the core pullout tests as performed provided very little information. The remaining three tests, overall, showed several trends that agreed from test to test, specifically those discussed in Sections 5.1, 5.2, and 5.3.

The slant shear test was the only test in the battery that successfully provided a quantitative measure of bond stress. The testing procedure required little specialized equipment besides a compression testing machine and was much less labor intensive than the slab bending tests once an effective process was developed for casting mortar base sections. However, there were some difficulties in keeping the mortar half-sections from becoming damaged. The points of the base sections had a tendency to break off, which may have created a bearing area in the composite cylinder during testing. Such a condition may have contributed to the substantial variance that was seen in some of the slant shear data for the specimens that were not cast with the bonding agent.

The static bending test provided valuable information, based primarily on visual observation. Observation of cracking patterns and patch damage indicated trends that were also seen by more heavily instrumented cyclic test specimens.

Cyclic slab bending tests provided some useful data about the behavior of patch bond throughout the cycles from the strain gages for identifying qualitative trends in bond deterioration. Peak-valley data acquired during these tests did not provide much use besides to confirm the formation of plastic hinges in specimens during the later cycles of testing. The visual observation data agreed with other behavioral trends observed during testing. Although the cyclic tests better simulated traffic and temperature loading to which a rigid pavement would be exposed, the static slab bending tests provided most of the important behavioral trends in a shorter and less labor intensive test method.

5.5 Recommendations for Further Research

The results of the testing performed as part of this investigation prompt further research into the bond strength of partial-depth patching materials. It is still believed that the core pullout test as performed in this investigation can provide useful quantitative data on patching material bond strength if the capacity of the testing system is increased. The system as used in this investigation was able to apply 455 psi to the bond area, but the slant shear tests indicated that stresses nearing 3000 psi may be required to cause bond failure.

Although the bond strength did not seem to see improvement with the application of a cement paste bonding agent, cement paste is not the only bonding agent that is used in the field. Many of the tests conducted as a part of this program could be repeated substituting epoxy or latex bonding agents for the cement paste bonding agent.

As always, the most accurate way to evaluate the effect of field conditions on a product or technology is to observe how it actually performs in the field. Additional field studies and monitoring focused on bond strength could provide useful data on field behavior and be compared to the results of the slab bending tests performed for this investigation to determine the representativeness of these tests.

5.6 Summary and Recommendations

This report presents the procedures and results of an investigation of bond strength between patching materials used for partial-depth patching projects and concrete representative of the rigid pavements that are patched. Different test methods utilized included slant shear tests, core pullout tests, static slab bending tests, and cyclic slab bending tests. The battery of tests looked at the effects of several variables on bond

strength, including the patching material used, the addition of a cement paste bonding agent before patching material is applied to base concrete, and the method used to remove deteriorated concrete and prepare the bond surface of the base concrete.

Based on the results of this testing program, the following recommendations can be made:

1) Futura-45 should be selected over 3U18 in partial-depth repairs where bond is crucial.
2) The cement paste bonding agent should not be used in field applications. The application of the paste actually decreases the bond strength between the patching material and the concrete substrate and increases the necessary labor of the patching process.
3) The patch preparation method and the material being used for a particular application should be compatible. For most applications, a material with sufficient paste and limited coarse aggregate can be used in a milled prepared patch area to achieve high bond strength. If a harsher mix with high percentages of coarse aggregate is to be used as the patching material, a saw cut and chipped patch preparation will serve to promote the best bond. Harsh materials similar to 3U18 should not be used for partial-depth repairs that are milled to a shallow depth.
4) With careful sample preparation, usable data can be obtained from the slant shear test. Although the standard deviation is typically high for this test, the results correlate well with those from more complex tests. Slant

shear is a representative small scale test and is suitable for quality control and quality assurance applications.

BIBLIOGRAPHY

AASHTO. (2012, March 30). Rapid Set Concrete Patching Materials for Portland Cement Concrete. *National Transportation Product Evaluation Program*. AASHTO.

American Concrete Pavement Association. (2004). *Concrete Crack and Partial-Depth Spall Repair Manual.*

ASTM. (2008). Standard Test Method for Rock Bolt Anchor Pull Test. D 4435-08. West Conshohocken, PA: ASTM International.

ASTM. (2009). Standard Specification for Packaged, Dry, Rapid-Hardening Cementitious Materials for Concrete Repairs. C 928/C 928M-09. West Conshohocken, Pennsylvania, USA: ASTM International.

ASTM. (2012). Standard Test Method for Bond Strength of Epoxy-Resin Systems Used with Concrete by Slant Shear. C 882/C 882M-12. West Conshohocken, Pennsylvania, USA: ASTM International.

ASTM. (2012). Standard Test Method for Compressive Strength of Cylindrical Concrete Specimens. C 39/C 39M-12a. West Conshohocken, Pennsylvania, USA: ASTM International.

ASTM. (2012). Standard Test Method for Compressive Strength of Hydraulic Cement Mortars. C 109/C 109M-12. West Conshohocken, PA: ASTM International.

ASTM. (2013). Standard Test Method for Tensile Strength of Concrete Surfaces and the Bond Strength or Tensile Strength of Concrete Repair and Overlay Materials by Direct Tension (Pull-off Method). C 1583/C 1583M-13. West Conshohocken, PA: ASTM International.

Carbonell Muñoz, M. A., Harris, D. K., Ahlborn, T. M., & Froster, D. C. (2013, July 1). Bond Performance between Ultra-High Performance Concrete and Normal Strength Concrete. *Journal of Materials in Civil Engineering*, Accepted for publication.

Cervo, N. M., & Schokker, A. J. (2010, November/December). Bridge Deck Patching Material Evaluation. *Journal of Bridge Engineering*, 723-730.

Chen, D., Won, M., Zhang, Q., & Scullion, T. (2009, September). Field Evaluations of the Patch Materials for Partial-Depth Repairs. *Journal of Materials in Civil Engineering*, 518-522.

Frentress, D. P., & Harrington, D. (2011). *Partial-Depth Repairs for Concrete Pavaments.* FHWA.

Frentress, D. P., & Harrington, D. S. (2012). *Guide for Partial-Depth Repair of Concrete Pavements.* Iowa State University, Institute for Transportation. Ames, IA: Iowa State University.

Grace, N., Ushijima, K., Baah, P., & Bebawy, M. (2013, July/August). Flexural Behavior of a Carbon Fiber–Reinforced Polymer Prestressed Decked Bulb T-Beam Bridge System. *Journal of Composites for Construction*, 497-506.

Minnesot Department of Transportation. (2005). *Mn/DOT Standard Specifications for Construction.* St. Paul: Mn/DOT. Retrieved July 1, 2013, from http://www.dot.state.mn.us/pre-letting/spec/2005/3101-3491.pdf

Minnesota Department of Transportation. (2003). Concrete Pavement Rehabilitation. In *MnDOT Concrete Manual.* Maplewood, Minnesota: Minnesota Dept. of Transportation, Office of Materials and Road Research. Retrieved from http://www.dot.state.mn.us/materials/manuals/concrete/Chapter9.pdf

Parker Jr., F., & Shoemaker, W. (1991). PCC Pavement Patching Materials and Proceedures. *Journal of Materials in Civil Engineering*, 29-47.

Pennsylvania Department of Transportation. (2000). Section 516 - Concrete Pavement Patching. *Publication 408 PennDOT Construction Specifications*. Harrisburg, PA: PennDOT. Retrieved from http://www.dot.state.pa.us/Penndot/reginfo.nsf/infoTOCEnglish#500

Pennsylvania Department of Transportation. (2000). Section 525 - Concrete Pavement Spall Repair. *Publication 408 PennDOT Construction Specifications*. Harrisburg, PA: PennDOT. Retrieved from http://www.dot.state.pa.us/Penndot/reginfo.nsf/infoTOCEnglish#500

Pennsylvania Department of Transportation. (2004, April 19). Approved Construction Materials. *Publication 35 Bulliten 15*. Harrisburg, PA: PennDOT. Retrieved from http://innovativeproduct.org/wp-content/uploads/2012/03/PennDOT-Approved-Material-Report.pdf

W. R. Meadows, Inc. (2013, April). Futura-45. Hampshire, Illinois, USA: W. R. Meadows. Retrieved from http://www.wrmeadows.com/data/398A.pdf

APPENDIX A Static Bending Test Photos

APPENDIX A STATIC BENDING TEST PHOTOS

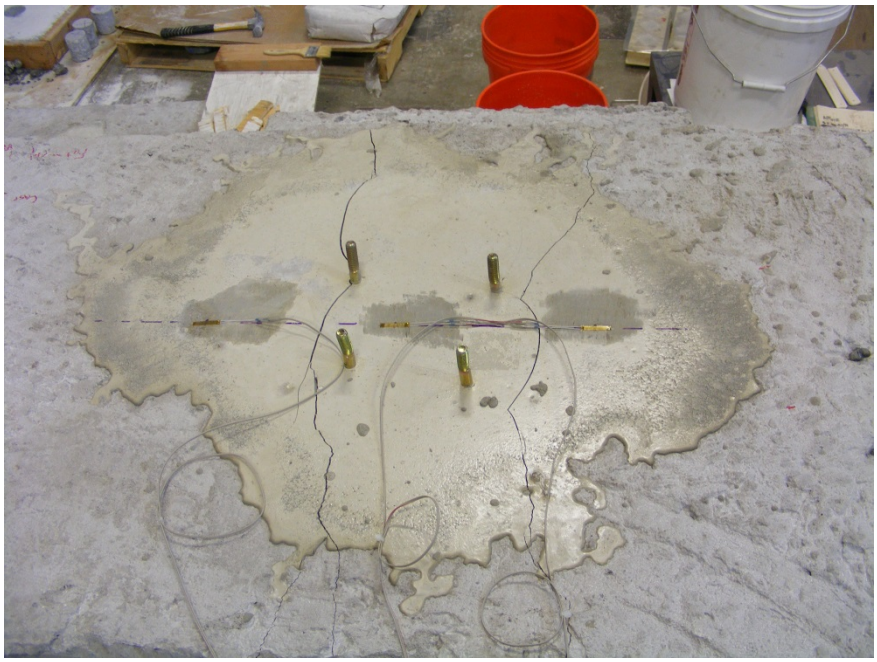

Figure A- 1 Fut M W 1

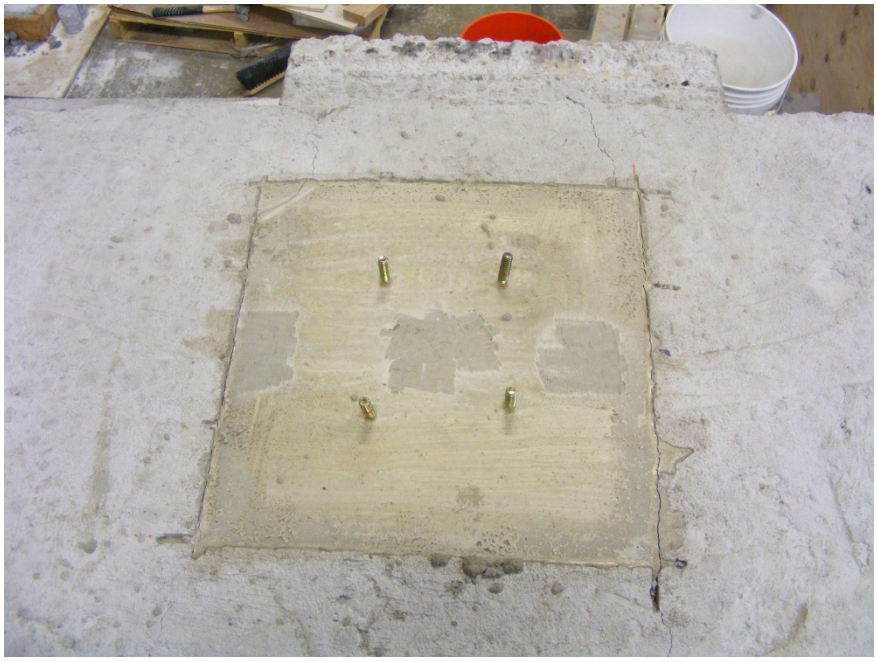

Figure A- 2 Fut S W 4

Figure A- 3 Fut M W 4

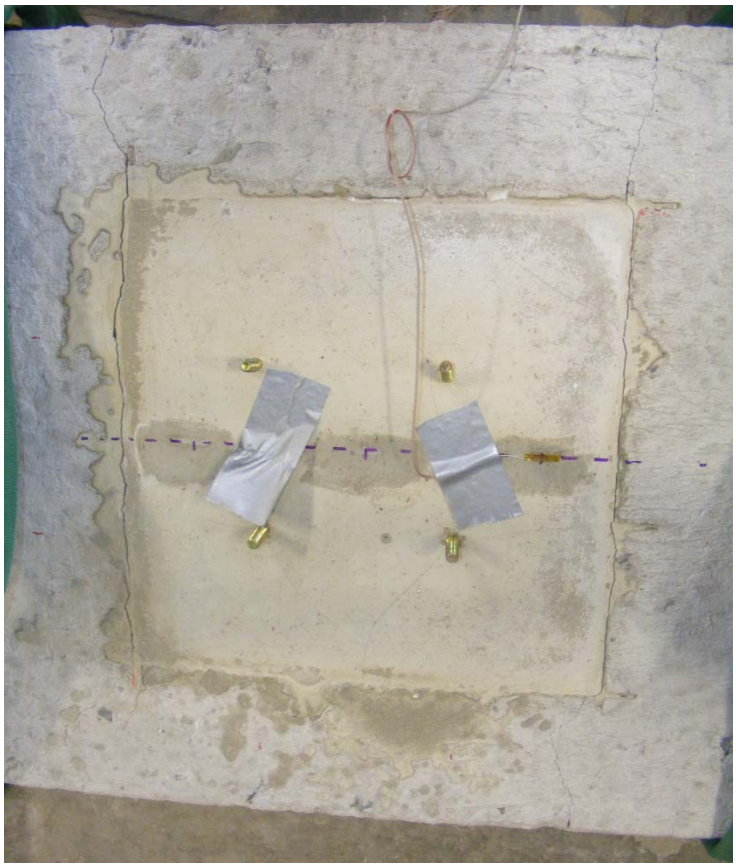

Figure A- 4 Fut S W 1

Figure A- 5 Fut S C 1

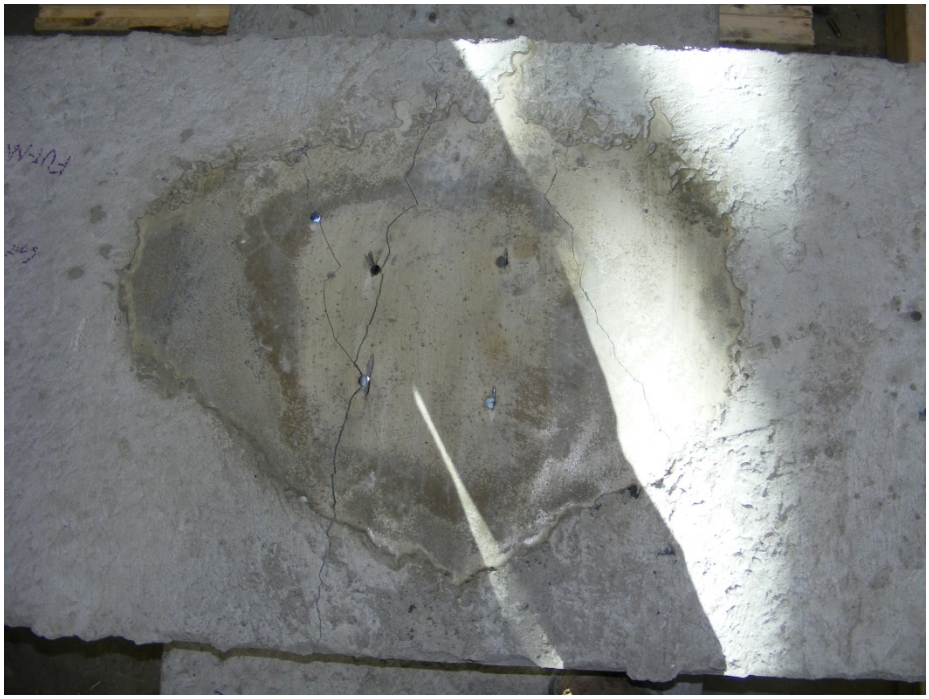

Figure A- 6 Fut M C 1

Figure A- 7 Fut S C 4

Figure A- 8 3U18 M W 1

Figure A- 9 3U18 S W 1

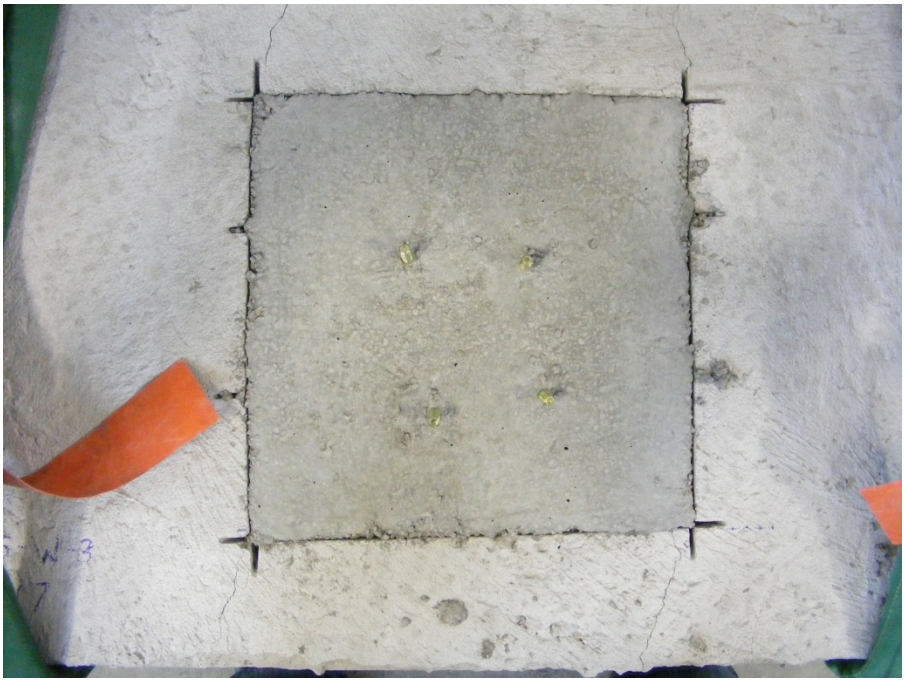

Figure A- 10 3U18 S W 3

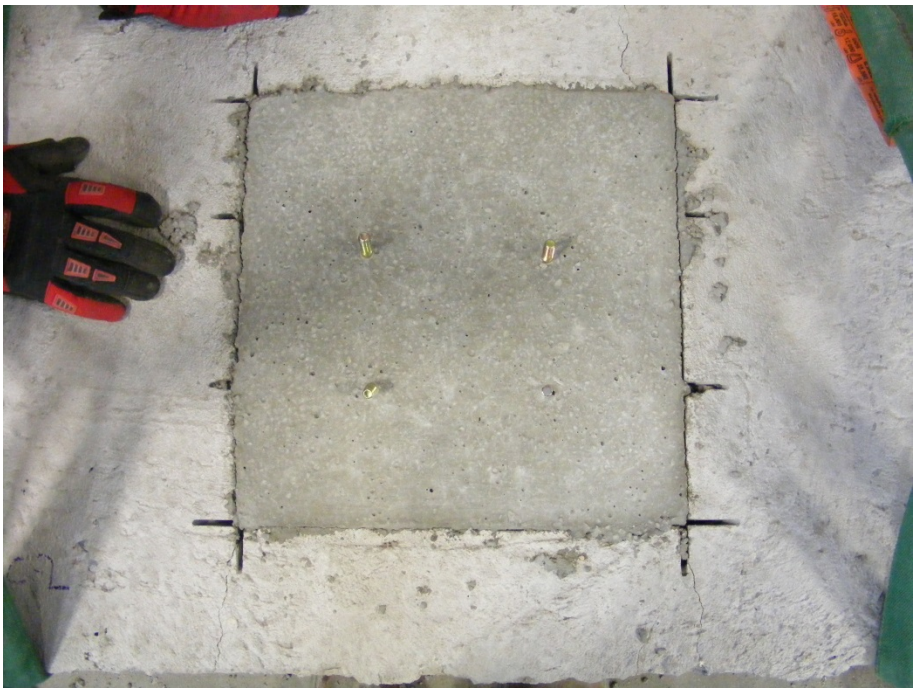

Figure A- 11 3U18 S C 2

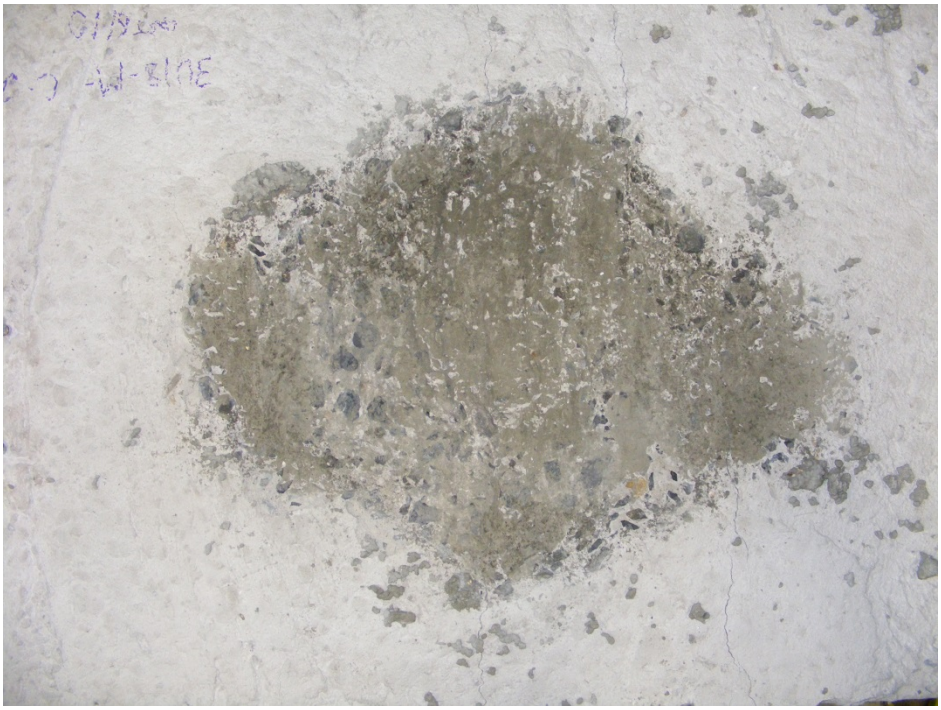

Figure A- 12 3U18 M C 2

Figure A- 13 3U18 S C 3

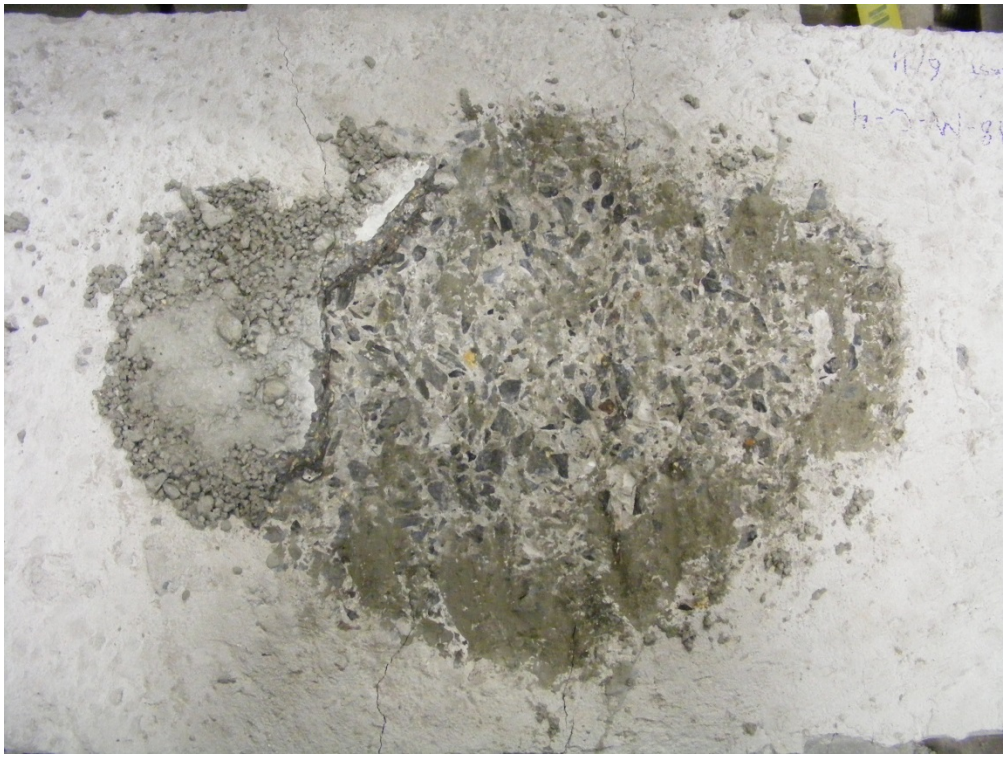

Figure A- 14 3U18 M C 4

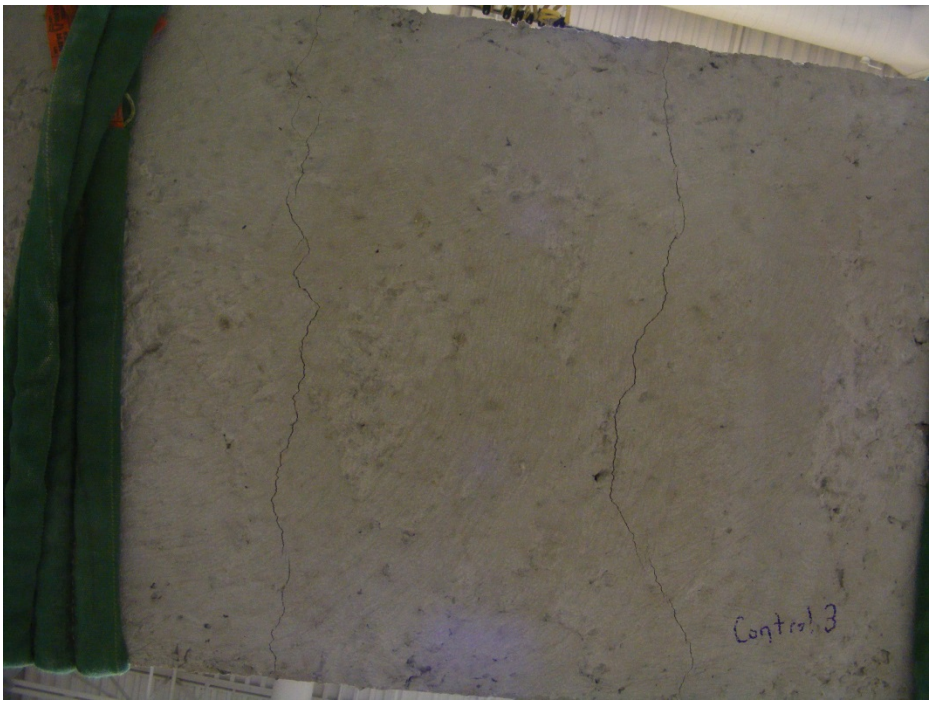

Figure A- 15 Control 3

APPENDIX B CYCLIC SLAB BENDING TEST PHOTOS AND STRAIN DATA

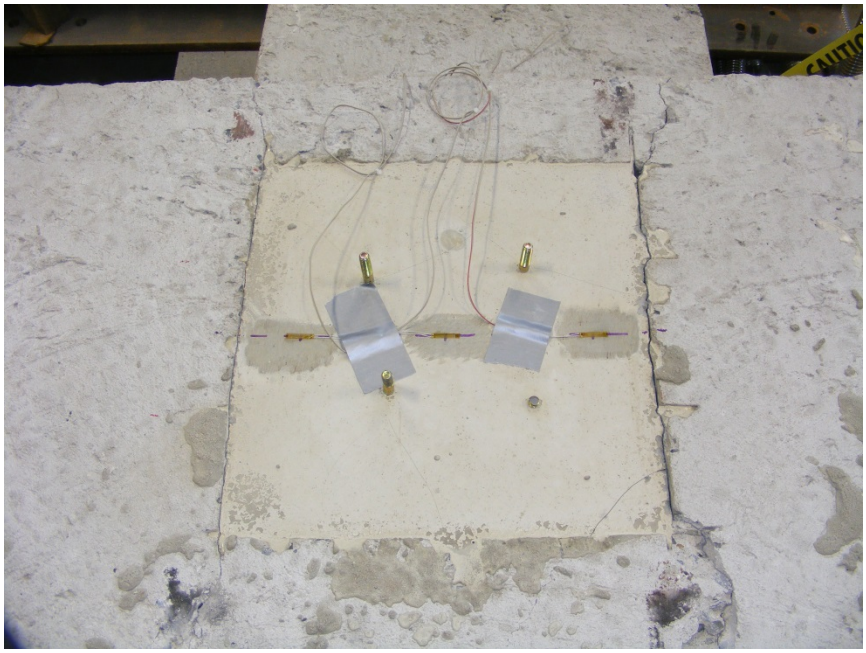

Figure B- 1 Fut S W 2

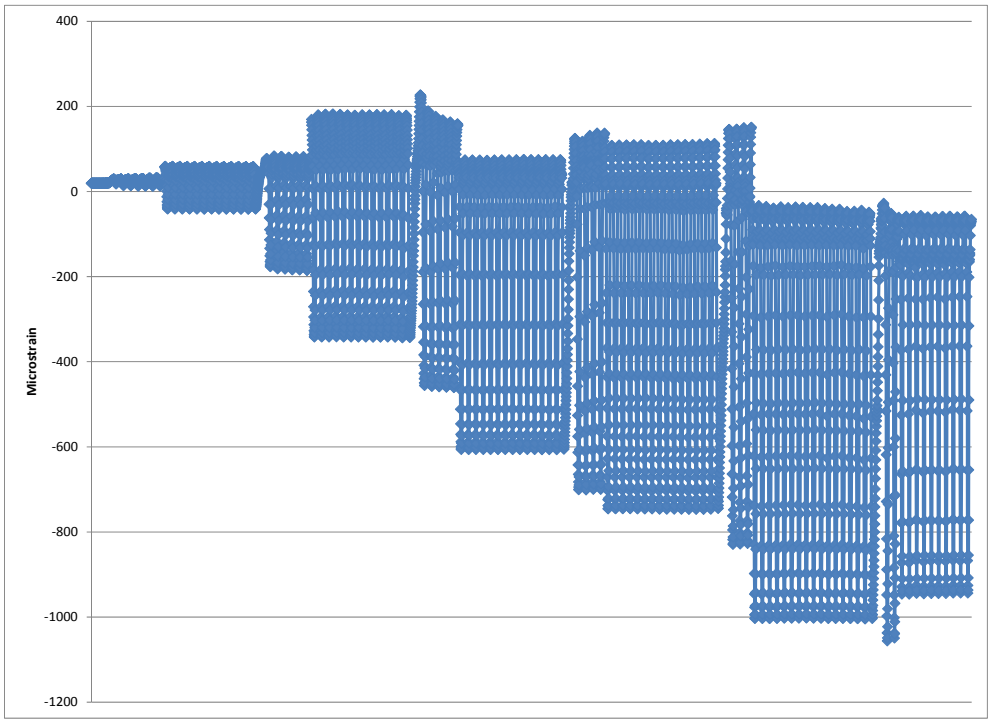

Figure B- 2 Fut S W 2 strain gage 2

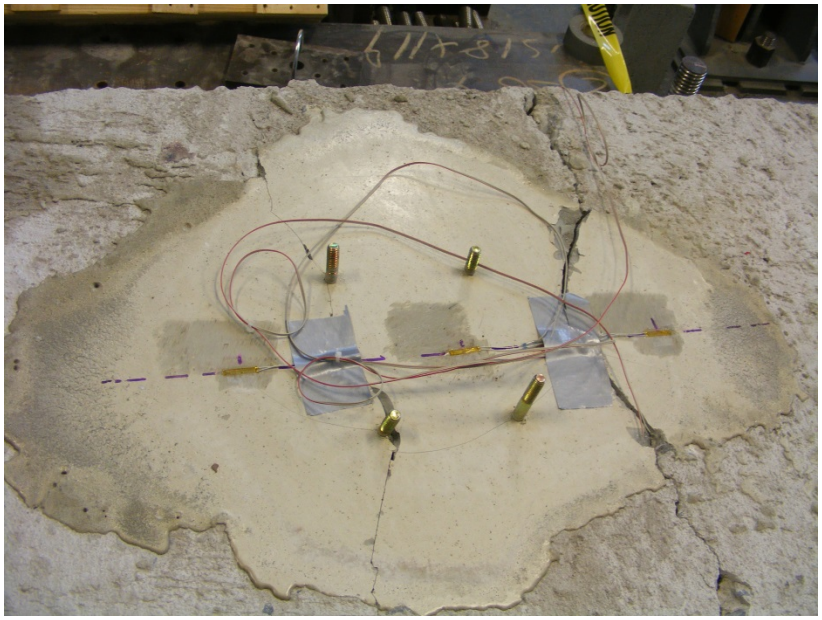

Figure B- 3 Fut M W 2

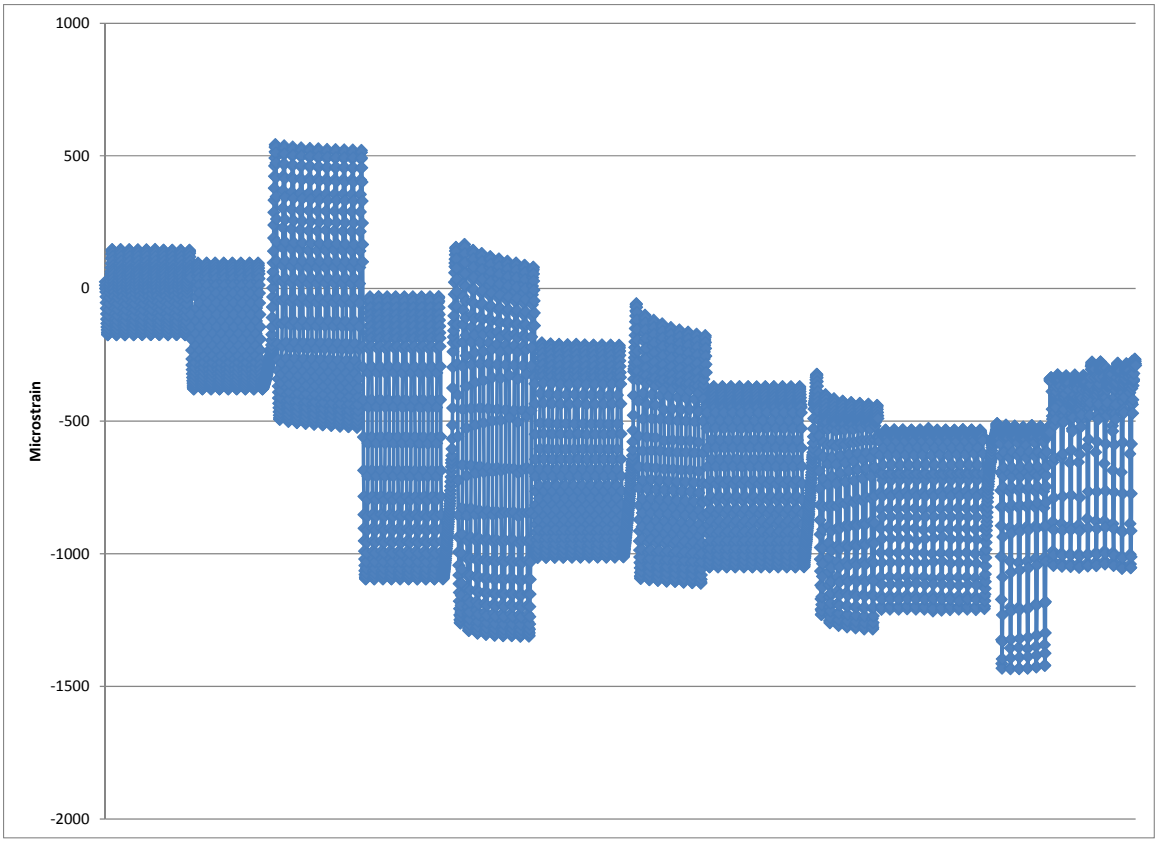

Figure B- 4 Fut M W 2 strain gage 1

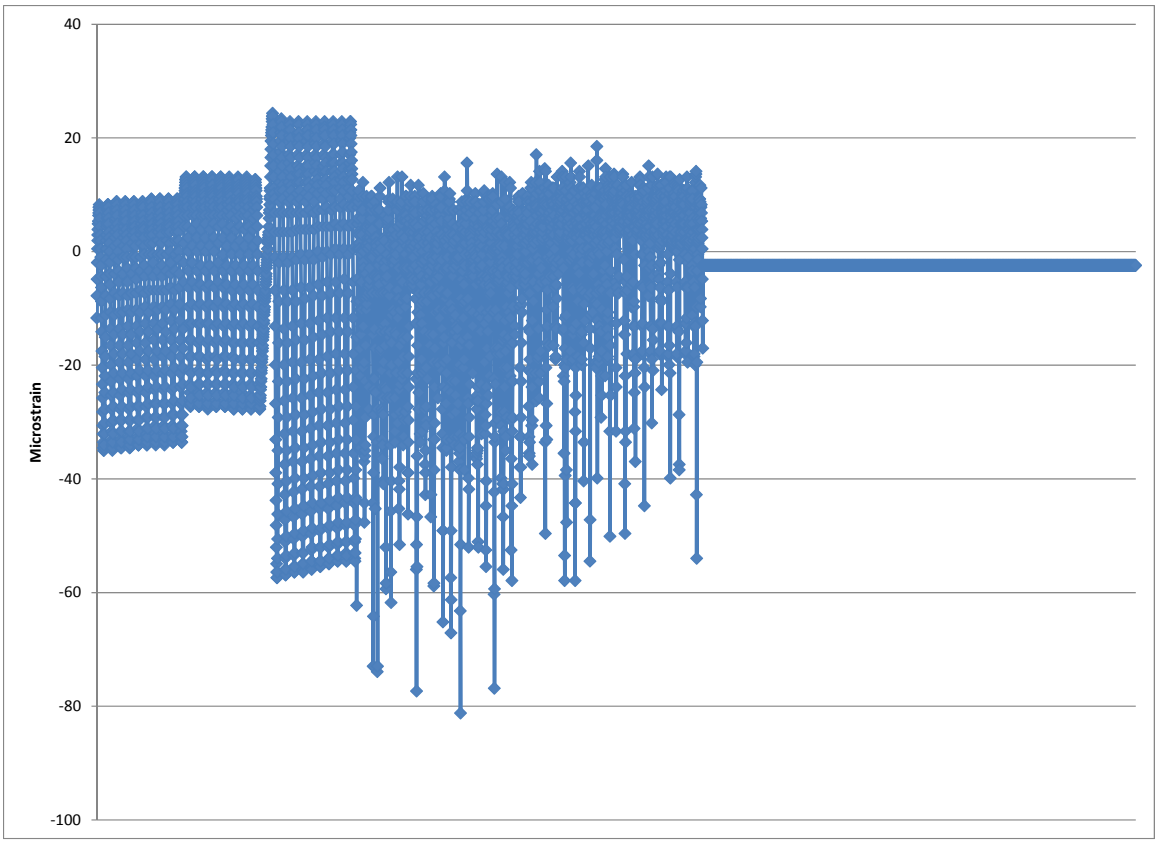

Figure B- 5 Fut S W 3 strain gage 2

Figure B- 6 Fut M W 3

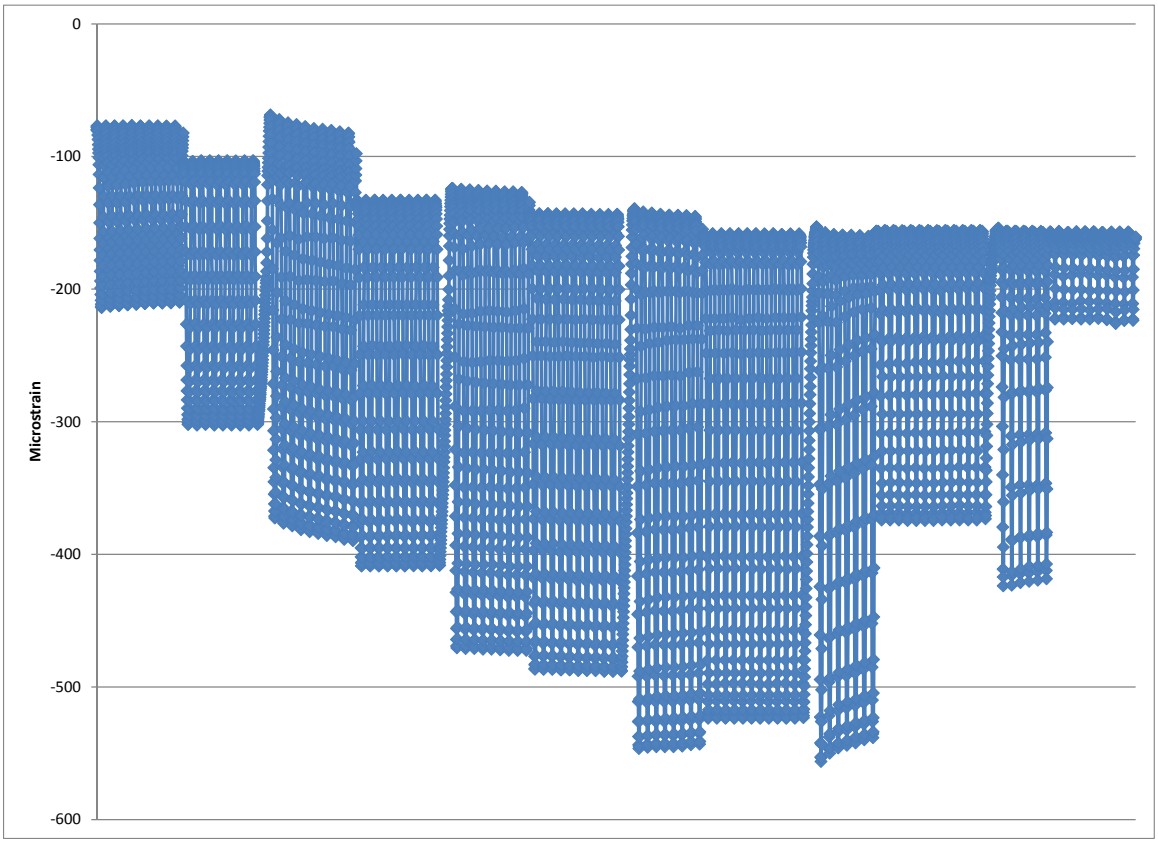

Figure B- 7 Fut M W 3 strain gage 2

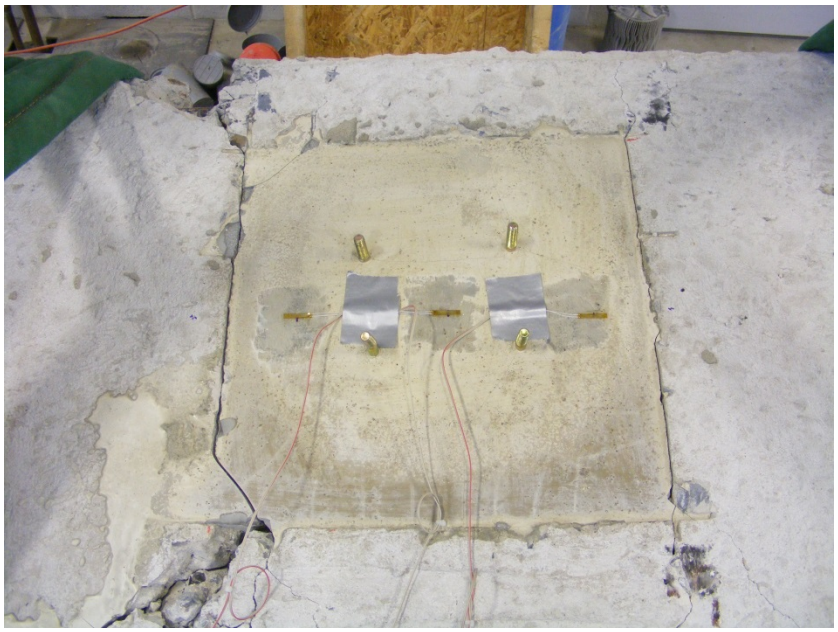

Figure B- 8 Fut S C 2

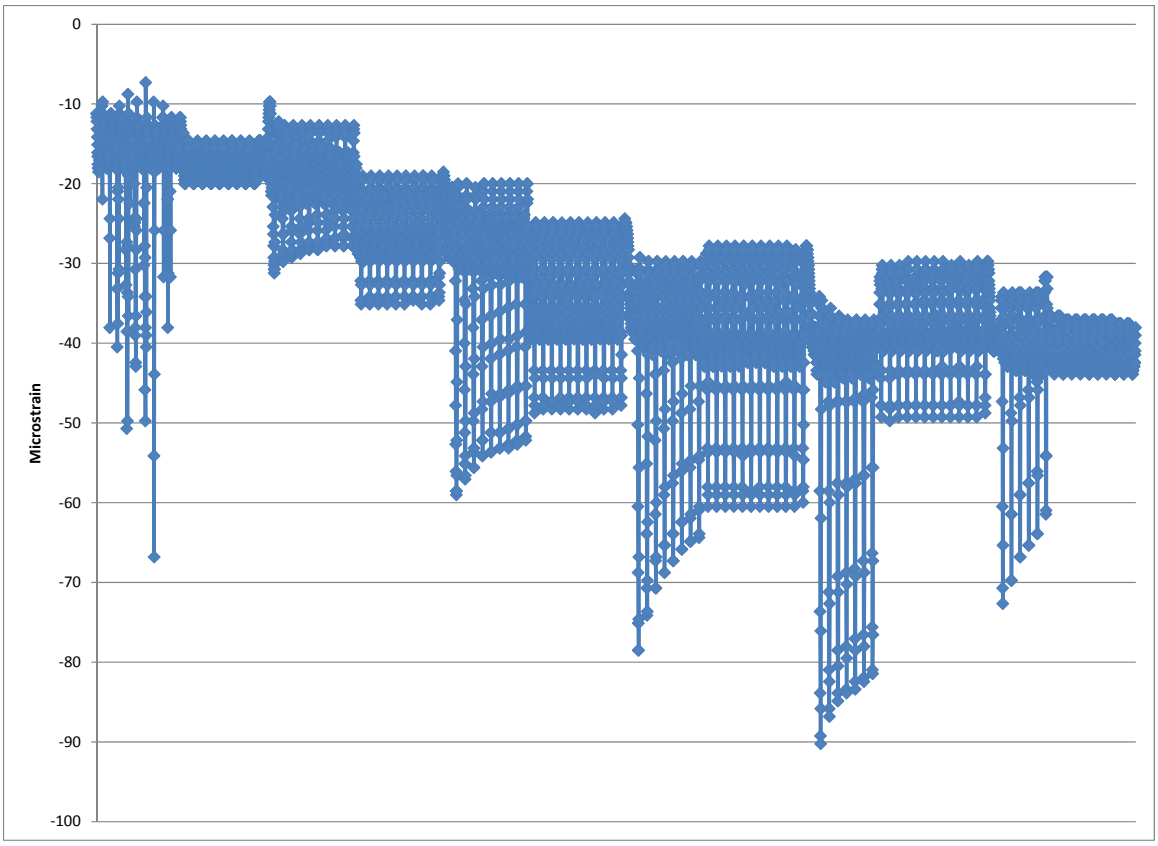

Figure B- 9 Fut S C 2 strain gage 2

Figure B- 10 Fut S C 3

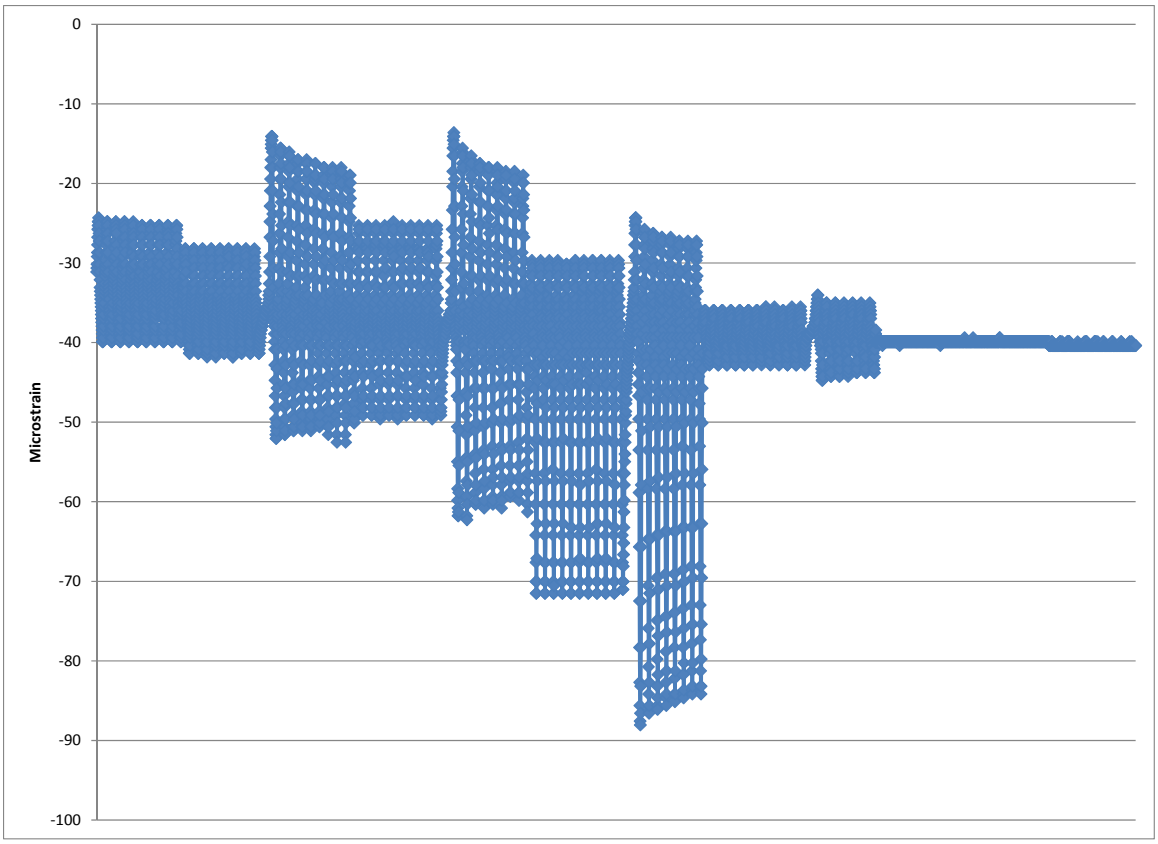

Figure B- 11 Fut S C 3 strain gage 2

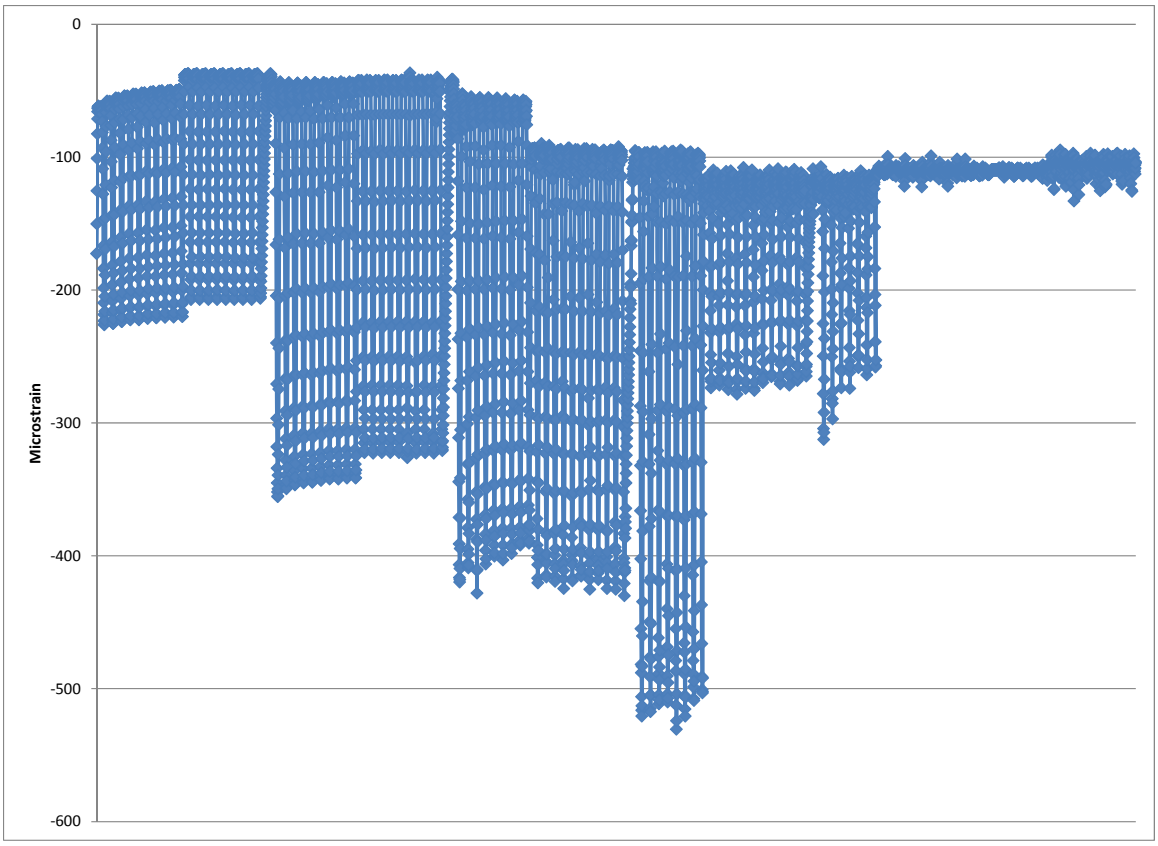

Figure B- 12 Fut M C 4 strain gage 2

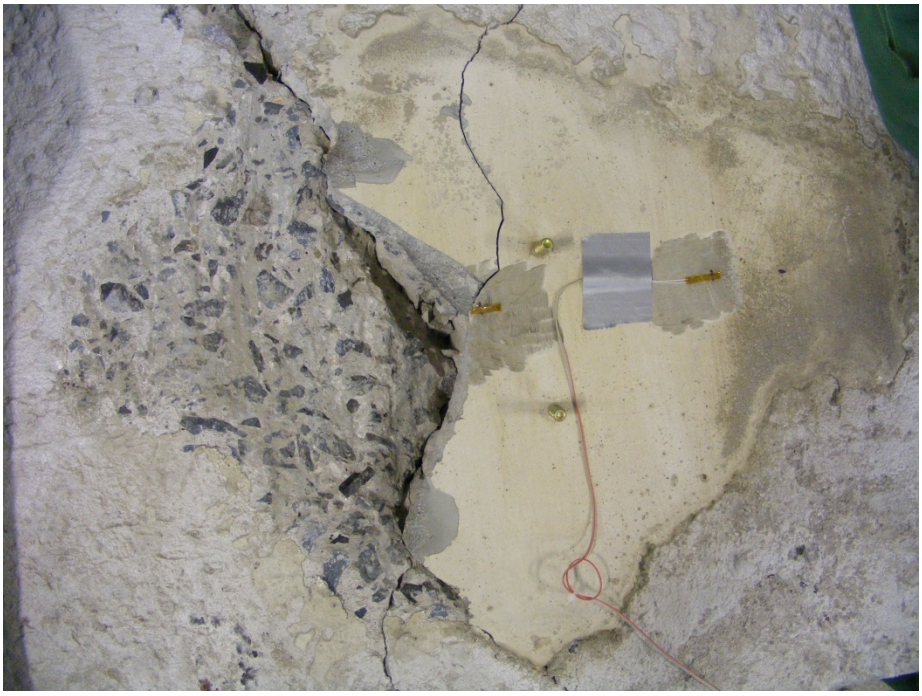

Figure B- 13 Fut M C 3

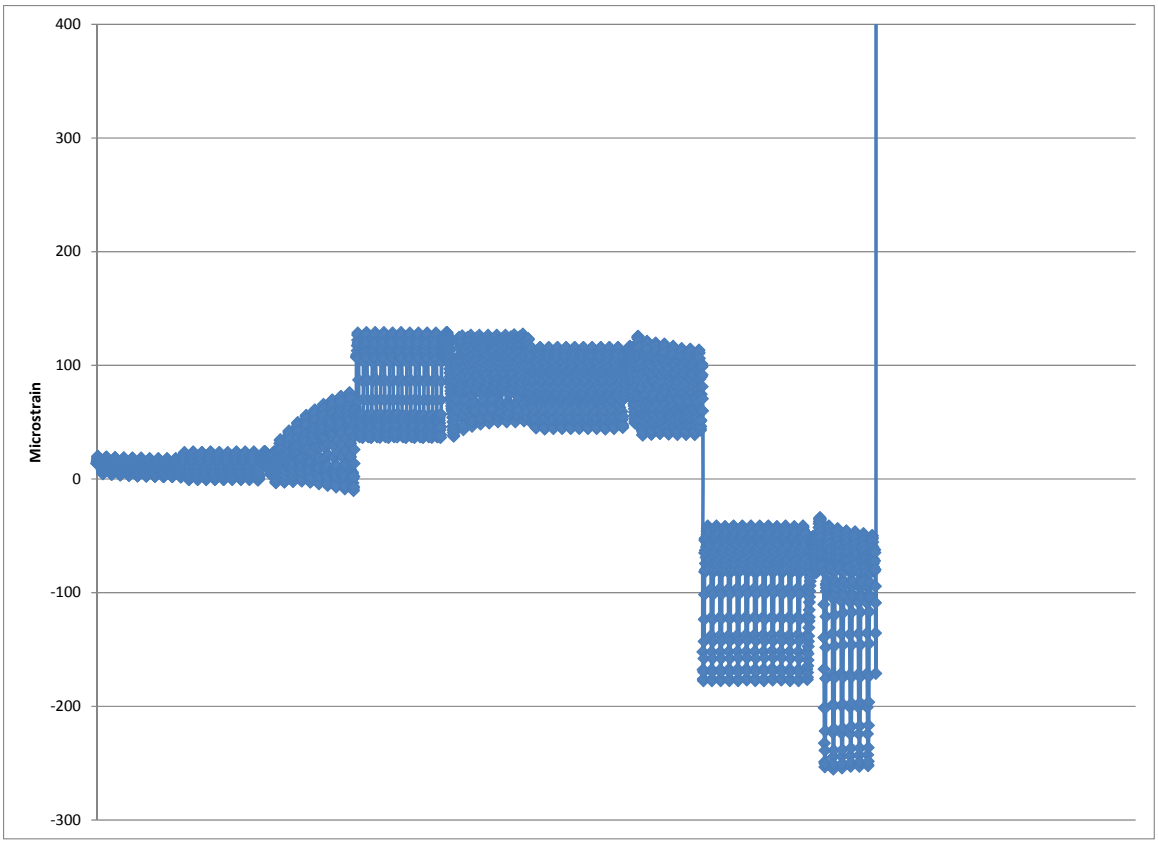

Figure B- 14 Fut M C 3 strain gage 2

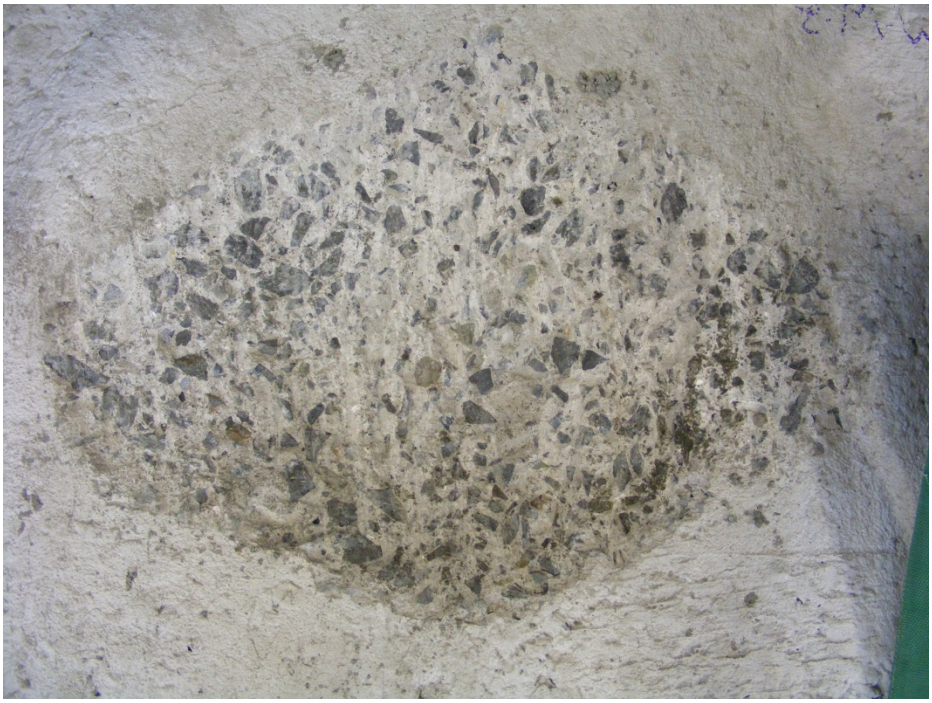

Figure B- 15 3U18 M W 2

Figure B- 16 3U18 M W 2 strain gage 1

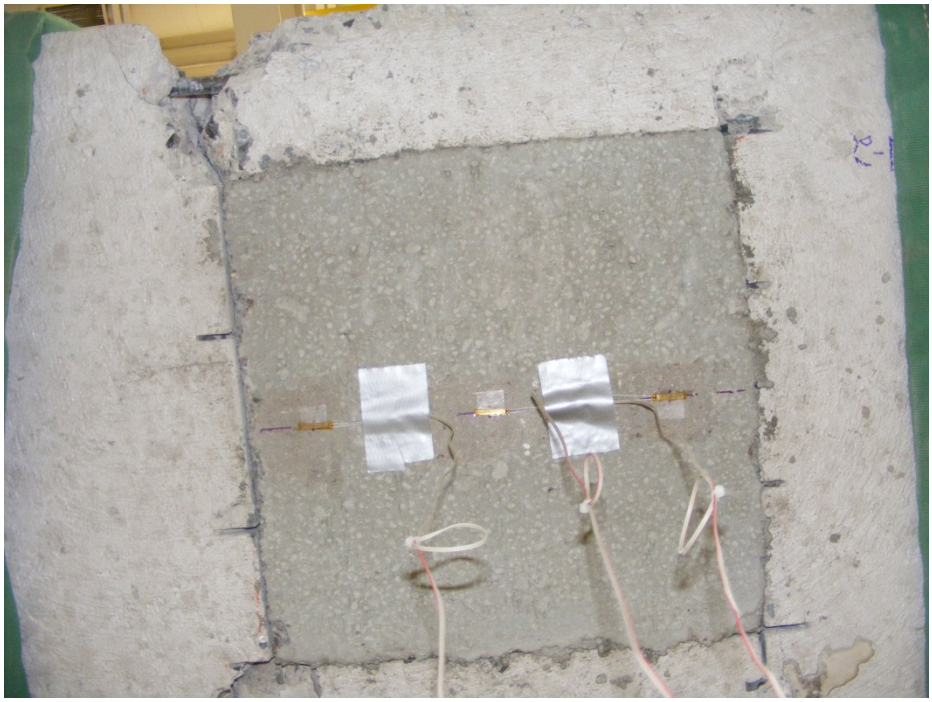

Figure B- 17 3U18 S W 2

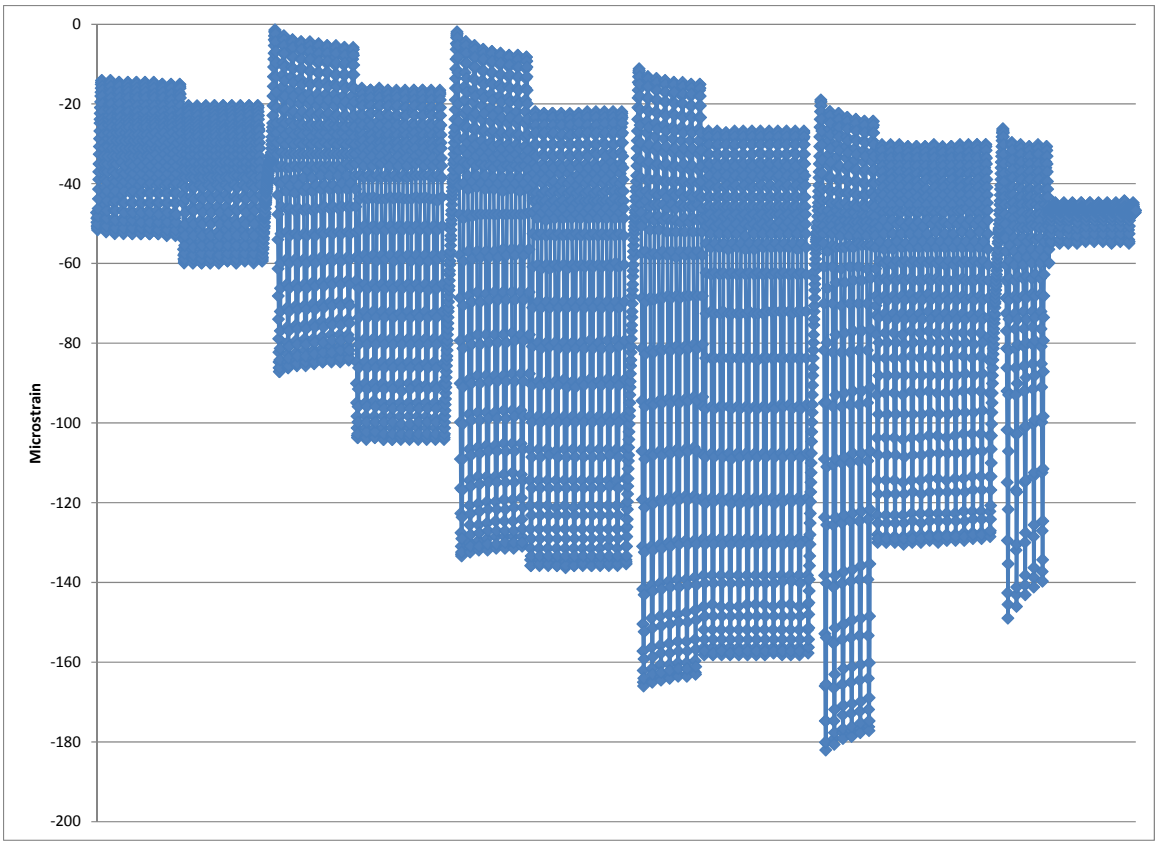

Figure B- 18 3U18 S W 2 strain gage 2

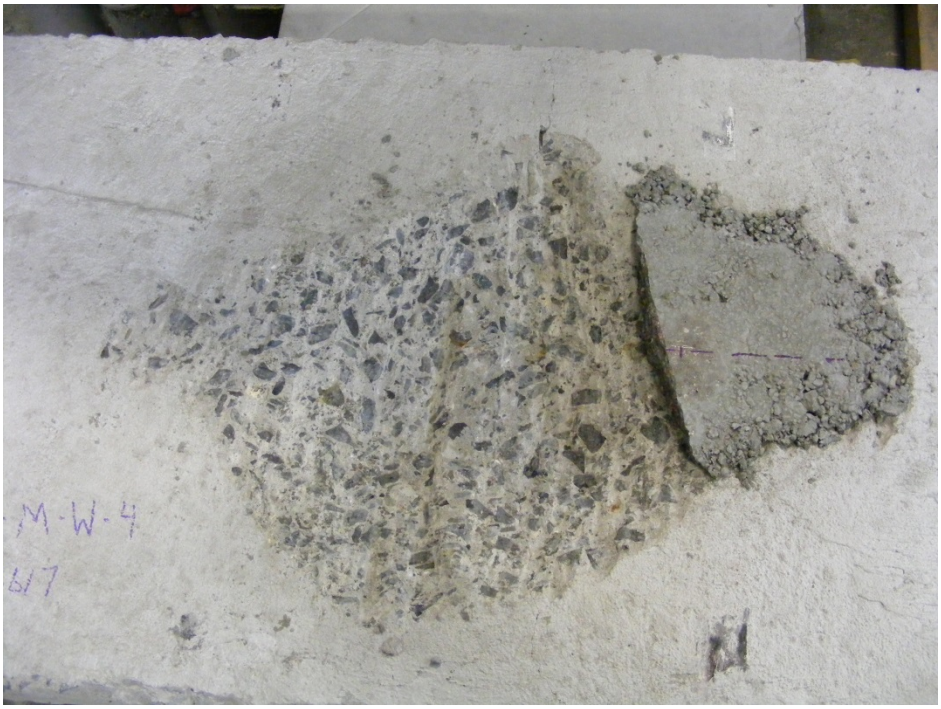

Figure B- 19 3U18 M W 4

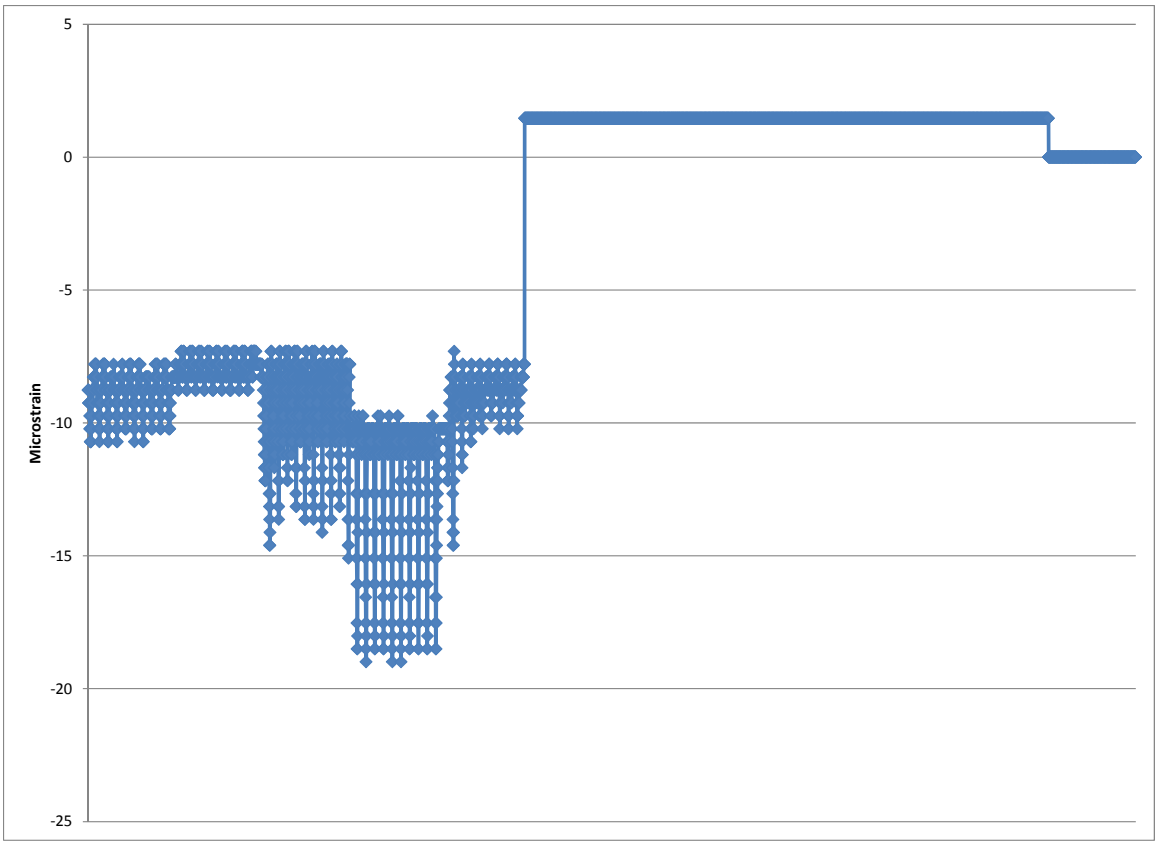

Figure B- 20 3U18 M W 4 strain gage 2

Figure B- 21 3U18 S W 4

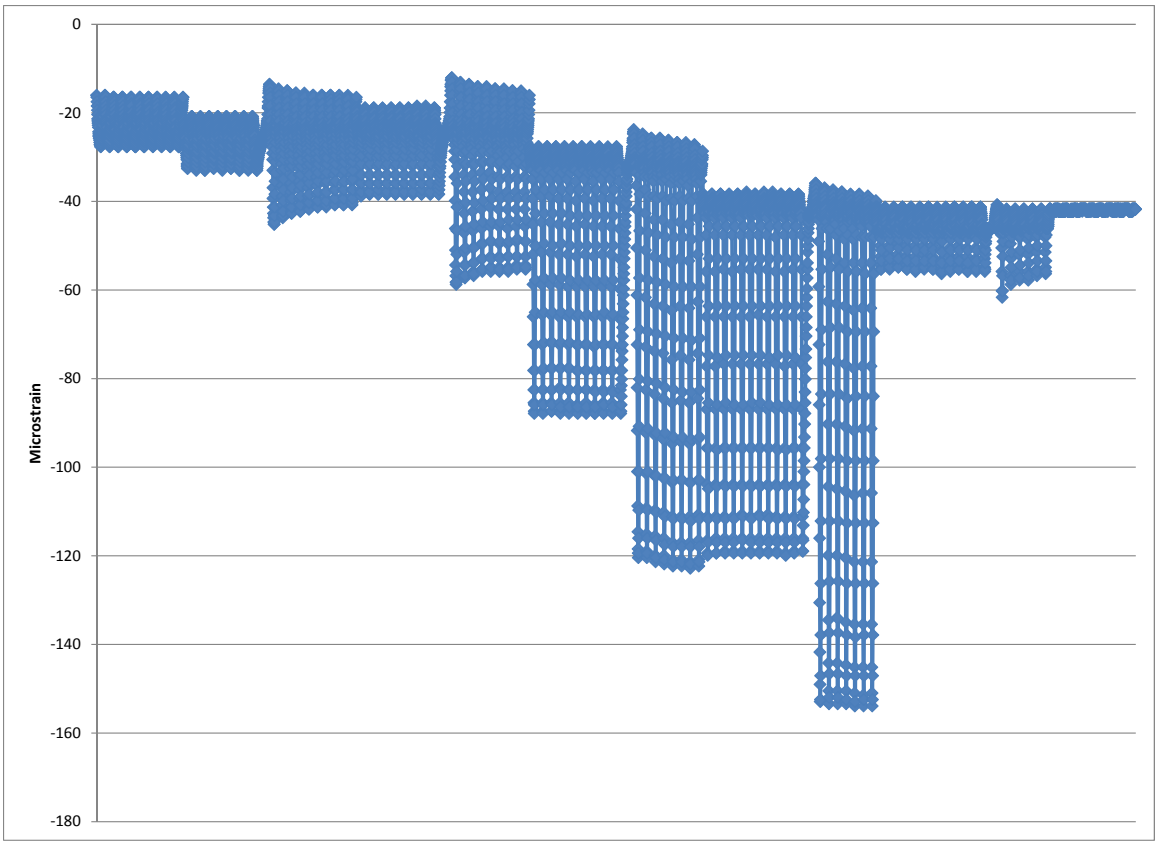

Figure B- 22 3U18 S W 4 strain gage 2

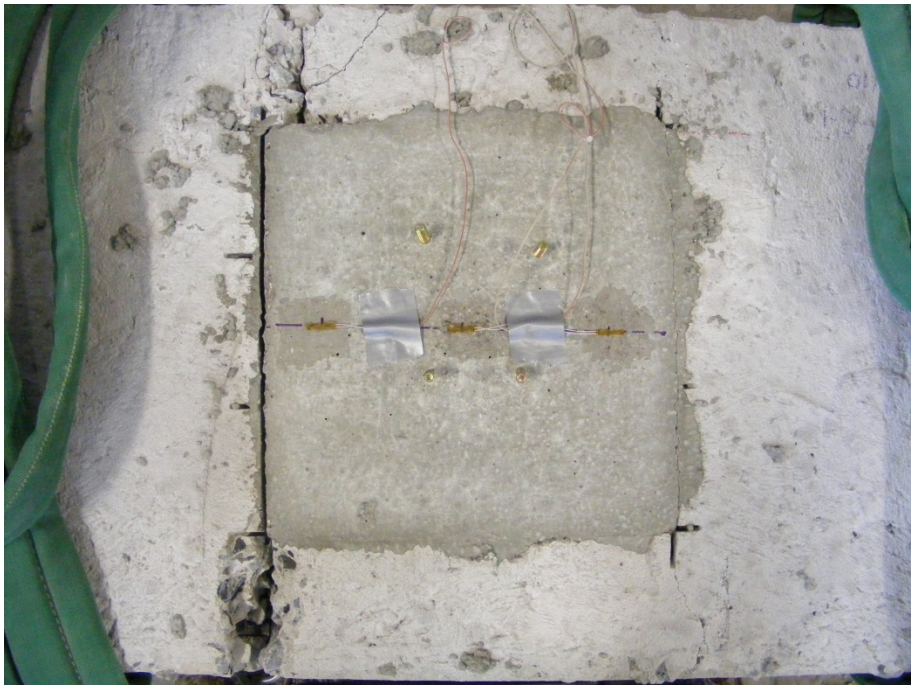

Figure B- 23 3U18 S C 1

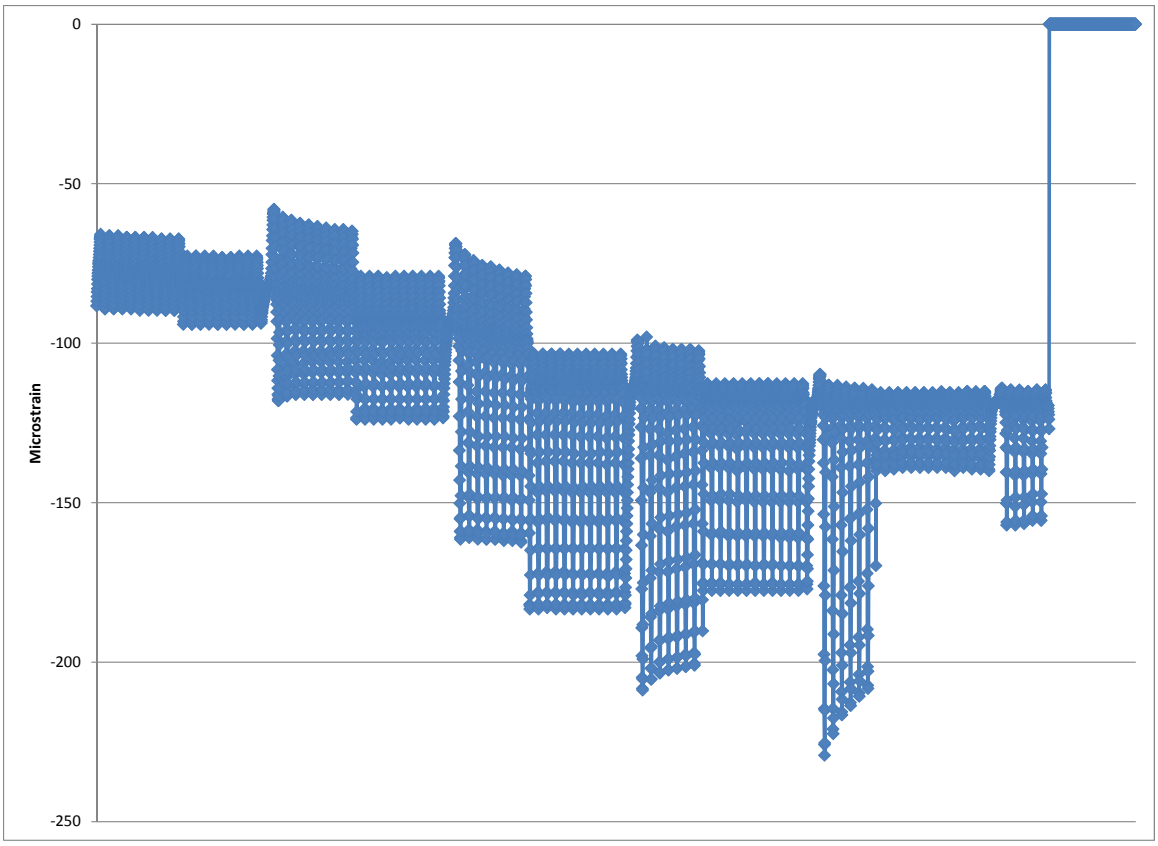

Figure B- 24 3U18 S C 1 strain gage 2

Figure B- 25 3U18 M C 1

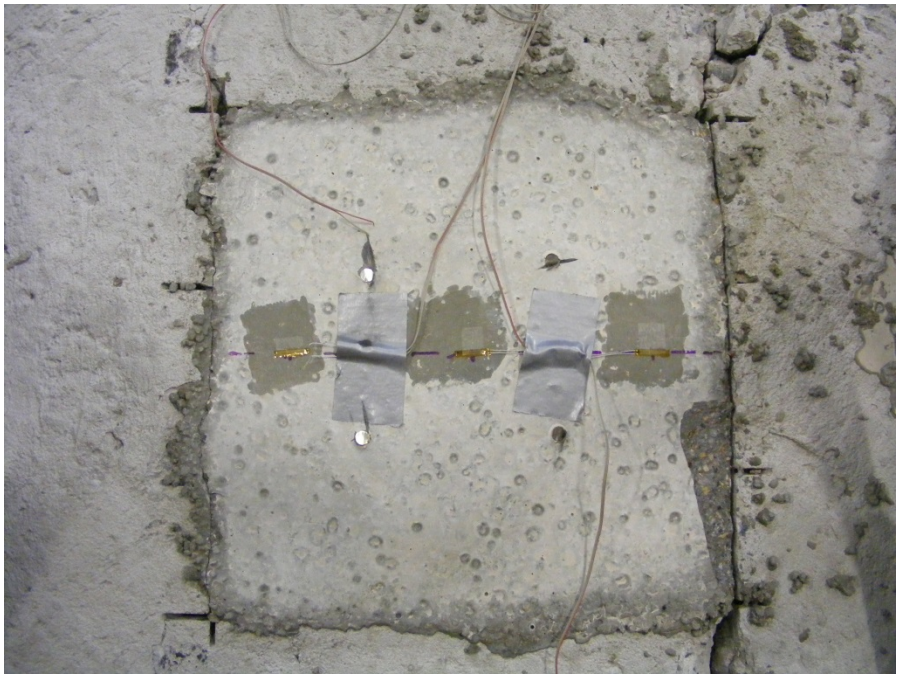

Figure B- 26 3U18 S C 4

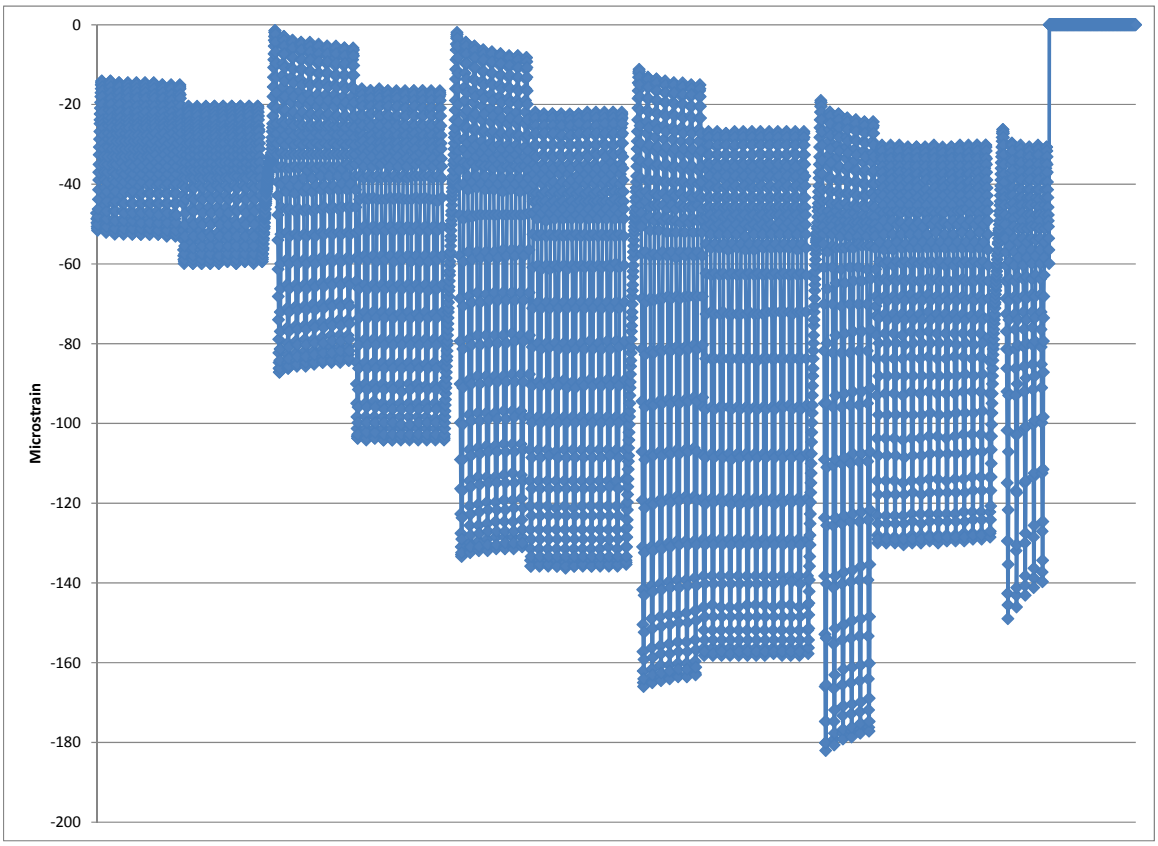

Figure B- 27 3U18 S C 4 strain gage 2